

Division of Pharmaceutical Biosciences  
Faculty of Pharmacy  
University of Helsinki  
Finland

**Investigation of Bacterial Biofilms  
on Clinically Relevant Materials and  
Effects of Antimicrobials**

*Anna Katariina Hiltunen*

**DOCTORAL DISSERTATION**

To be presented for public examination with the permission of the Faculty of Pharmacy of the University of Helsinki, in Auditorium 1041, Biocenter 2 (Viikinkaari 5), on the 24<sup>th</sup> of September 2021 at 13 o'clock.

Helsinki 2021

## **SUPERVISORS**

**Docent Adyary Fallarero, PhD**  
Microbiology Division  
Specialty Diagnostics Group  
Thermo Fisher Scientific, Vantaa  
Finland

**Professor Pia Vuorela, PhD**  
**(Deceased 1.10.2017)**  
Division of Pharmaceutical Biosciences  
Faculty of Pharmacy  
University of Helsinki  
Finland

## **REVIEWERS**

**Associate Professor Jaime Esteban Moreno, PhD**  
Department of Preventive Medicine, Public Health and  
Microbiology  
Faculty of Medicine  
Autonomous University of Madrid  
Spain

**Professor Markus Linder, PhD**  
Department of Bioproducts and Biosystems  
School of Chemical Engineering  
Aalto University, Espoo  
Finland

## **OPPONENT**

**Docent, Adjunct Professor Veli-Matti Tiainen, PhD**  
Director of the Diamond Group  
Orton Research Institute, Helsinki  
Finland

## THESIS COMMITTEE

### **Docent Kirsi Savijoki, PhD**

Division of Pharmaceutical Biosciences  
Faculty of Pharmacy  
University of Helsinki  
Finland

### **Docent Teemu Kinnari, PhD**

Department of Otorhinolaryngology-  
Head and Neck Surgery  
Helsinki University Hospital  
University of Helsinki  
Finland

### **Docent Pirkko Pussinen, PhD**

Department of Oral and Maxillofacial  
Diseases  
Faculty of Medicine  
University of Helsinki  
Finland

Published in the Doctoral School in Health Sciences (DSHealth) series  
*Dissertationes Scholae Doctoralis Ad Sanitatem Investigandam Universitatis  
Helsinkiensis 42/2021.*

© Anna Katariina Hiltunen 2021

ISBN 978-951-51-7456-7 (paperback)

ISBN 978-951-51-7457-4 (PDF)

ISSN 2342-3161 (print) and ISSN 2342-317X (online)

Unigrafia Oy  
Helsinki 2021

The Faculty of Pharmacy uses the Urkund system (plagiarism recognition) to  
examine all doctoral dissertations.

## ABSTRACT

Biofilm, a major lifestyle of bacteria, refers to bacterial communities surrounded by a self-produced protective slimy matrix. Due to this matrix and the reduced metabolic activity of bacteria within them, biofilms usually withstand the eradication of conventional antibiotics, leading to recalcitrant and recurrent infections. Therefore, there is an immense need for discovering novel truly effective anti-biofilm treatment strategies that do not promote the development of antibiotic resistance.

Biofilms colonizing permanently inserted indwelling medical devices are particularly challenging as their eradication always requires some kind of invasive surgery. Even though a wide variety of biomaterials are used in medical devices, the thorough understanding of biofilm characteristics or formation on such materials is still limited. In this thesis, a multidimensional orthogonal approach was taken to characterize biofilm dynamics on different biomaterials (borosilicate glass, plexiglass, hydroxyapatite, titanium, and polystyrene) at different maturation points (18, 42, and 66 h) (study I). This study covered (i) biomaterial surface properties (and the correlation with material susceptibility to biofilm formation), (ii) biofilm matrix structures (via proteosurfaceomics and polysaccharide/protein content determinations), and (iii) biofilm functionality (antimicrobial tolerance studies). *Staphylococcus aureus*, which is a major pathogen in medical device-associated infections, was chosen as a model organism for this study.

The matrix-associated polysaccharide content was observed to play an important role in the initial stages of biofilm formation as its amount decreased towards the end of the observation period. In turn, the matrix-associated protein content seemed to increase over time. Interestingly, the classical surface proteins that have been deemed as the most attractive targets in antibiotic development, demonstrated high biomaterial-dependent variability in their amounts. In turn, the presence of non-classical surface proteins “moonlighting proteins”, forming the major portion of the core proteosurfaceome, did not appear to be strongly dependent on the material. It is known that biofilm inhabitants reutilize cytoplasmic proteins as moonlighting constituents in the extracellular space, offering enhanced bacterial attachment, virulence, and antibiotic tolerance. Therefore, inhibiting moonlighting activity would offer a novel target for anti-biofilm agent/material development. Finally, biofilms formed on hydroxyapatite were in many cases more susceptible to antibiotics than titanium-associated biofilms. Also, according to our findings, the biofilm age did not always correlate with the increased antibiotic tolerance.

To the best of our knowledge, study I is among the pioneer investigations shedding light onto the matrix-associated proteosurfaceomes of *S. aureus* biofilms developed on different biomaterials and at diverse biofilm formation points. The study offers further mechanistic insights into biofilm formation and the findings may facilitate the development of new anti-biofilm compounds.

After focusing on the more fundamental aspects of biofilm formation on different materials, the next goal was to study whether one of these biomaterials, hydroxyapatite, could be protected from biofilm colonization with a novel non-antibiotic combination product. This was studied in two *in vitro* biofilm infection models: for prosthetic joint infections (PJIs) (modelled using *S. aureus* and *Staphylococcus epidermidis*; study **II**) and periodontitis (using *Aggregatibacter actinomycetemcomitans*; study **III**). Both diseases cause significant individual burden and would benefit from an approach with both biofilm-eradicating and bone-preserving capabilities.

The rise of antibiotic resistance is a top threat to public health, and thus innovative treatment options reducing the use of conventional antibiotics are desired. Based on this, bioactive glass S53P4 (BAG), a bone-constructing material with a completely divergent (*i.e.* physical-based) bactericidal mechanism, was chosen as a focus here. Additionally, it has been previously reported that the bone construction ability of other bioactive glasses can be enhanced by combining them with anti-osteoporotic drugs, *i.e.* bisphosphonates (BPs). However, how the addition of BPs (alendronate, clodronate, etidronate, risedronate, and zoledronate) influences the anti-biofilm effect of BAG has not been previously studied, and this was the main research question in studies **II** and **III**.

Etidronate-BAG and risedronate-BAG were found to be the most promising combinations from the perspective of both studies (**II** and **III**), while clodronate-BAG was not effective against any of the strains. Risedronate was the only BP that had an intrinsic anti-biofilm effect against all the tested strains. Moreover, an enhanced anti-biofilm effect was systematically observed in study **III**, probably due to the longer treatment period (48 h) compared to the one used in study **II** (24 h).

Finally, a possible mechanistic perspective to the anti-biofilm effect of BP-BAG combinations was undertaken. The observed anti-biofilm effects could not be rationalized alone with lowered pH values. Increased osmotic pressure or another yet-unknown mechanism seems to contribute to the observed anti-biofilm effect. In conclusion, the results of studies **II** and **III** further support the use of the most effective BP-BAG combinations in protecting biomaterials from biofilm infections in PJI and periodontal applications.

## TIIVISTELMÄ

Biofilmi on bakteerien yleisin kasvutapa, ja sillä tarkoitetaan bakteeriyhdyskuntia, joita ympäröi bakteerin tuottama suojaava limamatriisi. Tästä limamatriisista ja bakteerien vähäisestä metabolisesta aktiivisuudesta johtuen tavanomaiset antibiootit osoittautuvat yleensä tehottomiksi biofilmi-infektioiden hoidossa. Seurauksena tästä voi syntyä sitkeitä ja toistuvia infektioita. Onkin suuri tarve löytää uusia aidosti tehokkaita biofilmien vastaisia hoitostrategioita, jotka eivät kuitenkaan edistäisi antibioottiresistenssin kehittymistä.

Biofilmit, jotka muodostuvat elimistön sisään pysyvästi asennetuille lääkinnällisille laitteille, ovat erityisen haastavia, koska niiden hävittäminen vaatii aina jonkinlaisen invasiivisen leikkauksen. Vaikka lääkinnällisissä laitteissa käytetään monenlaisia biomateriaaleja, perusteellinen ymmärrys biofilmien ominaisuuksista ja muodostumisesta näille materiaaleille on edelleen rajallista. Tässä väitöskirjassa hyödynnettiin moniulotteista ortogonaalista lähestymistapaa analysoitaessa eri-ikäisten (18, 42 ja 66 h) biofilmien dynamiikkaa eri biomateriaaleilla (borosilikaattilasi, pleksilasi, hydroksiapatiitti, titaani ja polystyreeni) (tutkimus I). Tämä tutkimus käsitti (i) näiden materiaalin pintaominaisuuksien määrittämisen, sekä analyysin ominaisuuksien korrelaatiosta biofilmin muodostumisherkkyuden kanssa. Seuraavaksi, (ii) näiden eri materiaaleille muodostettujen ja eri-ikäisten biofilmien matriisikoostumukset analysoitiin (käsittäen proteiinipitoisuuksien ja polysakkaridi-/proteiinipitoisuuksien määritykset). Lopuksi tutkittiin (iii) eroavatko eri materiaaleille muodostuneet ja eri-ikäiset biofilmit antibioottivastustuskyvyn suhteen. *Staphylococcus aureus* on merkittävä taudinaiheuttaja lääkinnällisiin laitteisiin liittyvissä infektioissa, ja se valittiin malliorganismiksi tähän tutkimukseen.

Matriisiin polysakkaridien havaittiin olevan tärkeässä roolissa biofilmin muodostumisen alkuvaiheessa, ja niiden määrät vähenivät tarkkailujakson edetessä. Matriisiin proteiinipitoisuus puolestaan näytti kasvavan ajan kuluessa. Perinteisesti houkuttelevina antibioottikehityskohteina pidettyjen klassisten pintaproteiinien määrät osoittautuivat olevan riippuvaisia käytetystä biomateriaalista. Ei-klassisten pintaproteiinien, nk. "moonlighting proteiini" (eng. moonlighting proteins) määrät eivät puolestaan näyttäneet olevan voimakkaasti riippuvaisia käytetystä materiaalista. Nämä moonlighting proteiinit muodostivat myös suurimman osan ydinproteiinisurfaseomista. Tiedetään, että biofilmi populaatio hyödyntää ensin näitä moonlighting proteiineja sytoplasmassa, jonka jälkeen ne siirtyvät uudiskäyttöön solunulkoiseen tilaan. Solunulkoisessa tilassa ne edistävät bakteerien kiinnittymis-, taudinaiheuttamis- ja antibioottien vastaista puolustautumiskykyä. Tämän moonlighting proteiini-ilmion estäminen voisikin toimia uutena kohteena biofilmin vastaisten lääkeaineiden/materiaalien kehityksessä. Lopuksi havaittiin, että hydroksiapatiitille muodostuneet biofilmit olivat monissa tapauksissa herkempiä antibiooteille kuin titaanille

muodostuneet biofilmit. Havaintojemme mukaan myöskään biofilmin ikä ei aina korreloinut lisääntyneen antibioottivastustuskyvyn kanssa.

Parhaan tietomme mukaan tutkimus I toimii edelläkävijänä valaisten *S. aureus*-biofilmmatriisien proteiinipinnoitusten koostumuksia, kun eri ikäisiä biofilmejä on muodostettu eri biomateriaaleille. Tutkimus tarjoaa uudenlaisia näkemyksiä koskien biofilmin muodostumista, ja nämä havainnot voivat helpottaa uusien biofilmien vastaisten yhdisteiden kehitystyötä.

Näiden perustavanlaatuisien muodostumistutkimusten jälkeen seuraavana tavoitteena oli tutkia, voisiko yhtä näistä biomateriaaleista, hydroksiapatiittia, suojata biofilmin muodostumiselta uudentyypisellä antibiootittomalla yhdistelmätuotteella. Tätä tutkittiin kahdessa *in vitro* biofilmi-infektioimallissa: nivelproteesi-infektioimallissa (*S. aureus*- ja *Staphylococcus epidermidis*-bakteereja vastaan; tutkimus II) ja parodontiittimallissa (*Aggregatibacter actinomycetemcomitans*-bakteeria vastaan; tutkimus III). Molemmat sairaudet aiheuttavat yksilölle merkittävää kuormitusta ja niissä hyödyttäisiin hoitomuodosta, jossa yhdistyisivät sekä biofilmejä tuhoavat, että luuta ylläpitävät omaisuudet.

Antibioottiresistenssin nousu on merkittävä uhka kansanterveydelle, ja siksi on tarvetta innovatiivisille hoitovaihtoehdoille, jotka vähentävät tavanomaisten antibioottien käyttöä. Siksi luunrakennusmateriaali (bioaktiivinen lasi S53P4; BAG), jolla on täysin poikkeava fysikaalinen bakteereja tappava mekanismi, valittiin näiden tutkimusten keskiöön. Aiempien raporttien mukaan joidenkin bioaktiivisten lasilaatujen luurakentamiskykyä voidaan parantaa osteoporoosilääkkeillä eli bisfosfonaateilla. Kuitenkaan sitä kuinka bisfosfonaattien (alendronaatti, klodronaatti, etidronaatti, risedronaatti ja tsoledronaatti) lisääminen vaikuttaa BAG:n biofilmien vastaiseen tehoon, ei ole aiemmin tutkittu. Tämä toimikin pääasiallisena tutkimuskysymyksenä tutkimuksille II ja III.

Etidronaatti-BAG ja risedronaatti-BAG todettiin lupaavimmiksi biofilmien vastaisiksi yhdistelmiksi molempien tutkimusten (II ja III) näkökulmasta, kun taas klodronaatti-BAG ei ollut tehokas mitään tutkittua bakteerikantaa vastaan. Risedronaatti oli ainoa bisfosfonaatti, jolla oli biofilmien vastainen vaikutus yksinään annosteltuna; vaikutus myös ilmeni kaikkia testattuja bakteerikantoja vastaan. Lisäksi biofilmien vastainen teho havaittiin olevan järjestelmällisesti parempi tutkimuksessa III, todennäköisesti johtuen pidemmästä hoitojaksosta (48 h) verrattuna tutkimuksessa II käytettyyn (24 h).

Lopuksi annoimme näkökulman selittämään bisfosfonaatti-BAG-yhdistelmien biofilmien vastaisia vaikutuksia. Havaittuja vaikutuksia ei voitu selittää yksinään laskeneilla pH-arvoilla. Kohonnut osmoottinen paine tai muu vielä tuntematon mekanismi näyttääkin osallistuvan tähän. Yhteenvetona voidaan todeta, että tutkimusten II ja III tulokset tukevat tehokkaimpien bisfosfonaatti-BAG-yhdistelmien käyttöä biomateriaalien suojaamisessa biofilmi-infektioilta nivelproteesi-infektio- ja parodontiitti-indikaatioissa.

## ACKNOWLEDGEMENTS

The research work of this dissertation was carried out at the Division of Pharmaceutical Biosciences (Faculty of Pharmacy, University of Helsinki, Finland). I would like to thank Professors Päivi Tammela and Heikki Vuorela for providing the facilities and scientific environment for this project. The dissertation was pre-examined by Associate Professor Jaime Esteban Moreno and Professor Markus Linder, whom I sincerely thank for their positive feedback. I would like to thank Docent and Adjunct Professor Veli-Matti Tiainen for acting as my opponent and Professor Päivi Tammela for acting as the custos in the public defense.

The dissertation was financially supported by the Doctoral Programme in Drug Research (DPDR), The Finnish Science Foundation for Technology and Economics KAUTE, The Finnish Pharmaceutical Society, Jane and Aatos Erkko Foundation, The Academy of Finland, and the University of Helsinki.

I would like to express my gratitude to my supervisors Docent Adyary Fallarero and Professor Pia Vuorela (deceased 2017). Unfortunately, Pia could not see the completion of this project. However, I am grateful that she welcomed me as a member of the AIR research team in 2014, and together with Adyary, introduced the fascinating world of bacteria and biofilms! I am thankful for having been able to work on such interesting and important research questions concerning antibiotic tolerance and chronic infections. I am extremely grateful to Adyary for being such an excellent and enthusiastic scientific mentor for me throughout these years. I have learned tremendously from her about biofilms, drug development, and the scientific way of thinking. I would also like to thank Docent Malena Skogman for guiding and supporting me during this project.

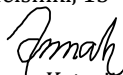
This thesis has benefited from the efforts of several professionals over the years: I would like to thank my co-authors Docent Kirsi Savijoki, Docent Tuula Nyman, Dr. Ilkka Miettinen, Docent Petri Ihalainen, Prof. Anne Juppo, Dr. Kirsi Rosenqvist, Prof. Jouko Peltonen, and Dr. Helka Juvonen for the productive cooperation. Furthermore, I would like to thank Dr. Fredrik Ollila for his co-operation during this project. Moreover, I want to thank MSc Sabina Pham and MSc Vincent Voet for their great assistance in laboratory work. I would also like to thank Docent Teemu Kinnari, Docent Pirkko Pussinen, and Docent Kirsi Savijoki for supporting the work as members of the thesis committee.

In addition, I wish to acknowledge my former and current research group members: Maarit, Ilkka, Sabina, Paola, Inés, Shella, Eveliina, Tuija, Krista, and Elina for creating such a warm-hearted and encouraging working atmosphere. Other pharmaceutical biology colleagues (Docent Leena Hanski, Dr. Karmen Kapp, Dr. Pia Fyhrquist, Docent Yvonne Holm, *et al.*) are also acknowledged. I would also like to thank Dr. Suvi Manner for the great traveling company in various conference trips throughout the years.

I want to express my gratitude to my family and friends, both in Finland and Switzerland, for their support. I am grateful to the Faculty of Pharmacy (University of Helsinki) for enabling me to finalize this project whilst living in Switzerland.

Finally, I am deeply grateful for my little family - Karri: I have been very privileged to have another (more senior) scientist living in the same household! Thank you for all the scientific discussions, perspective, and endless patience you have given. My little Kerttu – thank you for bringing so much happiness and delight to my life, every day!

Helsinki, 15<sup>th</sup> of August 2021



Anna Katariina Hiltunen



# TABLE OF CONTENTS

ABSTRACT .....	iv
TIIVISTELMÄ .....	vi
ACKNOWLEDGEMENTS .....	viii
TABLE OF CONTENTS .....	ix
LIST OF ORIGINAL PUBLICATIONS.....	xii
ADDITIONAL PUBLICATIONS NOT INCLUDED IN THE THESIS.....	xii
CONTRIBUTION OF THE AUTHOR.....	xiii
ABBREVIATIONS .....	xiv
<b>1. INTRODUCTION .....</b>	<b>1</b>
<b>2. LITERATURE REVIEW .....</b>	<b>3</b>
<b>2.1 Two bacterial lifestyles.....</b>	<b>3</b>
<b>2.2 Biofilm formation .....</b>	<b>4</b>
2.2.1 Attachment.....	4
2.2.2 Proliferation/maturation .....	5
2.2.3 Dispersal/detachment.....	5
<b>2.3 Biofilm tolerance and resistance.....</b>	<b>6</b>
<b>2.4 Biofilm matrix – more than a shield.....</b>	<b>7</b>
2.4.1 The biofilm matrix-accompanying polysaccharides .....	8
2.4.2 The biofilm matrix-associated protein fraction.....	9
2.4.3 The biofilm matrix-related extracellular DNA .....	11
<b>2.5 Biofilm infections.....</b>	<b>11</b>
2.5.1 Prosthetic joint infection .....	13
2.5.2 Periodontitis.....	16
<b>2.6 Biofilm treatment strategies.....</b>	<b>17</b>
<b>2.7 Relevant biofilm-forming bacteria .....</b>	<b>19</b>
2.7.1 <i>Staphylococcus aureus</i> and <i>Staphylococcus epidermidis</i> .....	19
2.7.2 <i>Aggregatibacter actinomycetemcomitans</i> .....	20
<b>2.8 Biofilm investigation methods.....</b>	<b>20</b>
2.8.1 Assays performed in liquid cultures .....	20
2.8.2 Assays performed in solid-state cultures.....	22
<b>2.9 Bisphosphonates.....</b>	<b>22</b>
2.9.1 Definition and pharmacological indications .....	22
2.9.2 Bisphosphonates in periodontitis .....	23
<b>2.10 Bioactive glass .....</b>	<b>24</b>
2.10.1 Definition.....	24
2.10.2 Bone regeneration .....	24

## TABLE OF CONTENTS

2.10.3 Antibacterial effect.....	25
2.10.4 Bioactive glasses in dental applications .....	26
2.10.5 Combination of bisphosphonates and bioactive glass .....	26
<b>3. AIMS OF THE STUDY .....</b>	<b>28</b>
<b>4. MATERIALS AND METHODS.....</b>	<b>29</b>
<b>4.1 Materials (studies I-III).....</b>	<b>29</b>
4.1.1 Test compounds, antimicrobials, culture media, and reagents (studies I-III) .....	29
4.1.2 Bacterial strains (studies I-III).....	30
<b>4.2 Methods (studies I-III).....</b>	<b>30</b>
4.2.1 Bacterial culturing (studies I-III) .....	30
4.2.2 Well plate-based assays (study I) .....	31
4.2.2.1 Biofilm formation on coupons in the well plate-based assay (study I).....	31
4.2.2.2 Quantification of the biofilm formation on different materials at different time points (study I) .....	31
4.2.2.3 Quantification of the coupon-associated biofilms (studies I-III) ....	32
4.2.2.4 Quantification of the biofilm matrix component polysaccharide intercellular adhesin/poly-N-acetyl- $\beta$ -(1-6)-glucosamine (study I) .....	32
4.2.2.5 Trypsin shaving of biofilm matrix-associated proteins (study I) ...	33
4.2.2.6 Identification of trypsin-released proteins/peptides by LC-MS/MS (study I).....	34
4.2.3 The Static Biofilm method-based assays (studies II, III).....	35
4.2.3.1 The biofilm formation in the prosthetic joint infection and dental biofilm models (studies II, III) .....	35
4.2.3.2 Selecting applicable biofilm formation substrate and time (studies II and III).....	35
4.2.3.3 Exploring anti-biofilm effects of bisphosphonate-bioactive glass and bisphosphonate-inert glass combinations (studies II and III) .....	35
4.2.3.4 Quantification of the biofilms (studies II-III) .....	37
4.2.4 Chemotolerance assays (studies I and III) .....	37
4.2.5 Imaging of biofilms (studies I and III).....	37
4.2.5.1 Atomic force microscopy (studies I and III).....	37
4.2.5.2 Fluorescence microscopy (study I).....	38
4.2.6 pH measurements (study III) .....	38
4.2.7 Data processing and statistical analysis (studies I-III).....	38
<b>5. RESULTS AND DISCUSSION .....</b>	<b>39</b>
<b>5.1 Characteristics and dynamical changes of <i>Staphylococcus aureus</i>   biofilms on clinically relevant materials (study I) .....</b>	<b>39</b>
5.1.1 Surface roughness analysis of tested substrate materials (study I)	39
5.1.2 Bacterial attachment on the materials (study I) .....	41
5.1.3 Quantification of polysaccharide intercellular adhesin/poly-N- acetyl- $\beta$ -(1-6)-glucosamine (study I) .....	42

5.1.4 Quantification of the protein fraction in the biofilm matrix (study I) .....	45
5.1.5 Qualification of the proteins in the biofilm matrix (study I) .....	47
5.1.5.1 Virulence factors.....	53
5.1.5.1.1 Adherence factors .....	53
5.1.5.1.2 Proteins contributing to immunoevasion.....	54
5.1.5.1.3 Host-damaging proteins.....	55
5.1.5.1.4 Exoenzymes.....	56
5.1.5.1.5 Antimicrobial resistance factors.....	56
5.1.5.2 Regulatory proteins.....	57
5.1.5.3 Clp family proteins.....	57
5.1.5.4 Cellular oxido-redox state-maintaining enzymes.....	57
5.1.5.5 Cytoplasmic proteins as moonlighters.....	57
5.1.5.5.1 Protein synthesis-associated adhesins .....	58
5.1.5.5.2 Glycolytic adhesins.....	59
5.1.5.5.3 Chaperones and other stress proteins .....	60
5.1.6 Chemotolerance assays (study I) .....	61
<b>5.2 Anti-biofilm effect of bisphosphonate-bioactive glass combinations against staphylococcal biofilms in the prosthetic joint infection biofilm model (study II) .....</b>	<b>64</b>
5.2.1 Optimization of the prosthetic joint infection biofilm model (study II).....	64
5.2.2 Examination of bisphosphonates in combination with inert glass and bioactive glass against staphylococcal biofilms (study II) .....	66
<b>5.3 Anti-biofilm effect of bisphosphonate-bioactive glass combinations against <i>Aggregatibacter actinomycetemcomitans</i> biofilms in the periodontal biofilm model (study III) .....</b>	<b>69</b>
5.3.1 Optimization of the dental biofilm model (study III) .....	69
5.3.2 Examination of bisphosphonates in combination with inert glass and bioactive glass against periodontal biofilms (study III) .....	73
<b>5.4 Mechanistic insight and possible targets of bisphosphonates and bisphosphonate-bioactive glass combinations on bacterial biofilms (studies I-III) .....</b>	<b>75</b>
<b>6. CONCLUSIONS AND FUTURE PERSPECTIVES .....</b>	<b>82</b>
<b>7. REFERENCES .....</b>	<b>84</b>
<b>APPENDIX (SUPPLEMENTARY MATERIAL) .....</b>	<b>105</b>

## LIST OF ORIGINAL PUBLICATIONS

- I. **Hiltunen AK**, Savijoki K, Nyman TA, Miettinen I, Ihalainen P, Peltonen J, Fallarero A: Structural and Functional Dynamics of *Staphylococcus aureus* Biofilms and Biofilm Matrix Proteins on Different Clinical Materials. *Microorganisms* 7: 584, 2019
- II. **Hiltunen AK**, Vuorela PM, Fallarero A: Bisphosphonates Offer Protection against Prosthetic Joint Infections Caused by *Staphylococcus aureus* and *Staphylococcus epidermidis* biofilms. *Journal of Drug Delivery Science and Technology* 40: 136–141, 2017
- III. **Hiltunen AK**, Skogman ME, Rosenqvist K, Juvonen H, Ihalainen P, Peltonen J, Juppo A, Fallarero A: Bioactive Glass Combined with Bisphosphonates Provides Protection Against Biofilms Formed by the Periodontal Pathogen *Aggregatibacter actinomycetemcomitans*. *International Journal of Pharmaceutics* 501: 211–220, 2016

The original publications have been reprinted with permission from the publishers/copyright holders.

The publications are referred to in the text by their Roman numerals (I–III).

## ADDITIONAL PUBLICATIONS NOT INCLUDED IN THE THESIS

- i. Fallarero A, Batista-González AE, **Hiltunen AK**, Liimatainen J, Karonen M, Vuorela PM: Online Measurement of Real-Time Cytotoxic Responses Induced by Multi-Component Matrices, such as Natural Products, through Electric Cell-Substrate Impedance Sensing (ECIS). *International Journal of Molecular Sciences* 16: 27044–27057, 2015
- ii. Fallarero A, Skogman M, Manner S, **Hiltunen A**, Vuorela PM: Counteracting Bacterial Biofilms: The Potential of Natural Product-Based Anti-Infectives. *Dosis* 32: 40–54, 2015
- iii. **Hiltunen A**, Skogman M, Vuorela PM, Fallarero A: Exploration of Microbial Communities Using the Thermo Scientific Varioskan LUX Multimode Reader and the Invitrogen EVOS FL Cell Imaging System. *BioTechniques* 61: 214–215, 2016

## CONTRIBUTION OF THE AUTHOR

The author has contributed to the publications in the thesis in the following manner:

- I.** The study was planned by the author and Dr. Adyary Fallarero. Most of the experimental biofilm work was performed by the author. MSc Sabina Pham and MSc Vincent Voet assisted in producing replicate samples for the proteomic analysis. The manuscript was primarily written by the author with suggestions and feedback from the co-authors. The LC-MS/MS-analysis was performed by Dr. Tuula Nyman. The AFM studies were performed by Dr. Petri Ihalainen. Most of the data analysis was performed by the author. Dr. Kirsi Savijoki contributed to the analysis and written part of the proteomic results. The principal component analysis was planned and performed by Dr. Ilkka Miettinen.
  
- II.** The author was the lead author and responsible for the planning, execution, and data analysis of the study. The manuscript was primarily written by the author with feedback from the co-authors.
  
- III.** All the experimental biofilm work and data analysis were performed by the author. The manuscript was primarily written by the author with feedback from the co-authors. The study was planned by the author, Dr. Malena Skogman, and Dr. Adyary Fallarero. The AFM studies were performed by Dr. Petri Ihalainen and Dr. Helka Juvonen.

## ABBREVIATIONS

<b>3D</b>	Three-dimensional
<b>AFM</b>	Atomic force microscopy
<b>Agr</b>	Accessory gene regulator
<b>AhpC/F</b>	Alkyl hydroperoxide reductase C/F
<b>AIP</b>	Autoinducing peptide
<b>AMP</b>	Antimicrobial peptide
<b>Asp23</b>	Alkaline shock protein 23
<b>ASTM</b>	American Society for Testing and Materials
<b>Atl</b>	Bifunctional autolysin
<b>ATP</b>	Adenosine triphosphate
<b>BA</b>	Blood agar
<b>BAG</b>	Bioactive glass S53P4
<b>Bap</b>	Biofilm-associated protein
<b>Bbp</b>	Bone sialoprotein-binding protein
<b>BP</b>	Bisphosphonate
<b>CcpA</b>	Catabolite control protein A
<b>CHX</b>	Chlorhexidine
<b>ClfA/B</b>	Clumping factors A/B
<b>Coa</b>	Staphylocoagulase
<b>Cra</b>	Catabolite repressor/activator protein
<b>CvfB</b>	Conserved virulence factor B
<b>DAIR</b>	Debridement, antibiotics and implant retention
<b>DMSO</b>	Dimethyl sulphoxide
<b>ECM</b>	Extracellular matrix
<b>eDNA</b>	Extracellular deoxyribonucleic acid
<b>EsxA</b>	Ess extracellular protein A
<b>FbnBP</b>	Fibrinogen-binding protein
<b>FmtA</b>	Teichoic acid <i>D</i> -alanine hydrolase
<b>FnBPA</b>	Fibronectin-binding protein A
<b>G</b>	Borosilicate glass
<b>HA</b>	Hydroxyapatite
<b>Hlg</b>	Gamma-hemolysin
<b>Ig</b>	Immunoglobulin
<b>IG</b>	Inert glass
<b>IsaA/B</b>	Immunodominant staphylococcal antigen A/B
<b>IsdB</b>	Iron-regulated surface determinant protein B
<b>iv.</b>	Intravenous
<b>logR</b>	Logarithmic reduction
<b>LTA</b>	Lipoteichoic acid
<b>LyrA</b>	Lysostaphin resistance protein A
<b>MBEC</b>	Minimal biofilm eradication concentration
<b>MIC</b>	Minimal inhibitory concentration
<b>mRNA</b>	Messenger ribonucleic acid
<b>MRSA</b>	Methicillin-resistant <i>Staphylococcus aureus</i>
<b>MRSE</b>	Methicillin-resistant <i>Staphylococcus epidermidis</i>
<b>MscL</b>	Large-conductance mechanosensitive channel
<b>MSCRAMM</b>	Microbial surface components recognizing adhesive matrix molecule
<b>N/A</b>	Not available

## ABBREVIATIONS

<b>NAG</b>	N-acetylglucosamine
<b>NEAT</b>	Near iron transporter
<b>OD</b>	Optical density
<b><i>p.o.</i></b>	Per oral
<b>PAMPs</b>	Pathogen-associated molecular patterns
<b>PBS</b>	Phosphate-buffered saline
<b>PCA</b>	Principal component analysis
<b>PG</b>	Plexiglass
<b>PIA/PNAG</b>	Polysaccharide intercellular adhesin/ poly-N-acetyl- $\beta$ -(1-6)-glucosamine
<b>PJ</b>	Prosthetic joint
<b>PJI</b>	Prosthetic joint infection
<b>PMMA</b>	Polymethyl methacrylate
<b>PS</b>	Polystyrene
<b>PSM</b>	Phenol-soluble modulins
<b>ROS</b>	Reactive oxygen species
<b>r-protein</b>	Ribosomal protein
<b>RT</b>	Room temperature
<b>SD</b>	Standard deviation
<b>SdrC/D</b>	Serine-aspartate repeat-containing protein C/D
<b>SEM</b>	Standard error of the mean
<b>SERAM</b>	Secretable expanded repertoire adhesive molecule
<b>SodA</b>	Superoxide dismutase [Mn/Fe] 1
<b>Spa</b>	Immunoglobulin G-binding protein A
<b>SsaA2</b>	Staphylococcal secretory antigen
<b>SspP</b>	Staphopain A
<b>TEAB</b>	Triethylammonium bicarbonate buffer
<b>TEAB<sub>S16</sub></b>	100 mM TEAB containing sucrose (16%)
<b>TFA</b>	Trifluoroacetic acid
<b>TI</b>	Titanium
<b>tRNA</b>	Transfer ribonucleic acid
<b>TSA</b>	Tryptic soy agar
<b>TSB</b>	Tryptic soy broth
<b>TSB-YE/Glc</b>	TSB supplemented with 0.6% (w/v) yeast extract and 0.8% (w/v) glucose
<b>Usp</b>	Universal stress protein SAV1710
<b>WGA</b>	Wheat germ agglutinin Alexa Fluor® 488 conjugate
<b>WP</b>	Well plate
<b>WTA</b>	Wall teichoic acid





## 1. INTRODUCTION

Bacteria are now proposed to exist in two lifestyles: <sup>(1)</sup> freely swimming single cells “planktonic bacteria” and <sup>(2)</sup> bacteria growing as aggregates surrounded by a protective slimy matrix, called “biofilms”. Planktonic bacteria are nowadays regarded to be responsible for acute infections (e.g. bloodstream infections) which can potentially be resolved with antibiotics in a relatively short period of time (excl. multi-drug resistant bacteria) (Bjarnsholt et al. 2013b). In contrast, bacterial biofilms are associated with persistent and chronic infections. These biofilms are responsible not only for high morbidity and mortality but also for prolonged hospitalization periods, significant financial losses, and a heavy burden on the already limited healthcare resources (Mandakhalikar 2019; Bjarnsholt 2013). Bacterial biofilms exhibit a high tolerance towards antibiotics. This tolerance causes highly recalcitrant and recurrent chronic infections, often reappearing soon after the termination of the antibiotic course (Costerton et al. 1999). Therefore, there is an immense need for discovering truly effective anti-biofilm treatment strategies utilizing novel modes of action that can help reducing the spread of antibiotic resistance (Grønseth et al. 2020; Bjarnsholt et al. 2013b).

Particularly challenging biofilm infections are encountered when biofilms colonize indwelling medical devices, which have been inserted into the human body permanently. Eradicating these types of infections always requires some kind of invasive surgery. Even though numerous different biomaterials employed in medical devices are currently in clinical use, there are only a limited number of systematic studies comparing biofilm formation and biofilm characteristics on such materials (e.g. Roehling et al. 2017; Drago et al. 2016). In contrast, the recent focus of research has been on distinctive approaches for incorporating antimicrobial agents on implantation materials (e.g. Reigada et al. 2020a; 2020b; Sankar et al. 2017; Jennings et al. 2015; Tran et al. 2015; Drago et al. 2014b). However, it is known that the dynamic changes related to biofilm growth (Payne and Boles 2016) make biofilm eradication from biomaterials even more challenging. As the used biomaterial and the biofilm growth conditions greatly affect structural and functional features of biofilms (Roehling et al. 2017; Koseki et al. 2014; Patel et al. 2016), there is an evident need for thorough investigations on biofilm dynamics on these materials. The biofilm matrix is a key component contributing to biofilm dynamics, as it is known that biofilms adjust the matrix composition and quantity as a response to prevailing conditions. Changes in the biofilm matrix may in turn contribute to increased pathogenesis, antibiotic tolerance, and immune evasion (Gupta et al. 2019; Flemming and Wingender 2010). Hence, in the first part of this thesis (study I), a multidimensional orthogonal approach is taken to characterize biofilm dynamics covering (i) biomaterial surface properties (correlated with material susceptibility to biofilm formation), (ii) biofilm structures (via proteosurfaceomics and exopolysaccharide/protein contents), and (iii) biofilm functionality

## 1. INTRODUCTION

(antimicrobial tolerance studies). This allows performing side-by-side comparisons of biofilms formed on different biomaterials (borosilicate glass, plexiglass, hydroxyapatite, titanium, and polystyrene) at different maturation time points (18, 42, and 66 h). *Staphylococcus aureus*, a very common causative pathogen of foreign body-associated infections, is used as a model organism in study I.

After focusing on the more basic aspects of biofilm formation on different biomaterials, the next main objective of this thesis is to study whether one such biomaterial, hydroxyapatite, could be protected from biofilm formation with a novel combination product. This research question is assayed in two *in vitro* biofilm infection models: first in prosthetic joint infection (PJI) (study II; against *S. aureus* and *Staphylococcus epidermidis*), and then in a more novel target disease, periodontitis (study III; against *Aggregatibacter actinomycetemcomitans*). PJIs are a serious complication of implantation surgery, leading to prolonged hospitalization periods, a serious economic burden (Davidson et al. 2019), and a decreased quality of life for the patients (Helwig et al. 2014). In turn, periodontitis is a significant disease that affects 20–50% of the global population (Nazir 2017) and causes destruction of the attachment tissues/bone of teeth, leading eventually to tooth loss (Kwon et al. 2020). In both conditions, biofilms are a key pathogenic factor (Kwon et al. 2020; Izakovicova et al. 2019), and bone defects are ultimately associated with the progress of both diseases. Therefore, bone-constructing biodegradable materials with potential anti-biofilm properties would be an attractive option for PJI and periodontitis management. In addition, the rise of antibiotic resistance is a top threat to public health and from that perspective, innovative new treatment options reducing the use of conventional antibiotics are also desired (Grønseth et al. 2020).

Based on this, bioactive glass S53P4 (BAG), a bone-constructing material with known anti-biofilm activity is the focus of our investigation here. In contrast to conventional antibiotics, it has a completely divergent (*i.e.* physical) bactericidal mechanism, which makes it an attractive option for preventing antibiotic resistance (Drago et al. 2015). Moreover, it has been previously reported that enhanced bone construction ability of other bioactive glass grades can be improved by combination with osteoporotic drugs, bisphosphonates (BPs) (Srisubut et al. 2007; Välimäki et al. 2006). However, how the addition of BPs affects the anti-biofilm effect of BAG against *Staphylococcus* spp. and *A. actinomycetemcomitans* has not been previously studied, and this is the main objective in studies II and III.

## 2. LITERATURE REVIEW

### 2.1 Two bacterial lifestyles

It is proposed that bacteria exist in two lifeforms: <sup>(1)</sup> free-floating single cells (planktonic bacteria), which are usually responsible for acute infections and <sup>(2)</sup> sessile multicellular bacterial communities, “biofilms”, associated with chronic infections. Planktonic cells have been postulated to be essential in colonizing and spreading bacteria to new niches in the host. It has been assessed that only <0.1% of the total microbial biomass on Earth is in the planktonic form (Bjarnsholt et al. 2013b). By contrast, biofilms are the predominant bacterial lifestyle and an ancient survival strategy utilized by bacteria in every natural ecosystem (Donlan and Costerton 2002). It has been estimated that around 99.9% of bacteria can form biofilms (Donlan and Costerton 2002), meaning that most, if not all medically relevant bacteria, have the capabilities to form biofilms (Bjarnsholt et al. 2013b). Alhede et al. (2014) describe biofilms as: *“Aggregated, often sessile bacteria, which differ from free-floating cells by slow growth and tolerance to antibiotics and immune cells”*.

Biofilms offer microorganisms a protective survival strategy in hostile environments, such as those encountered at the infection site (Donlan and Costerton 2002). It has been estimated that 65% of microbial and 80% of chronic infections are caused by biofilms (Jamal et al. 2018). Indeed, biofilms are ubiquitous in many chronic pathologies, such as in chronic otitis media, chronic rhinosinusitis, chronic otitis media, cystic fibrosis, endocarditis, recurrent urinary tract infections, osteomyelitis, chronic wound infections, periodontitis, and indwelling medical device-associated infections, including orthopedic devices, endotracheal tubes, central venous catheters, urinary catheters, contact lenses, cardiac pacemakers, and breast implants (Mandakhlikar 2019; Bjarnsholt 2013). Still, significantly much less is currently known about biofilms in comparison to planktonic bacteria (Bjarnsholt et al. 2013b).

Biofilms were first observed by Anthony van Leeuwenhoek already in 1684 when he observed “animalcules” in his dental plaque. At the same time, Leeuwenhoek also demonstrated the extreme ability of such formations to tolerate chemicals by using vinegar as a proof-of-concept agent in his experiments. Interestingly, medical microbiology did not readily accept the concept of bacteria living preferentially in biofilms (Bjarnsholt 2013), and the first biofilm-related studies were published as late as the 1970s (Marshall 1976; Høiby and Olling 1977; Costerton et al. 1978). Nowadays, research around biofilms is very active: the total number of biofilm-focusing publications in PubMed is approaching 60,000 (December 2020). One key reason as to why biofilms are an intriguing and important topic for ongoing research of the medical community is their incredibly challenging eradication. Although conventional antibiotics decrease the number of bacteria in biofilms to some extent, the eradication remains incomplete. Due to a small population of bacterial cells that remain alive after treatment, relapses of biofilm-mediated infections

## 2. LITERATURE REVIEW

occur frequently. Therefore, biofilm infections are often chronic, recalcitrant, and relapsing in nature (Bjarnsholt et al. 2013b; Costerton et al. 1999).

### 2.2 Biofilm formation

Biofilms can be surface-associated (on biotic or abiotic surfaces; e.g. on dentine or catheters/implants), tissue-related (e.g. in chronic wounds), or mucus-embedded aggregates (without attachment to any surface; e.g. in cystic fibrosis) (Bjarnsholt et al. 2013b; Bjarnsholt et al. 2009). Altogether, biofilm formation has been commonly described with three main stages, as depicted in **Figure 1**: (1) attachment to a surface, (2) proliferation/maturation, and (3) dispersal/detachment (Otto 2018). The mechanisms mediating biofilm formation vary from species to species, but this section emphasizes especially *Staphylococcus aureus*, as this is one of the key model bacteria used in this thesis. However, many of the processes described here are applicable to other clinically relevant bacteria.

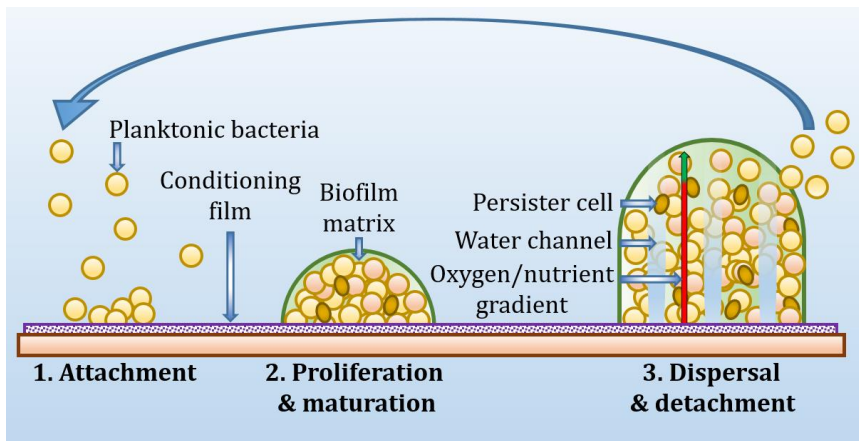


**Figure 1.** Three main stages of biofilm formation.

#### 2.2.1 Attachment

First, rapid surface attachment of planktonic bacteria to the abiotic or biotic surface occurs (**Figure 1**). The following factors mediate attachment: bacterial motility, (non)-proteinaceous adhesins, Van der Waals interactions, pH of the medium, material surface charge and hydrophobicity/hydrophilicity, as well as the formation of a conditioning film (Mandakhlikar 2019; Heilmann 2011). *S. aureus* has traditionally been considered as non-motile, but lately, it has been demonstrated to move on soft agar by spreading and comet formation (Pollitt and Diggle 2017). Examples of non-proteinaceous staphylococcal adhesins are positively charged PIA/PNAG (polysaccharide intercellular adhesin/poly-N-acetyl- $\beta$ -(1-6)-glucosamine) (described in 2.4.1) and negatively charged wall teichoic acid (WTA) and lipoteichoic acid (LTA) (Otto 2018; Joo and Otto 2012;

Heilmann 2011). For example, WTA seems to be essential for the adhesion of *S. aureus* to the nasal epithelium (Weidenmaier et al. 2004). *S. aureus* can also attach to host tissue (e.g. epithelium, endothelium, and bones) using specific proteinaceous adhesins that bind to a variety of extracellular matrix (ECM) components. The ECM is composed of an assortment of (glyco)proteins and proteoglycans, which form a structured meshwork surrounding cells in tissues. Examples of ECMs are bone-sialoprotein, collagen, elastin, fibronectin, and vitronectin. Moreover, indwelling medical devices become coated within nanoseconds after insertion with a layer called a conditioning film, which is composed of the extracellular matrix proteins, plasma proteins (e.g. fibrinogen and von Willebrand factor), and platelets. Hence, all these host components could serve as ligands for proteinaceous bacterial adhesin receptors and promote bacterial colonization (Geraci et al. 2017; Heilmann 2011). These proteinaceous adhesins will be further discussed in 2.4.2. As a result of the attachment phase, microcolonies are formed (Otto 2018).

### 2.2.2 Proliferation/maturation

In this second stage, the formed microcolonies start to proliferate and mature. In this phase, the self-produced polymeric biofilm matrix is secreted. The matrix offers architectural stability to the bacteria inside the biofilms and it protects against external threats, as it will be further described in 2.4. (Otto 2018; Flemming and Wingender 2010). As a result, a complex three-dimensional (3D)-structure is developed (Otto 2018). Because access for oxygen and nutrients decreases towards the base of the biofilm, fluid-filled channels are formed, which provide better availability of pivotal elements for deeper layers. Surfactant molecules (phenol-soluble modulins; PSMs) are responsible for producing such channels (Schilcher and Horswill 2020; Otto 2018; Periasamy et al. 2012). Once a mature biofilm has formed, the resulting construction is extremely viscoelastic. It has been demonstrated that the shear stress encountered during the biofilm formation correlates directly with the tensile strength of formed biofilms (Donlan and Costerton 2002; Stoodley et al. 1998).

### 2.2.3 Dispersal/detachment

The final stage of the biofilm cycle includes the dispersal of single cells and/or detachment of cell clusters from the biofilm. In this phase, bacteria transition from the biofilm lifestyle to planktonic form, allowing bacteria to disseminate to the bloodstream and spread the infection to other locations (Otto 2018). In this phase, a key role has been attributed to PSMs, as they reduce the surface tension of the biofilm matrix (Periasamy et al. 2012) as well as to degradative exoenzymes, such as proteases and nucleases (Schilcher and Horswill 2020; Otto 2018). Both PSMs and exoenzymes are regulated via an accessory gene regulator (*agr*) quorum sensing system. In addition to contributing to biofilm dispersal/detachment, the *agr*-system has been suggested to regulate motility and pathogenesis of *S. aureus*. Therein, the growth of the bacterial community

## 2. LITERATURE REVIEW

increases “autoinducing peptide” (AIP) signal molecule concentrations. When a critical AIP concentration “quorum” is reached, a regulatory cascade is initiated causing the production of e.g. exoenzymes, PSMs, and toxins. Correspondingly, the expression of adhesins is downregulated. Therefore, there is a negative correlation between *agr* induction and the accumulation of biofilm biomass (Schilcher and Horswill 2020; Pollitt and Diggle 2017).

### 2.3 Biofilm tolerance and resistance

The biofilm mode of growth is a bacterial survival strategy to withstand several human host- or environment-related hostile conditions. These harsh conditions may be caused by extreme pH values, anaerobic conditions, salinity, the host’s immune cells (such as phagocytes), bacteriophages, amoebae, desiccation, UV radiation, metal ions, and administered antibiotics, among others. Indeed, antibiotics typically have a significantly lower effect against biofilms in comparison to planktonic bacteria and this difference can be even 1000-fold (de la Fuente-Núñez et al. 2013). Basically, biofilm resilience to antimicrobials can be attributed to biofilm tolerance or bacterial resistance, which are two completely different concepts. The resistance mechanisms are not specifically associated with biofilms but with bacteria in general, and the involved mechanisms are illustrated in **Figure 2**.

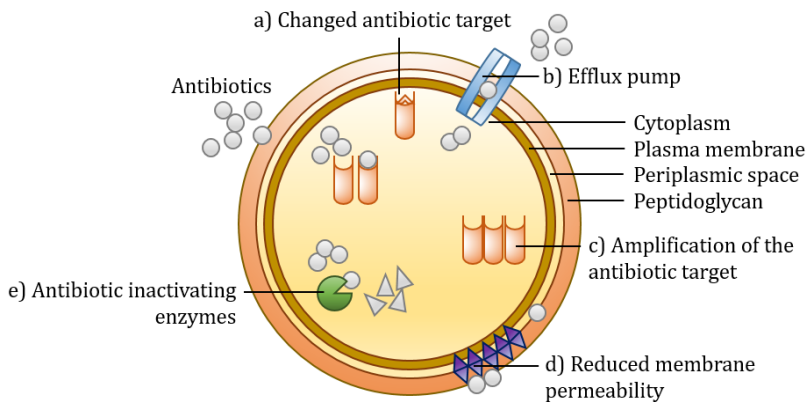


**Figure 2.** The most commonly described antibiotic resistance mechanisms. The figure has been inspired by Alav et al. (2018).

However, although resistance and tolerance are separate concepts, it has been found that biofilms promote the development of resistance. For instance, it has been observed that the biofilm growth mode increases dramatically horizontal transfer of plasmid-borne antibiotic resistance determinants when compared to planktonic bacteria. The close proximity of cells within the biofilm and more stabilized contacts between neighboring bacteria due to the biofilm matrix have been hypothesized to contribute to this (Savage et al. 2013).

With antibiotic tolerance, biofilm-associated bacteria can survive despite the presence of an antibiotic. However, if the biofilm is disrupted or naturally dispersed, the bacteria return to the antibiotic-susceptible planktonic state, as described in **Figure 1** (Bjarnsholt et al. 2013b). Antibiotic tolerance can be roughly explained with three mechanisms. First, the inner core of biofilm enters a slow-growing physiological status owing to depletion of metabolic substances, oxygen, and nutrients as well as accumulation of waste products (Bjarnsholt et al. 2013b). This leads to the low activity of cellular processes such as cell wall/protein biosynthesis or DNA replication. As many antibiotics target those processes, certain antibiotics do not have activity against biofilm cells (Ciofu et al. 2017). Secondly, ca. 1% of biofilm cells are in a metabolically inactive and non-dividing state, called “persisters”. These dormant cells are tolerant to multiple antibiotics simultaneously even without carrying the antibiotic resistance genes. A number of mechanisms have been suggested for the formation of persisters, such as induction of the SOS response, overexpressed toxin/antitoxin modules, and adenosine triphosphate (ATP) depletion. Persisters are a significant clinical problem as antibiotics kill only metabolically active cells and the remaining dormant cells can be re-activated later, thus causing an infection relapse (Podlesek and Žgur Bertok 2020; Lewis 2010; Lewis 2008). The third mechanism associated with biofilm tolerance to antibiotics is the restricted penetration of certain antimicrobials through the biofilm matrix (Ciofu et al. 2017), and this phenomenon will be further described in the following chapter, and it further highlights the importance of the matrix for biofilm persistence (2.4).

### 2.4 Biofilm matrix – more than a shield

Typically, 5–35% (by volume) of the biofilm is composed of bacterial cells, while the remaining 65–95% is formed by the biofilm matrix. The biofilm matrix is a self-produced gelatinous complex mixture of hydrated extracellular polymeric substances, such as proteins (>2%), polysaccharides (1–2%), DNA (<1%), RNA (<1%), some ions, and water (Jamal et al. 2018). These components may be species-specific, such as in the case of polysaccharides and proteins. Others may be common for a large subset of bacteria, such as teichoic acids for gram-positive bacteria (Otto 2014a). The biofilm matrix provides architectural stability by “gluing” bacteria to each other and the cellular agglomerates to surfaces (Flemming and Wingender 2010). Electrostatic interactions between oppositely charged matrix polymers are in a key role in maintaining the biofilm matrix cohesivity (Gupta et al. 2019).

In conjunction with shielding bacteria living in the biofilm, the biofilm matrix plays a number of roles. First, as it has already been earlier mentioned, it holds cells in close proximity enabling cellular communication and horizontal gene transfer. Furthermore, it scavenges nutrients and minerals, providing also a source of energy, carbon, nitrogen, and phosphorus elements for the biofilm community. It also retains water protecting biofilms from desiccation (Flemming and Wingender 2010). Additionally, it works as a barrier offering protection from

## 2. LITERATURE REVIEW

unfavorable environmental conditions (such as UV radiation), predation, chemicals/antimicrobials, and host clearance (Gupta et al. 2019; Flemming and Wingender 2010).

Indeed, one of the mechanisms behind the tolerance of biofilms to some antibiotics is the matrix-generated diffusion barrier that prevents certain antibiotics from reaching their cellular targets. This hindered penetration may occur if antibiotics bind to biofilm matrix components or the antibiotics are deactivated by matrix enzymes, such as beta-lactamases (Ciofu et al. 2017). For example, Singh et al. (2010) demonstrated the reduced penetration of some beta-lactams and glycopeptides through *S. aureus* and *S. epidermidis* biofilms, while the permeation of aminoglycosides and fluoroquinolones remained unaffected. Additionally, the biofilm matrix aids in evading the host immune system. For example, it provides a mechanical shield against neutrophilic phagocytosis (de Vor et al. 2020) as neutrophils can engulf only fragments up to their own cell size (~ 10 µm) (Herant et al. 2006). As biofilms are typically 4–200 µm in tissues and 5–1200 µm on medical devices (Bjarnsholt et al. 2013a), biofilms should be disintegrated into smaller units. For that purpose, phagocytic lysosomes contain e.g. proteases and DNases, but it is not fully understood how these can work extracellularly in disintegrating complete biofilms (de Vor et al. 2020). The biofilm matrix also shelters bacterial surface-expressed PAMPs (pathogen-associated molecular patterns) by incorporating fibrin into the biofilm matrix with aid of coagulase (de Vor et al. 2020; Zapotoczna et al. 2015). The PAMPs of *S. aureus* are e.g. peptidoglycan, lipoproteins, and LTA (Askarian et al. 2018). Because the biofilm matrix protects PAMPs from innate immune cell receptors (e.g. Toll-like receptors), the proper activation of the innate immune system is hampered (e.g. cytokines that recruit more defensive cells are not released) (de Vor et al. 2020; Tortora et al. 2014, p. 470).

### 2.4.1 The biofilm matrix-accompanying polysaccharides

The key staphylococcal biofilm matrix polysaccharide is PIA/PNAG. It is responsible for cell-cell adhesion in the initial attachment phase of biofilm development (Nguyen et al. 2020; Cramton et al. 1999). It has been observed that the synthesis of the PIA/PNAG by *S. aureus* progresses promptly during the first 24 hours of biofilm formation (Oja et al. 2014). Its biosynthesis and secretion are mediated by gene locus *icaADBC* (Cramton et al. 1999). It is synthesized inside the cell by enzymes (N-acetyl-glucosamine transferases: *icaA* and *icaD*) and exported by a putative PIA exporter (*icaC*) (Haghi Ghahremanloi Olia et al. 2020). After secretion, ~15–20% of N-acetyl groups are deacetylated by a PIA deacetylase (*icaB*), which generates a cationic charge (Nguyen et al. 2020). Due to its cationic character, it possibly has an important role in promoting the biofilm matrix cohesivity by interacting with negatively charged cell surfaces and matrix components, such as anionic extracellular DNA (eDNA) and proteins (Otto 2018; Speziale et al. 2014). The expression of *ica*-locus is induced by harsh environmental conditions (such as low oxygen levels, high NaCl concentration,



extreme osmolarity, or temperature (Gupta et al. 2019) and also by sub-inhibitory concentrations of certain antibiotics (Skogman et al. 2012), contributing to increased resistance against antimicrobials and phagocytosis (Vuong et al. 2004). It has been observed that *S. aureus* and *S. epidermidis* can form biofilms without *ica*-locus (Rohde et al. 2007; Fitzpatrick et al. 2005). However, in the case of *S. epidermidis*, it seems that the absence of *ica* decreases the robustness of biofilms indicating that *S. epidermidis* relies on PIA/PNAG for biofilm formation (Rohde et al. 2007). In contrast, inactivation of the *icaADBC* operon of *S. aureus* does not affect biofilm formation. In fact, it was observed that *S. aureus* can maintain the biofilm cohesivity without the presence of PIA/PNAG by replacing it with various surface proteins, such as the biofilm-associated protein (Bap) (Merino et al. 2009).

The PIA/PNAG also plays several roles in the immunoevasion of *S. aureus* biofilms. First, phagocytic lysosomes do not include PIA/PNAG-degrading enzymes, which might explain why PIA/PNAG-dependent *S. epidermidis* biofilms seem to be more tolerant to phagocytosis than *S. aureus* (Günther et al. 2009a; 2009b), which can rely more on proteins for matrix formation (de Vor et al. 2020). The PIA/PNAG also seems to protect *S. epidermidis* biofilms against neutrophilic phagocytosis (Vuong et al. 2004) e.g. via preventing deposition of C3b and immunoglobulin G (IgG) opsonins on the biofilm (Kristian et al. 2008). Moreover, PIA/PNAG also seems to capture antibodies by preventing them to reach the bacterial cell surface impeding opsonic killing of *S. epidermidis* (Cerca et al. 2006). The highly positively charged PIA/PNAG also repels cationic antimicrobial peptides (AMPs; such as human  $\beta$ -defensin 3 and LL-37) while sequestering negatively charged AMPs (such as dermcidin) (Vuong et al. 2004).

#### 2.4.2 The biofilm matrix-associated protein fraction

Adhesion to the ECM of the host tissue is a crucial step in the pathogenesis of *S. aureus*. For that purpose, *S. aureus* expresses various proteinaceous adherence factors. These can be covalently anchored to the bacterial cell wall (*i.e.* peptidoglycan), such as microbial surface components recognizing adhesive matrix molecules (MSCRAMMs) and near iron transporter (NEAT) motif family members. The MSCRAMMs form the most important staphylococcal protein family mediating attachment, and examples of MSCRAMMs utilized by *S. aureus* are clumping factors A and B (ClfA, ClfB), fibronectin-binding proteins A and B (FnBPA, FnBPB), bone sialoprotein-binding protein (Bbp), and serine-aspartate repeat-containing protein C, D, and E (SdrC, SdrD, and SdrE). To the NEAT family belong iron-regulated surface determinants (IsdA, IsdB, IsdC, and IsdH). Additionally, non-covalently cell wall-associated (anchorless) proteins exist, such as the secretable expanded repertoire adhesive molecules (SERAM). The SERAM proteins are secreted but after that, they re-bind to the bacterial cell surface via ionic and hydrophobic interactions. Fibrinogen-binding protein (FbnBP) is an example of such SERAMs. There are also other non-covalently bound adhesins that do not belong to SERAMs, such as a membrane-spanning

## 2. LITERATURE REVIEW

elastin-binding protein (EbpS). Certain proteins also seem to mediate the transition of planktonic *S. aureus* towards the biofilm lifestyle by promoting attachment and intercellular adhesion, such as the already mentioned biofilm-associated protein (Bap) (Geraci et al. 2017; Ko et al. 2013; Heilmann 2011).

Other pivotal tasks of the protein fraction in the biofilm matrix are to maintain biofilm matrix cohesivity, to enable redox activity, and to participate in enzymatic macromolecule degradation for nutritional acquisition (Flemming and Wingender 2010). Furthermore, *S. aureus* has been shown to produce an arsenal of proteins with various immunoevasive functions (de Vor et al. 2020). Some of these proteins bind antibodies and prevent complement fixation by the classical pathway and opsonophagocytosis (Atkins et al. 2008). Some others block neutrophil-chemoattractant interaction, thus preventing neutrophilic activation (de Vor et al. 2020). Furthermore, a variety of enzymes with different functions are included in the matrix with functions associated with immune system evasion. These participate e.g. in protection from reactive oxygen species (Karavolos et al. 2003), degradation of neutrophil extracellular traps (NETs) (Sultan et al. 2019), isolation of the pathogens from the immune responses (Thomer et al. 2013; Vanassche et al. 2013; Cheng et al. 2010), and tissue degradation for spreading the infection to other locations (Tortora et al. 2014, pp. 450–451). Lastly, *S. aureus* produces an arsenal of host-harming cytolytic toxins, such as hemolysins (e.g.  $\alpha$ -,  $\beta$ -, and  $\delta$ -hemolysins) and leukocidins (in human-associated strains: LukAB (*i.e.* LukGH), LukSF (*i.e.* Panton-Valentine leukocidin), LukED, and  $\gamma$ -hemolysins (HlgAB and HlgCB) (de Vor et al. 2020; de Jong et al. 2019; Cheung et al. 2015; Otto 2014b).

Traditionally, every bacterial protein has been considered to have only a single function. However, an emerging number of bacterial proteins have been recognized as multifunctional. These “moonlighting proteins” refer to proteins with pleiotropic functions, which are not caused by gene fusions, RNA splice variants, or multiple protein fragments (Kainulainen and Korhonen 2014). In fact, the proteinaceous fraction of the *S. aureus* biofilm matrix has been observed to be largely composed of these moonlighting proteins (Foulston et al. 2014). The canonical functions of such currently known moonlighting proteins include essential cellular processes, such as protein synthesis, glycolysis, chaperone activity, and nucleic acid stabilization. Their moonlighting activities contribute e.g. in establishing the infection in the host for instance via bacterial attachment to host tissues, immunomodulatory and biofilm formation stimulating properties (Kainulainen and Korhonen 2014).

In order to “moonlight”, typical cytoplasmic proteins are excreted into the culture supernatant. It has been subjected to debate how moonlighting proteins translocate to the extracellular space. It has been generally considered that the release of these cytoplasmic proteins into the extracellular milieu is simply caused by cell lysis (Kainulainen and Korhonen 2014). However, this explanation appears to be too straightforward since numerous lines of evidence suggest the existence of a yet undiscovered mechanism regulating active cytoplasmic protein excretion. For example, it has been noted that the excretion is augmented when

the autolysins are upregulated, and peptidoglycan cross-linking is weakened (Ebner et al. 2016). Further, the secretion of proteins has been observed to be deterministic. For example, certain sequence motifs such as  $\alpha$ -helices, have been observed to contribute to this to some extent (Yang et al. 2014). However, it is known that moonlighting proteins are “unconventionally/non-classically secreted proteins”, as their sequences do not contain known secretion or cell surface-anchoring sequence motifs (Jeffery 2018; Kainulainen and Korhonen 2014). Indeed, none of the classical secretion machinery types seems to be involved, such as ESAT-6 secretion system, TAT (twin-arginine transport) system, or ATP-binding cassette transporters, all of which are generally utilized by *S. aureus*. One potential excretion mechanism of cytoplasmic proteins has been suggested to involve membrane vesicles (Pasztor et al. 2010). Indeed, several matrix-associated moonlighting proteins have been earlier recognized from membrane vesicles of *S. aureus* 06ST1048 (Gurung et al. 2011) and *S. aureus* ATCC14458 (Lee et al. 2009), which are also employed in transportation of e.g. hemolysins, leukocidins, response regulatory proteins, and antibiotic resistance enzymes (Jeon et al. 2016; Lee et al. 2013; Gurung et al. 2011; Lee et al. 2009).

In any case, it has been observed that cytoplasmic proteins are excreted from the cells and aggregated to the interstitial space around cells to be assembled to form the biofilm matrix (Foulston et al. 2014). This appears to occur during the stationary phase as a response to a decrease in medium pH, which in turn takes place due to the accumulation of fermentation products. Indeed, preferably than exploiting devoted matrix proteins to form the biofilm matrix, *S. aureus* seems to recycle cytoplasmic proteins as moonlighting constituents in the biofilm matrix. This strategy has been suggested to offer enhanced adaptability for biofilms when grown in stressful conditions. Selected moonlighting proteins with their primary and moonlighting functions are further discussed in this thesis.

### 2.4.3 The biofilm matrix-related extracellular DNA

The last major biofilm matrix component, eDNA, has been reported to originate from lysed neutrophils (Alhede et al. 2020). Due to its highly polymeric (sticky) nature and anionic charge, it interacts with many other surface matrix components, such as cationic exopolysaccharides and proteins, contributing to matrix network cohesivity and increasing the overall structural stability of biofilms (Otto 2018).

## 2.5 Biofilm infections

The nature of biofilm infections differs considerably from acute infections that are caused by planktonic bacteria. Acute infections can be effectively diagnosed and treated with antibiotics. On the other hand, several biofilm infections may be challenging to diagnose. Moreover, the efficacy of antibiotics is unsatisfactory: frequently the clinical signs of infection remain despite the correct completion of the antibiotic course (Høiby et al. 2015; Bjarnsholt et al. 2013b; Costerton et al.

## 2. LITERATURE REVIEW

1999). In a nutshell, the clinical relevance of biofilm infections can be related to the following features (**Table 1**).

**Table 1.** The clinical importance of biofilms in a nutshell (Mandakhalikar 2019; Li et al. 2018; Høiby et al. 2015; Bjarnsholt et al. 2013b; Savage et al. 2013; Costerton et al. 1999).

I.	Biofilms are involved in a large number of chronic infections
II.	Diagnosing biofilms is challenging
III.	Biofilms are often impossible to eradicate completely, leading to the recurrence of infections → in this manner, they can remain a lifelong problem
IV.	Biofilms often cause multiple surgical operations, when involved in medical device-associated infections ( <i>i.e.</i> removal and replacement of the infected medical device)
V.	Biofilms may lead to severe systemic infections (especially in immunocompromised individuals)
VI.	Biofilms are often responsible for long hospital stays
VII.	Biofilms are associated with high morbidity and mortality
VIII.	Biofilms cause a heavy burden on healthcare
IX.	Biofilms incur a massive financial cost to society
X.	Biofilms aid in the rapid spread of multidrug-resistant bacteria: the transfer of genetic material between bacteria occurs more frequently in biofilms

The presence of biofilms is connected to several chronic infections. Selected biofilm infections and their causative pathogens are presented in **Table 2**.

**Table 2.** Selected biofilm infections and their common causative pathogens. References in this table are listed below.

Biofilm infections	Causative pathogens
<b>Host tissue-associated infections</b>	
Chronic otitis media	<i>Haemophilus influenzae</i> , <i>Streptococcus pneumoniae</i> , <i>Moraxella catarrhalis</i> <sup>1</sup>
Chronic rhinosinusitis	<i>Staphylococcus aureus</i> , <i>Pseudomonas aeruginosa</i> , coagulase-negative staphylococci, <i>S. pneumoniae</i> , <i>M. catarrhalis</i> , <i>H. influenzae</i> <sup>2</sup>
Chronic wounds	<i>S. aureus</i> , <i>P. aeruginosa</i> , <i>Enterococcus faecalis</i> , coagulase-negative staphylococci, <i>Proteus</i> spp., anaerobic bacteria <sup>3</sup> (often polymicrobial)
Recurrent urinary tract infection	<i>Escherichia coli</i> , <i>E. faecalis</i> , <i>Klebsiella</i> spp., <i>Proteus</i> spp., <i>Staphylococcus saprophyticus</i> <sup>4</sup>
Cystic fibrosis	<i>P. aeruginosa</i> , <i>Burkholderia cepacia</i> , <i>S. aureus</i> , <i>H. influenzae</i> <sup>5</sup>
Endocarditis	<i>S. aureus</i> , coagulase-negative staphylococci, viridans group streptococci, <i>Enterococcus</i> spp. <sup>6</sup>
Periodontitis	<i>Aggregatibacter actinomycetemcomitans</i> , <i>Porphyromonas gingivalis</i> , <i>Tannerella forsythia</i> , <i>Treponema denticola</i> , <i>Fusobacterium nucleatum</i> , <i>Micromonas micros</i> , <i>Prevotella intermedia</i> , <i>Campylobacter rectus</i> , <i>Eikenella corrodens</i> <sup>7</sup>
Dental caries	Mutans streptococci (main species: <i>Streptococcus mutans</i> , <i>Streptococcus sobrinus</i> ), lactobacilli <sup>8</sup>
Osteomyelitis	<i>S. aureus</i> , <i>S. epidermidis</i> , <i>P. aeruginosa</i> , <i>Enterococcus</i> spp., <i>Streptococcus</i> spp., <i>Enterobacter</i> spp., <i>Mycobacterium</i> spp., <i>Candida</i> spp., anaerobes <sup>9,10</sup>
<b>Medical device-related infections</b>	
Prosthetic joint	<i>S. aureus</i> , <i>E. coli</i> , <i>Enterobacter</i> spp., <i>Klebsiella</i> spp., <i>P. aeruginosa</i> , coagulase-negative staphylococci (e.g. <i>S. epidermidis</i> ), <i>Cutibacterium</i> spp., <i>Propionibacterium</i> <sup>11,12,13</sup>
Cardiac pacemaker	Coagulase-negative staphylococci, <i>S. aureus</i> , enteric gram-negative bacilli <sup>14</sup>
Mammary implant	Coagulase-negative staphylococci, <i>S. aureus</i> , <i>P. aeruginosa</i> <sup>15</sup>
Dental implant	<i>P. gingivalis</i> , <i>P. intermedia</i> , anaerobic gram-negative cocci such as <i>Veillonella</i> spp. and <i>T. denticola</i> <sup>16</sup>
Intravenous catheter	Coagulase-negative staphylococci, <i>S. aureus</i> , <i>Klebsiella pneumoniae</i> , <i>E. coli</i> , <i>P. aeruginosa</i> , <i>Acinetobacter baumannii</i> , <i>Candida</i> spp. <sup>17</sup>
Urinary catheter	<i>E. coli</i> , <i>K. pneumoniae</i> , <i>P. aeruginosa</i> , <i>S. aureus</i> , <i>Proteus mirabilis</i> , <i>S. epidermidis</i> <sup>18</sup>
Contact lenses	Coagulase-negative staphylococci, corynebacteria, bacilli, <i>S. pneumoniae</i> , <i>P. aeruginosa</i> , <i>Serratia marcescens</i> , <i>Candida albicans</i> , <i>Fusarium</i> ssp. <sup>19</sup>

<sup>1</sup> Hall-Stoodley et al. 2006; <sup>2</sup> Leid et al. 2011; <sup>3</sup> Gjødsbøl et al. 2006; <sup>4</sup> Delcaru et al. 2016; <sup>5</sup> Rajan and Saiman 2002; <sup>6</sup> Que and Moreillon 2011; <sup>7</sup> Demmer et al. 2008; <sup>8</sup> Hoceini et al. 2016; <sup>9</sup> O'May et al. 2011; <sup>10</sup> Kavanagh et al. 2018; <sup>11</sup> Izakovicova et al. 2019; <sup>12</sup> Zimmerli et al. 2004; <sup>13</sup> Li et al. 2018; <sup>14</sup> Chua et al. 2000; <sup>15</sup> Cohen et al. 2015; <sup>16</sup> Pye et al. 2009; <sup>17</sup> Parameswaran et al. 2011; <sup>18</sup> Cortese et al. 2018; <sup>19</sup> Otto 2014a.

### 2.5.1 Prosthetic joint infection

Many vital body functions can be improved, or pain alleviated with transiently or permanently implanted medical devices (Zimmerli and Trampuz 2011). Transiently inserted devices comprise e.g. endotracheal tubes, central venous and urinary catheters (Mandakhalikar 2019). Permanently inserted devices can be classified based on their insertion location: they are either

## 2. LITERATURE REVIEW

intravascular or extravascular devices. Intravascular devices are e.g. artificial heart valves, vascular prostheses, and electrophysiologic devices. Extravascular devices are e.g. aesthetic implants, neurosurgical devices, dental implants, intrauterine devices, and orthopedic implants, such as internal fixation devices and prosthetic joints (PJs) (Zimmerli and Trampuz 2011).

The PJs can be utilized to alleviate pain and movement restrictions caused by joint destruction. Joint destruction can be caused by e.g. osteoarthritis, rheumatoid arthritis, or a physical injury. In developed countries, the utilization of PJs has significantly increased during the last decades (Singh et al. 2019). Increasing life span, constantly aging populations, more active elder populations, increasing osteoarthritis incidence associated with obesity, evolving medical sciences, and more comprehensive health insurances have contributed to this (Izakovicova et al. 2019; Singh et al. 2019; Zimmerli and Trampuz 2011). In 2019, for instance in Finland, ca. 10,500 hip and 13,500 knee primary replacement surgeries were performed. Additionally, in 20 years (1999–2019) the performed hip and knee primary replacement surgeries were reported to increase in Finland, by a factor of two and three, respectively (National Institute for Health and Welfare: Finnish Arthroplasty Register 2020). As a result, this evolving trend has contributed to an increasing number of prosthetic joint infections (PJIs) (Izakovicova et al. 2019).

The PJIs are one of the most common and feared complications of joint replacement surgeries (Davidson et al. 2019) affecting 1–2% of primary and 4% of revision arthroplasty patients (Izakovicova et al. 2019). It has been estimated that up to 1.7% of hip, 2% of knee, and 9% of ankle prostheses (Zimmerli 2014) as well as 5–10% of internal fixation devices become infected (Zimmerli and Trampuz 2011). Predisposing factors for these infections are young age (<60 years), male gender, high body mass index ( $\geq 30$  kg/m<sup>2</sup>), and smoking. Furthermore, the presence of certain medical conditions, such as diabetes, dementia, renal disease, hemodialysis, and immunomodulatory or steroid-based therapy are associated with higher infection risk (Stewart and Bjarnsholt 2020; Lenguerrand et al. 2018). Moreover, near-surface body inserts that are poorly covered by soft tissue are more prone to get infected (Nymer et al. 2008).

The PJIs are caused by prosthetic joint material-colonizing biofilms. The most common causative pathogens of PJIs are biofilm-forming *Staphylococcus aureus* and *Staphylococcus epidermidis* (Davidson et al. 2019; Arciola et al. 2018). The geographical location influences this trend: while *S. epidermidis* causes most cases in Europe, *S. aureus* is responsible for most PJIs in the United States (Aggarwal et al. 2014).

The insertion of a PJ causes a locally acquired immune defect by damaging the tissues, leading to a decreased blood supply, forming necrotic tissue, and frustrated phagocytosis (*i.e.* the impaired activity of phagocytic cells). In frustrated phagocytosis, phagocytes undergo apoptosis when facing an object of a size that is outside their phagocytic capability. The consequential release of reactive oxygen species (ROS), enzymes, and defensins causes unintentional injury to host tissue/vasculature as well as de-activation of other neutrophils

(Izakovicova et al. 2019 (Winkler 2012; Nymer et al. 2008). All of these factors can promote biofilm formation, and the existence of a medical device has been observed to decrease the minimal infecting dose of *S. aureus* by more than 100,000-fold (Izakovicova et al. 2019). Moreover, some substrate materials such as polymethyl methacrylate (PMMA) hamper the complement system and leukocytic activity, which also promotes biofilm formation. Finally, phagocytes typically focus on breaking down the medical device itself, hence having a lower impact on the actual biofilm (Nymer et al. 2008).

The PJIs are very difficult to treat solely with antibiotics: the diminished local tissue perfusion and the damaged vasculature prevent that satisfactory antibiotic concentrations are reached at the biofilm infection site (Gergely et al. 2014). Because of this, removal of the infected device, debridement of the necrotic tissue, and insertion of a new device are often needed (Izakovicova et al. 2019). Overall, PJIs are frequently associated with poor clinical outcomes, high costs, and prolonged hospitalization periods (Davidson et al. 2019). Long hospitalization periods in turn increase the risk for re-infections (Rosman et al. 2015). For instance, it has been estimated the average price in the UK for treating a knee or hip PJI is £100,000 (per patient), including the revision surgery, a new prosthesis, extended hospitalization period, and antibiotics (Davidson et al. 2019). Classification of PJIs and their preferred treatment protocols are presented in **Table 3** (Izakovicova et al. 2019; Li et al. 2018; Zimmerli et al. 2004).

**Table 3.** The most recent classification of PJIs and suggested treatment protocols. Adapted from (Izakovicova et al. 2019; Li et al. 2018; Zimmerli et al. 2004).

	Acute PJI	Chronic PJI
Perioperative origin	Early postoperative <4 weeks after surgery <sup>a</sup>	Delayed postoperative ≥4 weeks after surgery
Typical causative pathogens in perioperative PJI	High virulence organisms: <i>S. aureus</i> , <i>E. coli</i> , <i>Enterobacter</i> spp., <i>Klebsiella</i> spp., <i>P. aeruginosa</i>	Low virulence organism: coagulase-negative staphylococci (e.g. <i>S. epidermidis</i> ), <i>Cutibacterium</i> spp., <i>Propionibacterium</i> spp.
Hematogenous origin	<3 weeks duration of symptoms	≥3 weeks duration of symptoms
Examples of typical causative pathogens in hematogenous PJI	<i>S. aureus</i> (from skin/soft tissue infection), <i>S. pneumonia</i> (from respiratory tract infection), <i>Bacteroides</i> spp., <i>Salmonella</i> spp., and <i>Streptococcus gallolyticus</i> (from gastrointestinal infection), <i>E. coli</i> , <i>Klebsiella</i> spp., and <i>Enterobacter</i> spp. (from urinary tract infection), viridans group streptococci (from dental procedures)	
Symptoms	Fever, acute pain, red and swollen joint, prolonged postoperative discharge (>7–10 days)	Chronic pain, sinus tract (fistula), loosening of the prosthesis
General treatment protocol	Debridement, antibiotics, and implant retention (DAIR) and change of the mobile parts	Prosthesis removal, debridement, antibiotics, and <sup>b</sup> one- or <sup>c</sup> two-stage exchange of the new device
Systemic antibiotic therapy	E.g. in staphylococcal infections: cefazoline <i>iv.</i> and rifampicin <i>p.o.</i> (oxacillin-/methicillin susceptible) / vancomycin <i>iv.</i> and rifampicin <i>p.o.</i> (oxacillin-/methicillin-resistant) for 2 weeks, then rifampicin + levofloxacin/doxycycline/cotrimoxazole <i>p.o.</i> (total antibiotic therapy duration: 12 weeks)	

<sup>a</sup> According to a new recommendation (Löwik et al. 2020), the DAIR can also be considered with cases that occur later than the indicated time, on condition that it is performed within 1 week after the onset of symptoms. <sup>b</sup> Can be performed when the soft tissues are intact or slightly damaged. <sup>c</sup> Recommended when moderately and severely damaged soft tissues, abscess formation, sinus tract, or difficult-to-treat micro-organisms (such as methicillin-resistant *S. aureus*, other multidrug resistant organisms, *Enterococcus* spp., fungi) are present. *iv.* = intravenous; *p.o.* = per oral.

### 2.5.2 Periodontitis

Periodontitis is a very common oral condition affecting 20–50% of the global population (Nazir 2017). In Finland, gingival and dental connective tissue diseases are a significant public health problem among the  $\geq 30$ -year-old population. Among that population, the prevalence of gingivitis is 74%, periodontitis with recessed ( $\geq 4$  mm) dental pockets is 64% and with deep ( $\geq 6$  mm) dental pockets is 21%. The prevalence of rapidly progressing periodontitis (previously localized aggressive/juvenile periodontitis) located on the cheek or anterior teeth in Finland is ca. 0.1% (Current Care Guidelines: Periodontitis 2019). Periodontitis is initiated by dental biofilms *i.e.* plaque (Kwon et al. 2020), and if not removed, causes gingivitis that may progress further on periodontitis (Current Care Guidelines: Periodontitis 2019).

The dental plaque is generally composed of multi-species bacterial biofilms (Peterson et al. 2011b). Oral biofilm formation includes several steps that are summarized in **Figure 3**. In periodontitis, the host immune system responds to the dental biofilms (e.g. bacterial lipopolysaccharides or virulence factors) by producing proinflammatory cytokines, such as tumor necrosis factor- $\alpha$ , interleukin-1 $\beta$ , and prostaglandin E2. As a response to these cytokines and virulence factors, matrix metalloproteinases are produced, that mediate the destruction of collagen fibers in periodontal attachment tissues (**Figure 3**). In addition, these cytokines induce osteoclast precursors, that mediate alveolar bone damage, and all of these contribute to tooth loss (Kwon et al. 2020).

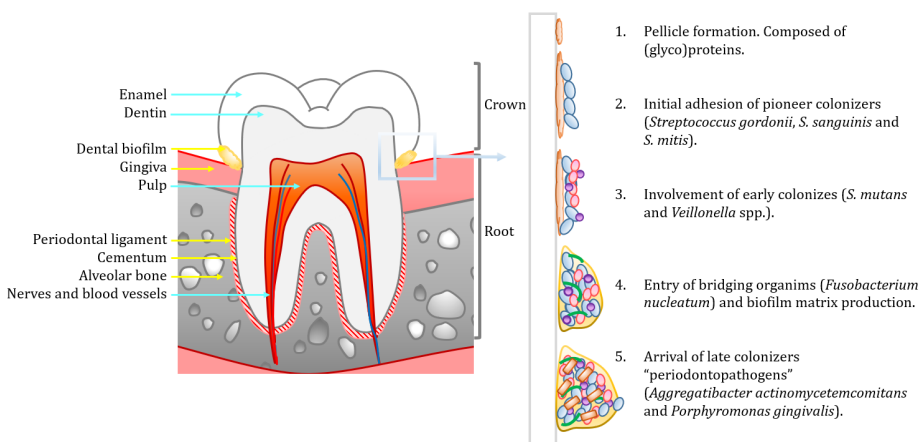


**Figure 3.** The structures of the tooth and periodontium are shown on the left. Periodontitis-associated structures are indicated with yellow arrows. Oral biofilm formation steps are displayed on the right (Peterson et al. 2011b; Sánchez et al. 2011; Darveau et al. 1997). The figure has been inspired by Clais (2014).

Typical symptoms of periodontitis are redness, swelling, and bleeding of the gingiva, mobile or migrated teeth, formed dental gaps, and discharge (Current Care Guidelines: Periodontitis 2019). Periodontitis has been observed to



predispose to several systemic diseases: cancer (oral, pancreatic, head, neck, and lung) (Michaud et al. 2017), stroke (Lafon et al. 2014), coronary artery disease (Bahekar et al. 2007), respiratory infections (e.g. pneumonia, Gomes-Filho et al. 2014), Alzheimer's disease (Kamer et al. 2009), type 2 diabetes (Demmer et al. 2015), and preterm birth (Lin et al. 2007). Moreover, periodontitis affects negatively to the glycemic control of diabetic patients (Stanko and Izakovicova Holla 2014).

Good daily oral hygiene including powered toothbrush (Yaacob et al. 2014) and interdental brushes is a cornerstone in the prevention of periodontitis (Slot et al. 2008). Once diagnosed, the treatment includes quitting smoking, mechanical debridement (scaling and root planning), gingival surgery, and possible topical chlorhexidine or systemic antibiotic therapy (typically metronidazole +/- amoxicillin) (Current Care Guidelines: Periodontitis 2019).

### 2.6 Biofilm treatment strategies

Until recent decades, clinical microbiology research focused primarily on diagnosing and finding solutions to acute infections. Thereby characterizing the physiology of planktonic bacteria has been the main task. As a result, all drug discovery effects resulting in currently available antibiotics have been developed to treat infections caused by planktonic bacteria. However, data collected from planktonic bacteria, including the discovery of new antibiotics, cannot be extrapolated into biofilms (Parsek and Fuqua 2004).

As mentioned earlier, planktonic bacteria-associated infections can potentially be resolved with the right antibiotic within a few days. However, this is not the case with biofilms (Bjarnsholt et al. 2013b). In fact, the use of conventional antibiotics against biofilms frequently eliminates the symptoms caused by the released planktonic bacteria. However, they are not capable of eradicating the existing biofilm, which causes recurrence of the symptoms after completing the antibiotic course (Costerton et al. 1999). For example, according to a case report, a cystic fibrotic patient with a *P. aeruginosa* biofilm infection received 1 kg tobramycin, 1 kg colistin, and 10 kg of beta-lactam antibiotic during a 20 year-long treatment period. Still, it was not possible to reach a complete eradication of the biofilm (Bjarnsholt et al. 2009). Toxicity is often the main limitation when applying high antibiotic concentrations to treat biofilms (Winkler 2012). On the other hand, applying sub-inhibitory concentrations of antibiotics on biofilms may even promote biofilm formation (Bjarnsholt et al. 2013b).

Indeed, to this day, despite extensive research endeavors, established anti-biofilm therapies exist for a very narrow range of clinical conditions, and even for these approaches, deficiencies exist. For example, there are strategies that aim in biofilm formation prevention by killing planktonic bacteria before aggregation, when they are still in an antibiotic susceptible state (Bjarnsholt et al. 2013b). This is performed via coating catheters with antimicrobials (Mandakhalikar et al. 2016). For that purpose, there are available central venous

## 2. LITERATURE REVIEW

catheters coated with chlorhexidine-silver sulfadiazine (Arrowg+ard®, Teleflex, Gurnee, US), minocycline-rifampicin (Cook Spectrum®, Cook Medical LLC, Bloomington, US), and miconazole-rifampicin (Premistar™, Vygon, Ecouen, France). Also, urinary catheters coated with silver alloy-hydrogel (Bardex® I.C., Bard Medical, Sussex, UK) and nitrofurazone (ReleaseNF, Rochester Medical, Stewartville, US) are available. However, a drawback of the coating-based approach is the quick release of the antimicrobial agents, which provides only short-term prevention. Furthermore, the deposition of the conditioning film on the device occurs rapidly, which neutralizes the effect of the coating (Mandakhalikar 2019). Therefore, antimicrobial coatings do not totally prevent biofilm formation on medical devices, but they decelerate it (Otto 2018). Moreover, there is a great risk for the emergence of antibiotic resistance when antibiotic coatings are used (Mandakhalikar et al. 2016).

Another applied strategy is to disrupt the existing biofilms to liberate planktonic bacteria and eradicate these released single bacteria with systemic antibiotics. These approaches include mechanical or surgical removal, but these can be performed only on surfaces that are easily accessible. Treating chronic wounds with ultrasound is currently in clinical trials (ClinicalTrials.gov ID: NCT03516422). Another option is to disrupt biofilm enzymatically: dornase alfa is an inhaled recombinant human DNase (Pulmozyme®) that degrades the eDNA in the biofilm matrix and is used in the treatment of cystic fibrosis to decrease the viscosity of the sputum (Terveysportti: Lääkkeet ja hinnat -database 2021; Kaplan 2009). It is used in conjunction with e.g. acetylcysteine, colistin, tobramycin, levofloxacin (as inhalation), and ciprofloxacin (*p.o.*) (Terveysportti: Lääkkeet ja hinnat -database 2021). Still, these kinds of combination strategies only postpone but are not capable of eradicating the biofilms in cystic fibrosis (Bjarnsholt et al. 2009). There is also another enzyme DispersinB® (Kane Biotech Inc., Winnipeg, Canada) that hydrolyzes biofilm matrix-associated PIA/PNAG (Kaplan 2009), and this enzyme is under development/commercialization process against chronic wounds. Additionally, small cell clusters and planktonic cells can be dispersed from biofilms with different chemical agents. An example of this, nitric oxide, is presently in phase 2 of clinical trials in the treatment of chronic rhinosinusitis (ClinicalTrials.gov ID: NCT04163978).

Indeed, the eradication of biofilms is a significant but unmet clinical need in several biofilm-associated diseases (Baker et al. 2014; Bjarnsholt et al. 2013b). There are several reasons why the discovery efforts of anti-biofilm compounds have been so scarce. First, the presence of biofilms was neglected by the medical community for decades (Bjarnsholt 2013). Moreover, the lack of internationally harmonized and accepted anti-biofilm screening methods and metrics (similar to methods for antibiotic susceptibility testing provided by e.g. EUCAST “European Committee on Antimicrobial Susceptibility Testing”) has in turn negatively affected the development of anti-biofilm compounds. Additionally, biofilm-associated infections are considered extremely problematic to tackle. Therefore, insufficient financial incentives offered to pharmaceutical developers remain

very limited considering how demanding, risky, and expensive the antimicrobial development process is. This is associated with the fact that diseases, where medications are taken daily for extended periods (such as high blood pressure or diabetes), are more economically attractive targets for the pharmaceutical industry than antibiotic courses that are used for a limited period. Therefore, bacterial biofilms have unfortunately not been a priority disease area of the pharmaceutical industry (Baker et al. 2014; Otto 2014a; Tortora et al. 2014, p. 531).

### 2.7 Relevant biofilm-forming bacteria

In this thesis, three biofilm-forming bacteria were studied: *Staphylococcus aureus* (I, II), *Staphylococcus epidermidis* (II), and *Aggregatibacter actinomycetemcomitans* (III). Their clinical relevance is described briefly in this chapter.

#### 2.7.1 *Staphylococcus aureus* and *Staphylococcus epidermidis*

*S. aureus* and *S. epidermidis* are major opportunistic pathogens causing a wide arsenal of biofilm-associated infections, such as chronic rhinosinusitis (Leid et al. 2011), chronic wounds (Gjødsbøl et al. 2006), endocarditis (Que and Moreillon 2011), and osteomyelitis (Kavanagh et al. 2018; O'May et al. 2011). Furthermore, these pathogens are key pathogens in indwelling medical device-associated infections (Zimmerli and Trampuz 2011), such as those related to PJs (Davidson et al. 2019; Arciola et al. 2018), cardiac pacemakers (Chua et al. 2000), mammary implants (Cohen et al. 2015), and intravenous catheters (Parameswaran et al. 2011). This is attributed to the staphylococcal presence in the normal microbiota: *S. epidermidis* is a very ubiquitous bacterium of the human normal microbiota on the skin and mucous membranes of all individuals, while *S. aureus* colonizes the normal microbiota of ca. 20% and 30% of the adult population permanently and transiently, respectively (Otto 2018; Otto 2010). Therefore, both species are the most likely pathogens to be introduced as contaminants during indwelling medical device insertion operations, either from healthcare personnel or the patient (Otto 2014a).

The incidence of antibiotic resistance of both strains has also increased tremendously worldwide during the last decades, such as MRSA and MRSE (methicillin-resistant *S. aureus* and *S. epidermidis*) (European Centre for Disease Prevention and Control 2015; Namvar et al. 2014), to which the biofilm lifestyle contributes (Savage et al. 2013). For example, it is estimated in Europe that 75–90% of nosocomial-associated *S. epidermidis* infections are currently caused by MRSE (Namvar et al. 2014). In Southern and Northern Europe, the predominance of MRSA in *S. aureus* infections is 10–50% and 0–5%, respectively (European Centre for Disease Prevention and Control 2015).

### 2.7.2 *Aggregatibacter actinomycetemcomitans*

*Aggregatibacter actinomycetemcomitans* (previously *Actinobacillus actinomycetemcomitans*) is a periodontal pathogen causing the following biofilm-associated diseases: rapidly progressing periodontitis (*i.e.* localized aggressive/juvenile periodontitis), endocarditis, bacterial arthritis, osteomyelitis, and cerebral/brain abscess (Herbert et al. 2016; Rahamat-Langendoen et al. 2011). Its presence in the human host is also a risk factor for certain systemic diseases, such as coronary artery disease (Liljestrand et al. 2018), type 2 diabetes (Demmer et al. 2015), Alzheimer's disease (Díaz-Zúñiga et al. 2019), and rheumatoid arthritis (Konig et al. 2016).








## 2.8 Biofilm investigation methods

As previously indicated, most of the existing antimicrobial compounds have been developed to eradicate planktonic bacteria. Therefore, the existing methods utilized in antimicrobial research have also been established to assay planktonic bacteria (Mandakhalikar 2019). Hence, standardized and reliable *in vitro* models for studying biofilms are required. These methods should take the unique features of biofilms into consideration and at the same time be rapid, simple, reasonable cost-efficient, and automation-friendly (Skogman 2012).

### 2.8.1 Assays performed in liquid cultures

Existing *in vitro* biofilm assays can be divided into liquid or solid cultures. The research question and the infection type that are under interest determine the choice of the method (Lebeaux et al. 2013). Selected biofilm assay types are summarized in **Table 4**. Four of the presented methods are standardized by ASTM International (American Society for Testing and Materials), which is a globally recognized leader in developing and delivering standardized methods (ASTM International 2020). All of these ASTM-approved methods have been standardized for *P. aeruginosa*.

**Table 4.** Selected *in vitro* biofilm models (Oja et al. 2014; Lebeaux et al. 2013; Peterson et al. 2011a; Coenye and Nelis 2010; Charaf et al. 1999). Modified from Blomqvist (2014) and Hiltunen (2015). MBEC = minimum biofilm eradication concentration; HTS = high-throughput screening.

	Biofilm model	Culture	Fluid shear	Substratum	Advantages
<b>LIQUID CULTURES</b>	 <b>CDC Biofilm Reactor</b>	Continuous culture	High	Various	ASTM Standard Method (E2562)
	 <b>Rotating Disk Reactor</b>	Continuous culture	Medium	Various	ASTM Standard Method (E2196)
	 <b>Drip Flow Biofilm Reactor</b>	Continuous culture	Low	Various	ASTM Standard Method (E2647)
	 <b>MBEC Assay "Calgary device"</b>	Batch culture	Low	Plastic pegs (coating possible)	ASTM Standard Method (E2799)
	 <b>Well plate assays *</b>	Batch culture	Low	Plastic wells (coating possible)	HTS, fairly cheap
<b>SOLID CULTURES</b>	 <b>Static Biofilm method *</b>	Batch culture	No	Various	Inexpensive, versatile
	 <b>Colony Biofilm model</b>	Batch culture	No	Polycarbonate filter paper	Antibiotic penetration assays

\* The methods were used in the thesis.

The Drip Flow Biofilm Reactor, the Rotating Disk Reactor, and the CDC Biofilm Reactor are continuous cultures. Therein, consumed medium that includes waste, metabolic byproducts, and dead cells, are constantly replaced with fresh medium ensuring continuous nutrient availability (Lebeaux et al. 2013). Once formed, the biofilms can be challenged with different anti-biofilm compounds. The disadvantages of these models are their low throughput, the requirement for continuous medium flow, and therefore susceptibility to contamination and leakage (Peterson et al. 2011a).

On the other hand, the MBEC Assay and the commonly used well plates are batch cultures. Batch cultures have a fixed volume of medium without a constant supply of fresh medium. They allow higher throughput for simultaneous testing of many compounds, several concentrations, and even different bacterial strains. The MBEC method refers to a plate that has a lid with pegs and a receiver plate with wells containing the bacterial suspension. Once biofilms are formed on the pegs, the peg-containing lid is transferred to a new receiver plate which includes compounds for efficacy testing. The well plate format offers a cheap and user-friendly option that is frequently utilized in the field of biofilm research for rapid compound screening (Coenye and Nelis 2010). Typically, in biofilm assays, 96-

## 2. LITERATURE REVIEW

well plates made of polystyrene are utilized. Therein, the bacterial suspension is dispensed in the wells and the biofilms are formed on the bottom and the walls of the wells. In one variation of this, coupons made of various materials are inserted into a well plate with larger wells, e.g. on a 12-well plate (Park et al. 2014). With this kind of assembly, the formation of biofilms can be studied on more clinically relevant materials than on polystyrene. The coupon-based well plate assay format was used in study **I** of this thesis.

### 2.8.2 Assays performed in solid-state cultures

In solid-state methods, biofilms grow in a solid-air interface since the growth surfaces are not submerged into liquid (**Table 4**) (Oja et al. 2014). They are more labor-intensive and therefore less frequently used. They encompass the Colony Biofilm model and the Static Biofilm method (batch cultures). In the Colony Biofilm model, biofilms are grown on polycarbonate membrane filters and these filters are transferred regularly onto new agar (Peterson et al. 2011a). On the other hand, the Static Biofilm method consists of biofilms grown on a filter paper-covered agar plate. The biofilms of the Static Biofilm method are grown in the absence of fluid shear (Buckingham-Meyer et al. 2007), and therefore the method can be considered as proper for simulating certain infections (e.g. skin- or ear-associated). The Static Biofilm method represents a versatile, robust, simple, and cost-effective option, which can be performed without the need for sophisticated instrumentation (Oja et al. 2014). More importantly, it allows the possibility to test more complex drug formulations (e.g. semisolid pastes) than mere drug solutions. This essay type, the Static Biofilm method, was utilized in studies **II** and **III**.

## 2.9 Bisphosphonates

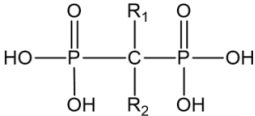
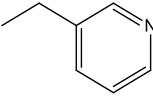
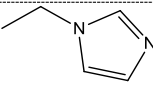
In this thesis (studies **II**, **III**) bisphosphonates and bioactive glass were used to form a test combination product under interest, and their properties are described in this and the following chapter (2.10).

### 2.9.1 Definition and pharmacological indications

Bisphosphonates (BPs) are analogs to endogenous blood serum pyrophosphates that regulate the mineralization of bones and chelate calcium (Kuźnik et al. 2020). Owing to the ability of BPs to inhibit the actions of osteoclasts, they are employed in various bone diseases that cause excessive bone resorption. These are e.g. osteoporosis, Paget's bone disease, hypercalcemia of malignancy as well as prevention of bone cancer-associated osteolytic metastases (Hillilä 2007). The BPs used in the experiments of this thesis are presented in **Table 5**. The mechanism of action depends on the structure of BPs: the non-nitrogen containing BPs (group 1 in **Table 5**) incorporate into ATP of the osteoclasts and lead to apoptosis, while nitrogen-containing BPs (groups 2 and 3) inhibit a farnesyl pyrophosphate synthase enzyme resulting in osteoclast

cytoskeleton disruption and apoptosis (Kuźnik et al. 2020). Osteoclast apoptosis slows the resorption of bone into the bloodstream (Hillilä 2007). This increases the total bone mass and the biomechanical strength of the bones. Furthermore, some BPs are used to prevent bone metastases: while they prevent the function of osteoclasts, the microenvironment of bones is more unfavorable for the growth of tumor cells (Terveysportti: Lääkkeet ja hinnat -database 2021).

**Table 5.** The bisphosphonates (BPs) used in the thesis (Terveysportti: Lääkkeet ja hinnat -database 2021; Hillilä 2007). \* Pharmacological potency factors compared to etidronate (Kuźnik et al. 2020).

The general structure of BPs				
				
Group	BP	R <sub>1</sub> side chain	R <sub>2</sub> side chain	Indication and dosing regimen
1. Non-nitrogen-containing structures	Etidronate (1x)*	—OH	—CH <sub>3</sub>	Not approved in Finland; 400 mg/day <i>p.o.</i> for 14 days every 3 months
	Clodronate (1–10x)*	—Cl	—Cl	Cancer-associated osteolytic bone metastases and hypercalcemia: 1600–3200 mg/day <i>p.o.</i>
2. Nitrogen-containing alkyl chains	Alendronate (100–1,000x)*	—OH	—(CH <sub>2</sub> ) <sub>3</sub> —NH <sub>2</sub>	Osteoporosis in men and postmenopausal women: 10 mg/day <i>p.o.</i> or 70 mg/week <i>p.o.</i>
3. Nitrogen-containing ring structures	Risedronate (1,000–10,000x)*	—OH		Osteoporosis in men and postmenopausal women: 35 mg/week <i>p.o.</i>
	Zoledronate (>10,000x)*	—OH		( <sup>1</sup> ) Paget's bone disease, osteoporosis in men and postmenopausal women, and osteoporosis associated with a long-term glucocorticoid treatment: 5 mg/year <i>iv.</i> ( <sup>2</sup> ) In cancer to prevent the bone incidence and to treat hypercalcemia: 4 mg every 3–4. week <i>iv.</i>

### 2.9.2 Bisphosphonates in periodontitis

Beyond their approved indications, BPs have also been observed to improve periodontal parameters (increased attachment tissue and/or alveolar bone levels) in several animal and human studies (**Table 6**). The tests have been performed against naturally occurring periodontitis (in humans and animals) and against experimentally induced periodontitis (in animals), which has been generated e.g. by a ligature around a tooth (Weinreb et al. 1994).

## 2. LITERATURE REVIEW

**Table 6.** Systemically and topically tested bisphosphonates (BPs) in periodontitis.

BP	Administration route	Species	References
<b>Alendronate</b>	Topical	Human	Pradeep et al. 2012; Sharma and Pradeep 2012a; Sharma and Pradeep 2012b; Veena and Prasad 2010; Reddy et al. 2005
	Systemic	Human	Jeffcoat et al. 2007; Rocha et al. 2004; El-Shinnawi and El-Tantawy 2003; Rocha et al. 2001
	Systemic	Beagle dogs	Reddy et al. 1995
	Systemic	Monkey	Weinreb et al. 1994; Brunsvold et al. 1992
	Topical	Rat	Binderman et al. 2000; Yaffe et al. 2000
	Systemic	Rat	Moreira et al. 2014; Menezes et al. 2005
<b>Clodronate</b>	Topical	Rat	Liu et al. 2004; Mitsuta et al. 2002
	Systemic	Rat	Alencar et al. 2002
<b>Etidronate</b>	Systemic	Human	Takaishi et al. 2003; Takaishi et al. 2001
<b>Risedronate</b>	Topical	Rat	Igarashi et al. 1996; Adachi et al. 1994
	Systemic	Rat	Shoji et al. 1995
	Systemic	Human	Palomo et al. 2005
<b>Zoledronate</b>	Topical	Rat	Yao et al. 2021

## 2.10 Bioactive glass

### 2.10.1 Definition

Bioactive glasses are an assembly of synthetic silica-based bioactive materials that are employed as bone graft substitutes (Välimäki and Aro 2006). The first bioactive glass, called 45S5 Bioglass®, was created by Larry Hench in the 1960s (Hench et al. 2010). Bioactive glass S53P4 (BAG), is a III class medical device from Bonalife® Biomaterials Ltd. (Turku, Finland) (**Figure 4**). It is composed of 53% silicon dioxide, 23% sodium oxide, 20% calcium oxide, and 4% phosphorus pentoxide (Coraça-Huber et al. 2014).

### 2.10.2 Bone regeneration

The BAG is indicated in the filling, reconstruction, and regeneration of bone defects with the following official indications: <sup>(1)</sup> bone cavity filling caused by trauma (e.g. Gergely et al. 2011), benign bone tumor (e.g. Syvänen et al. 2018), or spine fractures (e.g. Rantakokko et al. 2012); <sup>(2)</sup> bone cavity filling in chronic osteomyelitis (e.g. Malat et al. 2018); <sup>(3)</sup> mastoid cavity obliteration (e.g. de Veij Mestdagh et al. 2017). In general, BAG is regarded as a biocompatible, osteoconductive, osteopductive, and cost-effective material (Geurts et al. 2019; Gergely et al. 2014; Välimäki and Aro 2006).





**Figure 4.** BAG granules can be used to fill bone cavities (Bonalive® Biomaterials Ltd. 2021). Reprinted with permission from Bonalive Biomaterials Ltd.

When BAG gets in contact with an aqueous solution or a biological fluid, it releases ions ( $\text{Ca}^{2+}$ ,  $\text{Na}^+$ ,  $\text{PO}_4^{3-}$  and  $\text{Si}^{4+}$ ) into the surrounding medium (Stoor et al. 1998). Polycondensation of hydrated silica groups forms a silica-gel layer on the glass surface. The silica-gel works as a platform for calcium phosphate precipitation. This crystallizes into hydroxyapatite, which resembles the mineral phase of the natural bone. Hydroxyapatite bonds with the existing bone, resorbs slowly, and is replaced by natural bone over several years (Välimäki and Aro 2006).

### 2.10.3 Antibacterial effect

The antibacterial effect of BAG has been proved in many studies against several gram-positive and -negative bacterial strains including *S. aureus*, MRSA, *S. epidermidis*, MRSE, and *A. actinomycetemcomitans* (Grønseth et al. 2020; Cunha et al. 2018; Stoor and Frantzen 2017; Gergely et al. 2014; Drago et al. 2013; Leppäranta et al. 2008; Munukka et al. 2008; Waltimo et al. 2006; Stoor et al. 1998). The antibacterial results have been observed to be comparable with gentamicin/vancomycin-PMMA (the golden standard treatment in osteomyelitis) (Cunha et al. 2018). Moreover, the efficacy of BAG has been comparable to antibiotic-loaded bone substitutes in the treatment of chronic osteomyelitis (Romanò et al. 2014). In addition to its antimicrobial effects, BAG has proven to have anti-biofilm activity against various bacterial strains, including *S. aureus* (Grønseth et al. 2020; Höing et al. 2018; Coraça-Huber et al. 2014; Drago et al. 2014a) and *S. epidermidis* (Bortolin et al. 2016).

The antibacterial mechanism of BAG is based on raised pH and osmotic pressure (Drago et al. 2014a). This completely divergent (*i.e.* physical) bactericidal mechanism of BAG compared to regular antibiotics makes it an attractive option for controlling antibiotic resistance (Drago et al. 2015). First,

## 2. LITERATURE REVIEW

Na<sup>+</sup> -ions are released which elevates pH via NaOH formation. At a slower onset, Ca<sup>2+</sup>, PO<sub>4</sub><sup>(3-)</sup>, and Si<sup>4+</sup> along with remaining Na<sup>+</sup>-ions are released sustainably (Bonalive® Biomaterials Ltd. 2021), which increases osmotic pressure (Munukka et al. 2008). Increased osmotic pressure cause bacteria to plasmolyze *i.e.*, the cytoplasm of bacterium collapses as water flows out of the cell in a hypertonic environment. This causes inhibition of bacterial growth (Drago et al. 2015). A reduction in the particle size of BAG has been shown to result in a more drastic pH elevation (Zhang et al. 2008). Moreover, sodium-containing bioactive glasses have a faster bactericidal effect than sodium-free glasses via more aggressive pH elevation (ca. pH 12 vs. 9) (Gubler et al. 2008).

### 2.10.4 Bioactive glasses in dental applications

In dental applications, Biosilicate®-bioactive glass (Federal University of São Carlos, São Carlos, Brazil) has been used e.g. to treat hypersensitive teeth owing to its ability to mineralize dentine and enamel (Tirapelli et al. 2011). Furthermore, due to its bone-augmenting properties, bioactive glass can be used in the treatment of periodontitis (Chacko et al. 2014). Indeed, enhanced periodontal parameters (increased alveolar bone and attachment tissue levels) in humans have been achieved with PerioGlas®-bioactive glass (Chacko et al. 2014; Mengel et al. 2006; 2003). Indeed, PerioGlas® (NovaBone, Bangalore, India) has clinical applications in the management of oral or dental osseous defects.

### 2.10.5 Combination of bisphosphonates and bioactive glass

There has been a growing attraction to bioactive glasses (e.g. Grønseth et al. 2020; Cunha et al. 2018; Höing et al. 2018; Malat et al. 2018). One research theme concentrates on the augmentation of bioactive glass bone growth ability with other compounds, for instance with BPs. Indeed, the improved bone formation has been observed when bioactive glass and BPs have been used as a combination therapy in orthopedics: Biogran-glass supplemented with alendronate (Orthovita, Malvern, US; Srisubut et al. 2007) and 13-93-glass supplemented with zoledronate (Vivoxid Ltd., Turku, Finland; Välimäki et al. 2006). Therefore, such combinations have also attracted interest in periodontal applications (Rosenqvist et al. 2017; 2014). Indeed, locally administered clodronate-BAG has been tested in a pilot clinical trial (Rosenqvist et al. 2017). Therein, patients suffering from chronic periodontitis received two treatments simultaneously: clodronate-BAG (mixture ratio 1:5; granule size of BAG: 0.5–0.8 mm; based on Rosenqvist et al. (2014)) and mere BAG. As an outcome of the study, the patients experienced that the clodronate-BAG diminished the sensitivity symptoms slightly more than BAG alone without any safety issues (Rosenqvist et al. 2017). Indeed, it has been observed that the pH elevation of mere BAG is more aggressive than clodronate-BAG (Rosenqvist et al. 2014), which might explain the more prominent sensitivity symptoms of BAG *per se*. Furthermore, during physicochemical property characterization, clodronate-

BAG showed improved bioactivity via longer-lasting and more extensive ion exchange than mere BAG (Rosenqvist et al. 2013). It was also detected that large amounts of clodronate caused excessive calcium clodronate precipitation, which in turn inhibited hydroxyapatite formation of BAG. Therefore, Rosenqvist et al. (2014) concluded that the amount of BP (clodronate) should be enough for ion exchange augmentation, but not too much so that hydroxyapatite formation is hampered.

### 3. AIMS OF THE STUDY

In this thesis, the main objectives were (i) to shed light on the dynamics of bacterial biofilms formed on clinically relevant materials and (ii) to study how such materials could be protected against biofilms by using a new treatment strategy composed of bisphosphonates (BPs) and bioactive glass (BAG; S53P4). What first distinguishes this project is the pioneer exploration of the matrix-associated proteosurfaceomes of *Staphylococcus aureus* biofilms developed on different clinically relevant surfaces used in medical devices and at diverse biofilm formation points. Gathering relevant mechanistic insights into biofilm formation and dynamics is crucial to guide the development of new anti-biofilm approaches, particularly applicable to the protection of biomaterials. Beyond a basic exploration of biofilm physiology, it is also investigated here the anti-biofilm effects of a novel (non-antibiotic) BP-BAG combination product in two *in vitro* models, mimicking prosthetic joint infection and periodontitis.

The specific aims of the thesis were to:

- Study formation of *S. aureus* biofilms on five different clinically relevant materials (borosilicate glass, plexiglass, hydroxyapatite, titanium, and polystyrene) at different biofilm maturation points and their correlation with the surface properties of those biomaterials, as well to assess whether the material and biofilm age affect antibiotic tolerance (study **I**)
- Analyze the dynamic changes in exopolysaccharide/protein contents and proteosurfaceomes of the *S. aureus* biofilm matrix when biofilms were formed on these materials (study **I**)
- Study whether BPs (alendronate, clodronate, etidronate, risedronate, and zoledronate) as stand-alone compounds or when combined with BAG can protect biomaterial from biofilm formation in a prosthetic joint biofilm model (against *S. aureus* and *Staphylococcus epidermidis*; study **II**) and in a periodontal biofilm model (against *Aggregatibacter actinomycetemcomitans*; study **III**)
- Gain a mechanistic understanding of the possible anti-biofilm effects and targets of BPs and BP-BAG combinations (studies **I-III**)

## 4. MATERIALS AND METHODS

### 4.1 Materials (studies I-III)

#### 4.1.1 Test compounds, antimicrobials, culture media, and reagents (studies I-III)

The used test compounds, antimicrobials, culture media, reagents, buffer solutions, and solvents are presented in **Table 7**.

**Table 7.** The materials that were utilized in all studies (**I-III**) and their vendor information.

Material	Manufacturer
<b>Test compounds</b>	
Alendronate sodium trihydrate <sup>a</sup>	Cayman Chemical Company (Ann Arbor, US; <b>II</b> ); Kemprotec Limited (Carnforth, UK; <b>III</b> )
Clodronate disodium tetrahydrate <sup>b</sup>	PharmaZell GmbH (Raubling, Germany)
Etidronic acid monohydrate <sup>c</sup>	Sigma-Aldrich (Steinheim, Germany)
Risedronic acid monohydrate <sup>d</sup>	AK Scientific (Union City, US)
Zoledronic acid monohydrate <sup>e</sup>	Kemprotec Limited (Carnforth, UK)
Bioactive glass S53P4 (BAG; granule size: 500–800 $\mu\text{m}$ )	Bonalive® Biomaterials Ltd. (Turku, Finland)
Inert glass beads (IG; particle size: 230–320 $\mu\text{m}$ )	Jencons Ltd. (Bedfordshire, UK)
<b>Antimicrobials</b>	
Chlorhexidine dihydrochloride	Sigma-Aldrich (Steinheim, Germany)
Doxycycline hydrochloride	Sigma-Aldrich (Steinheim, Germany)
Levofloxacin	Sigma-Aldrich (Steinheim, Germany)
Penicillin G sodium salt	Sigma-Aldrich (Steinheim, Germany)
Vancomycin hydrochloride hydrate	Sigma-Aldrich (Steinheim, Germany)
<b>Others (culture media, reagents, buffer solutions, and solvents)</b>	
Bacto™ Yeast Extract	Becton, Dickinson and Company (Le Pont de Claix, France)
Dextrose	Sigma-Aldrich (Steinheim, Germany)
Dimethyl sulphoxide (DMSO)	VWR International (Fontenay-sous-Bois, France)
Sheep blood (aseptically collected, defibrinated)	Bio Trading (Mijdrecht, The Netherlands)
Triethylammonium bicarbonate buffer (TEAB; 1.0 M, pH 8.5)	Sigma-Aldrich (Steinheim, Germany)
Trifluoroacetic acid (TFA; 99%)	Sigma-Aldrich (Steinheim, Germany)
Tryptic soy agar (TSA)	Lab M Limited (Lancashire, UK; <b>I</b> ); Sigma-Aldrich (Steinheim, Germany; <b>II, III</b> )
Tryptic soy broth (TSB)	Lab M Limited (Lancashire, UK; <b>I</b> ); Sigma-Aldrich (Steinheim, Germany; <b>II, III</b> )
Tween® 20	Sigma-Aldrich (Steinheim, Germany)
Phosphate-buffered saline (PBS)	Lonza (Verviers, Belgium)
Sequencing grade modified trypsin (porcine)	Promega Corp. (Madison, US)
Sodium chloride	Sigma-Aldrich (Steinheim, Germany)
Sucrose	Merck (Darmstadt, Germany)
Wheat germ agglutinin Alexa Fluor® 488 conjugate (WGA)	Invitrogen™, Thermo Fisher Scientific (Eugene, US)

a, molecular weight (MW) = 325.12 g/mol; b, MW = 360.92 g/mol; c, MW = 224.04 g/mol; d, MW = 301.13 g/mol; e, MW = 290.10 g/mol.

## 4. MATERIALS AND METHODS

### 4.1.2 Bacterial strains (studies I-III)

The bacterial strain *Aggregatibacter actinomycetemcomitans* ATCC 33384 and *Staphylococcus aureus* Newman were kindly donated by Doctor Pirkko Pussinen (Institute of Dentistry, University of Helsinki, Finland) and Docent Pekka Varmanen (Faculty of Veterinary Medicine, University of Helsinki, Finland), respectively. *Staphylococcus aureus* ATCC 25923 and *Staphylococcus epidermidis* RP62A (ATCC 35984) were obtained from the Faculty of Pharmacy (University of Helsinki, Finland).

### 4.2 Methods (studies I-III)

#### 4.2.1 Bacterial culturing (studies I-III)

The storing and culturing conditions of the bacteria and the utilized media (studies I-III) are summarized in **Table 8**.

**Table 8.** The storing and culturing conditions of the used bacteria.

Bacterial strain	Storing conditions	Agar	Medium	Growth conditions	Study
<i>Staphylococcus aureus</i> ATCC 25923	-80°C in 20% (w/v) glycerol-TSB	TSA	TSB	Aerobic, +37°C, 220 rpm	I, II
<i>Staphylococcus aureus</i> Newman	-80°C in 20% (w/v) glycerol-TSB	TSA	TSB	Aerobic, +37°C, 220 rpm	II
<i>Staphylococcus epidermidis</i> RP62A (ATCC 35984)	-80°C in 20% (w/v) glycerol-TSB	TSA	TSB	Aerobic, +37°C, 220 rpm	II
<i>Aggregatibacter actinomycetemcomitans</i> ATCC 33384	-80°C in skim milk	BA	TSB-YE/Glc	Microaerophilic, +37°C, static	III

TSA = tryptic soy agar; TSB = tryptic soy broth; BA = blood agar; TSB-YE/Glc = TSB supplemented with 0.6% (w/v) yeast extract and 0.8% (w/v) glucose.

In study **I**, a 10- $\mu$ L sample of *Staphylococcus aureus* ATCC 25923 was taken from the glycerol stock, suspended into 3 mL of TSB, and grown under aerobic conditions at 37°C, 220 rpm overnight. Next, this pre-culture was diluted with fresh TSB in 1:1000, and grown under aerobic conditions at 37°C, 220 rpm for 4 h to reach the exponential phase (to a concentration of  $10^8$  CFU·mL<sup>-1</sup>) as in (Skogman et al. 2012).

In study **II**, a 10- $\mu$ L sample of *Staphylococcus aureus* ATCC 25923, *Staphylococcus aureus* Newman or *Staphylococcus epidermidis* RP62A (ATCC 35984) was taken from the glycerol stock, suspended into 100 mL of TSB, and grown under aerobic conditions at 37°C, 220 rpm for 20 h to reach a bacterial concentration of  $10^9$  CFU·mL<sup>-1</sup>, as in Oja et al. (2014).

In study **III**, a 20- $\mu$ L sample of the *Aggregatibacter actinomycetemcomitans* ATCC 33384 bacterial suspension in skim milk was spread on the blood agar (BA) plates. The BA-plates are TSA-plates that have been supplemented with 5%

defibrinated sheep blood. The bacteria were let to grow in microaerophilic conditions (3% CO<sub>2</sub>; 17% O<sub>2</sub>) at 37°C for 2 days. A sample of the formed bacterial colonies was taken (4 full 1-μL inoculation loops) and suspended into 1 mL of TSB-YE/Glc. TSB-YE/Glc is TSB supplemented with 0.6% (w/v) yeast extract and 0.8% (w/v) glucose. The bacterial suspension was adjusted to an optical density (OD) of 1 at 595 nm (approximately 10<sup>9</sup> CFU·mL<sup>-1</sup>). The culturing conditions were adapted from Paino et al. (2011).

In all cases, bacterial concentrations were estimated by measuring OD at 595 nm (Varioskan™ LUX Multimode Reader, Thermo Scientific, Vantaa, Finland), and verified by plating serial dilutions of bacterial suspensions on TSA- (I, II) or BA-plates (III), which were incubated under aerobic conditions at 37°C for 18 h (I, II) or in microaerophilic conditions at 37°C for 2 days (III). The viable colonies were counted, and the bacterial concentration (CFU·mL<sup>-1</sup>) was determined by using Equation 1:

$$CFU \cdot mL^{-1} = \frac{\text{Average of number of colonies} \times \frac{1}{\text{Dilution}}}{\text{Volume plated (mL)}} \quad (1)$$

#### 4.2.2 Well plate-based assays (study I)

##### 4.2.2.1 Biofilm formation on coupons in the well plate-based assay (study I)

*S. aureus* ATCC 25923 (bacterial culturing conditions described in 4.2.1) was used to form biofilms on 96-well plates (96-WPs) (Nunclon™ Δ surface polystyrene plates, Nunc™, Roskilde, Denmark) or on the following commercial coupons: borosilicate glass (G), plexiglass (PG), titanium (TI) (the dimensions of all three: 0.4 cm height, 1.27 cm diameter) and hydroxyapatite (HA: 0.25 cm height, 1.27 cm diameter) (BioSurface Technologies Corp., Bozeman, MT). For the assays with coupons, the coupons were incubated in 12-WPs (Costar®, polystyrene, well diameter 2.26 cm, flat bottom; Corning Inc., Corning, US). For the assays executed in 96-WPs or 12-WPs (with the coupons on them), 200 μL or 2.5 mL of the bacterial suspension (10<sup>6</sup> CFU·mL<sup>-1</sup>) were applied, respectively. All the plates were incubated under aerobic conditions at 37 °C, 150 rpm for 18, 42, or 66 h. The selected incubation times were similar to Skogman et al. (2012). The media of the 42- and 66-h-old biofilms were refreshed at 18 h, and at 18 and 42 h, respectively.

##### 4.2.2.2 Quantification of the biofilm formation on different materials at different time points (study I)

After 18, 42, or 66 h of incubation, *S. aureus* ATCC 25923 biofilms on PS (in 96-WPs) or on G, PG, HA, and TI coupons in 12-WPs, were disaggregated for quantification. In the case of coupons, the following biofilm quantification protocol (4.2.2.3) was used.

## 4. MATERIALS AND METHODS

In the case of biofilms grown on 96-wells, the wells were first washed once with 200  $\mu\text{L}$  of TSB to detach planktonic and loosely attached bacteria. Next, 200  $\mu\text{L}$  of 0.5% (w/v) Tween® 20-TSB solution was added on 96-wells and the 96-WPs were sonicated as described in 4.2.2.3. Correspondingly, the quantifications of biofilms grown on 96-WPs were performed as in 4.2.2.3. The size differences between the coupons and 96-wells were taken into account by converting the calculated colony forming units (CFU) per volume (mL) into CFU per surface area ( $\text{cm}^2$ ), based on the bacterial attachment area covered on the diverse materials. Those values of  $\text{CFU}\cdot(\text{mL}\cdot\text{cm}^2)^{-1}$  were then converted to a  $\log_{10}$  scale.

### 4.2.2.3 Quantification of the coupon-associated biofilms (studies I-III)

Following the incubation period, the coupons were immersed into TSB (I, II) or TSB-YE/Glc (III) to remove planktonic and loosely attached cells (except in 4.2.3.3). Next, the coupons were transferred into Falcon tubes (50 mL) holding 1 mL of 0.5% (w/v) Tween® 20-TSB (I, II) or Tween® 20-TSB-YE/Glc (III) solution. Thereafter, the tubes were sonicated in a water bath (Ultrasonic Cleaner 3800, Branson Ultrasonics, Danbury, US) at 25°C, 35 kHz for 5 min. In addition, the tubes were vortexed for 20 sec (Vortex mixer SA8, Stuart, Stone, UK) before and after the sonication step, as proposed by Mandakhlikar et al. (2018). The resulting bacterial suspensions were serially diluted and plated on TSA- (I, II) or BA-plates (III) and incubated under aerobic conditions at 37°C for 18 h (I, II) or in microaerophilic conditions at 37°C for 2 days (III). In study I, from these viable colonies,  $\text{CFU}\cdot(\text{mL}\cdot\text{cm}^2)^{-1}$  values were determined due to the different size areas of the materials. In turn, in studies II and III,  $\text{CFU}\cdot\text{mL}^{-1}$  values were determined, because the biofilm attachment areas (surface areas of the coupon bottoms), were the same among all used coupons. In all cases, the bacterial attachment on coupons was expressed on the  $\log_{10}$  scale.

### 4.2.2.4 Quantification of the biofilm matrix component polysaccharide intercellular adhesin/poly-N-acetyl- $\beta$ -(1-6)-glucosamine (study I)

The main staphylococcal biofilm matrix polysaccharide, polysaccharide intercellular adhesin/poly-N-acetyl- $\beta$ -(1-6)-glucosamine (PIA/PNAG), was quantified from *S. aureus* ATCC 25923 biofilms formed on 96-WPs and on coupons (G, PG, HA, and TI) in 12-WPs for 18, 42, and 66 h. Wheat germ agglutinin Alexa Fluor® 488 (WGA) conjugate stain was utilized as it recognizes the N-acetylglucosamine (NAG) component of the PIA/PNAG. In addition to PIA/PNAG, WGA may also attach to other NAG-containing components, such as peptidoglycan and teichoic acid (Cerca et al. 2006). The biofilms were formed as explained in 4.2.2.1. A WGA-staining protocol published by Skogman et al. (2012) was utilized with two adjustments: <sup>(1)</sup> WGA-conjugate was used with a lower concentration ( $2.5 \mu\text{g}\cdot\text{mL}^{-1}$ ) based on Hiltunen et al. (2017) and <sup>(2)</sup> 100% DMSO was used to substitute 33% acetic acid, as acetic acid is not compatible with acid-intolerable materials, such as HA. The election of 100% DMSO was made upon



preliminary tests where a lower concentration (10%) of acetic acid, 96% ethanol, and 100% DMSO were assayed.

First, to detach planktonic and loosely attached cells, the coupons were shortly immersed once into PBS while the 96-wells were washed once with PBS (200  $\mu\text{L}$ ). Next, WGA (2.5  $\mu\text{g}\cdot\text{mL}^{-1}$  in PBS) was pipetted into 96-wells (200  $\mu\text{L}$ ) or onto coupons (500  $\mu\text{L}$ ) in 24-WPs (Nunclon™  $\Delta$  surface, Nunc™, Roskilde, Denmark) and incubated in the darkness, at 4°C, for 2 h. Then, the biofilms were washed three times by soaking coupons briefly into PBS or washing 96-wells with 200  $\mu\text{L}$  of PBS. Next, they were let dry at room temperature (RT) for 15 min. Then, 200  $\mu\text{L}$  of DMSO was pipetted onto the 96-wells. In the case of coupons, they were moved into Falcon tubes (50 mL) containing 1.3 mL (for G, PG, and TI) or 1.11 mL (for HA coupons; the lower volume owing to the smaller surface area of HA coupons) of DMSO. The 96-WPs and the tubes were then sonicated in a water bath at 25°C, 35 kHz, for 30 sec and incubated at 37°C for 1 h. After the incubation, the sonication step was repeated. Lastly, 200  $\mu\text{L}$  of the remaining suspensions from Falcon tubes were pipetted onto a 96-WP and the top fluorescence ( $\lambda_{\text{excitation}} = 495 \text{ nm}$ ;  $\lambda_{\text{emission}} = 520 \text{ nm}$ ) with Varioskan™ LUX Multimode Reader was measured. In parallel, the resulting suspensions of 96-well-associated biofilms were diluted 1:10 before measuring the fluorescence signal, to be in correspondence with the coupon surface area. The measurements of emitted top fluorescence were conducted in the same manner ( $\lambda_{\text{excitation}} = 495 \text{ nm}$ ;  $\lambda_{\text{emission}} = 520 \text{ nm}$ ).

#### 4.2.2.5 Trypsin shaving of biofilm matrix-associated proteins (study I)

Next, proteins present in the biofilm matrix were identified and quantified. Before initiating the protein identifications, it was pivotal to assay whether trypsin used in the protein analyses would have detrimental effects on biofilm integrity. Therefore, biofilm viability with and without the trypsin treatment was tested. First, biofilms were formed on G coupons in 12-WPs (as in 4.2.2.1) and then moved into Falcon tubes (50 mL) containing 1 mL of acetate buffer (100 mM, 4°C, pH 4.7), which is a condition that has been shown to prevent the release of the adhesive moonlighting proteins (Savijoki et al. 2019). The tubes were sonicated at 25°C, 35 kHz, for 5 min and detached bacterial cells were collected by centrifugation at 4°C, 4,000g, for 2 min. The collected cells were suspended into 110  $\mu\text{L}$  of 100 mM TEAB containing 16% sucrose (TEAB<sub>S16</sub>; pH 8.5) with and without trypsin, at a final concentration of 51.9  $\text{ng}\cdot\mu\text{L}^{-1}$ . These mixtures were incubated at 37°C for 15 min, serially diluted in TSB, and plated onto TSA for CFU-determinations. There were no statistical differences in the viable counts ( $\text{CFU}\cdot(\text{mL}\cdot\text{cm}^2)^{-1}$ ) measured on the trypsin- and the control-treated samples, indicating that the trypsin-induced cell lysis did not take place (**Figure S1**) and thus confirming the suitability of the conditions for the trypsin shaving step during protein analyses.

After that, biofilm samples prepared in duplicates for each material and time point, were shaved with trypsin. To that end, coupon-associated biofilms were

#### 4. MATERIALS AND METHODS

first rinsed with TSB to remove planktonic and loosely attached bacteria and transferred onto 12-WPs. With a sterile plastic stick, the bacteria were scraped off from the coupon surface into acetate buffer (100 mM, 4°C, pH 4.7). Similarly, PS-associated biofilms were also first rinsed with TSB and scraped off from 96-wells into the acetate buffer. Next, in all cases, bacteria were collected by centrifugation at 4°C, 4,000*g*, for 2 min and suspended into 110 µL of TEAB<sub>S16</sub> (Espino et al. 2015) and trypsin, at a final concentration of 51.9 ng·µL<sup>-1</sup>. Following the trypsin treatment at 37°C for 15 min, cells were first removed by centrifugation at RT, 4,000*g*, for 2 min. Next, the digestions were purified through membranes (cellulose acetate, pore size: 0.22 µm, Costar® Spin-X Centrifuge Tube Filter, Corning Inc., Corning, US) by centrifugation at RT, 16,000*g* for 2 min. The digestions that had been incubated at 37°C for 16 h were blocked by adding trifluoroacetic acid (TFA) to reach a final concentration of 0.6% (v/v). Concentrations of released proteins/peptides were determined by employing low volume photometric quantification at 280 nm using the µDrop™ Plate (Thermo Scientific, Vantaa, Finland) with a Varioskan™ LUX Multimode Reader.

##### **4.2.2.6 Identification of trypsin-released proteins/peptides by LC-MS/MS (study I)**

Tryptic peptides were first purified and concentrated (ZipTips C18; Millipore®, Merck KGaA, Darmstadt, Germany). Next, they were analyzed as described in Lorey et al. (2017). In short, an equal amount of the purified tryptic peptides was submitted to an Easy-nLC 1000 Nano-LC system (Thermo Scientific, Vantaa, Finland) that was paired with a quadrupole Orbitrap mass spectrometer (Q Exactive™, Thermo Scientific, Bremen, Germany) and a nanoelectrospray ion source (Easy-Spray™, Thermo Scientific). Liquid chromatography separation was performed (Easy-Spray™, C18, 75 µm x 25 cm, 2-µm beads, 100 Å, Thermo Scientific) using 60 min LC separation gradient (2–30%; 100% acetonitrile and 0.1% formic acid) with 300 nL·min<sup>-1</sup> flow rate. The resulting MS raw data were submitted (MaxQuant version 1.6.2.1, built-in Andromeda search engine) (Cox et al. 2011; Cox and Mann 2008), and UniProt (*S. aureus* protein database, <https://www.uniprot.org/>) was used for database searches. Carbamidomethyl (C) and methionine oxidation was set as a fixed and a variable modification, respectively. First search peptide tolerance (20 ppm) and main search error (4.5 ppm) were utilized. Trypsin without proline restriction enzyme option was employed with two permitted miscleavages. The minimal unique + razor peptides number was adjusted to 1, and the false discovery rate (FDR) to 0.01 (1%) for peptide/protein identifications. Proteins identified as “reverse” or “only identified by site” and known contaminants (provided by MaxQuant), were excluded from further data analyses. Only proteins that could be identified in both replicates were included for the data set analyses.

### 4.2.3 The Static Biofilm method-based assays (studies II, III)

#### 4.2.3.1 The biofilm formation in the prosthetic joint infection and dental biofilm models (studies II, III)

The bisphosphonate-bioactive glass (BP-BAG) combinations were investigated in the prosthetic joint infection (PJI) (II) and dental (III) biofilm models. These models are based on the Static Biofilm method, originally developed by Charaf et al. (1999) and further optimized by Oja et al. (2014). Here, the method was additionally optimized to meet the special requirements of testing two-component semisolid samples (Figure 5). Based on the Static Biofilm method (Oja et al. 2014), the protocol was performed as follows. First, a sterile filter paper (Whatman, 70-mm diameter, qualitative grade 2, GE Healthcare, Little Chalfont, UK) was positioned on TSA- (II) or BA-plate (III). The filter paper, which is used to facilitate the even spread of the bacterial suspension, was inoculated with 1.5 mL of  $10^8$  CFU·mL<sup>-1</sup> suspension in the cases of *S. aureus* ATCC 25923 (II), *S. aureus* Newman (II), or *S. epidermidis* RP62A (ATCC 35984) (II) or 1.5 mL of  $10^7$  CFU·mL<sup>-1</sup> suspension in the case of *A. actinomycetemcomitans* ATCC 33384 (III). Next, sterile coupons without (4.2.3.2) or with treatments (4.2.3.3) were added on the filter paper, and this assembly was incubated under humidified aerobic (II) or in humidified microaerophilic (III) conditions at 37°C for 24 or 48 h (II, III). After the incubation periods, the biofilms were detached from the coupon surfaces and quantified as described in 4.2.2.3.

#### 4.2.3.2 Selecting applicable biofilm formation substrate and time (studies II and III)

Before initiating the susceptibility trials, a suitable biofilm formation time and substrate material were chosen. For that purpose, G, PG, HA, and TI coupons (the dimensions are described in 4.2.2.1) were tested. The applicable biofilm formation time was selected from two tested incubation periods: 24 and 48 h (II, III). Biofilms formed for 48 h were refreshed with 1.5 mL of TSB (1:10 diluted) (II) or TSB-YE/Glc (III) halfway through the incubation period. The plates were incubated in the conditions described in 4.2.3.1. The formed biofilms were quantified as described in 4.2.2.3.

#### 4.2.3.3 Exploring anti-biofilm effects of bisphosphonate-bioactive glass and bisphosphonate-inert glass combinations (studies II and III)

The combination samples of BP and BAG were prepared with a mixture ratio (1:10; BP-BAG), similar to Rosenqvist et al. (2014). Furthermore, the grade and particle size of BAG were similar to Rosenqvist et al. (2014). To investigate the anti-biofilm effects of BP-BAG combinations in study II: 25 mg of BP (alendronate, clodronate, etidronate, risedronate, or zoledronate) or vancomycin (as a positive control) or inert glass beads (IG; as a negative control) was combined with 250 mg of BAG in 225 µL of 0.9% (w/v) saline to form semisolid

#### 4. MATERIALS AND METHODS

paste-type samples. In study **III**, 50 mg of BP (alendronate, clodronate, etidronate, risedronate, or zoledronate), chlorhexidine (CHX, as a positive control) or IG; as a negative control) and 500 mg of BAG in 450  $\mu\text{L}$  of 0.9% (w/v) saline were combined. In both studies (**II** and **III**), IG was utilized as a negative control material to simulate BPs, due to its inert nature and similar particle size to BPs.

Second, selected BPs were assayed in terms of their intrinsic anti-biofilm activity. Herein, 25 mg of BP (alendronate, etidronate, or risedronate) or vancomycin (as a positive control) and 250 mg of IG in 225  $\mu\text{L}$  of 0.9% (w/v) saline (**II**) or 50 mg of BP (alendronate, clodronate, etidronate, risedronate, or zoledronate) or CHX (as a positive control) and 500 mg of IG in 450  $\mu\text{L}$  of 0.9% (w/v) saline (**III**) were mixed. A negative control composed of 275 mg of IG in 225  $\mu\text{L}$  of 0.9% (w/v) saline (**II**) or 550 mg of IG in 450  $\mu\text{L}$  of 0.9% (w/v) saline (**III**) was used. As earlier, IG was regarded as a suitable component to mimic the two-component formulation.

An additional layer of filter papers (diameter: 25 mm; one per coupon) was positioned on the larger filter papers to ease the scraping of the samples into Falcon tubes during the detachment phase (4.2.2.3) (**Figure 5**). The HA coupons, with the semisolid test samples applied on their undersides, were then transferred on this double layer of filter papers. These assemblies were incubated under humidified aerobic conditions at 37°C for 24 h (**II**) or in humidified microaerophilic conditions at 37°C for 48 h (**III**). The formed biofilms were quantified as described in 4.2.2.3. These sample-covered coupons were not immersed in the medium (to detach planktonic and loosely attached cells) prior to sonication.

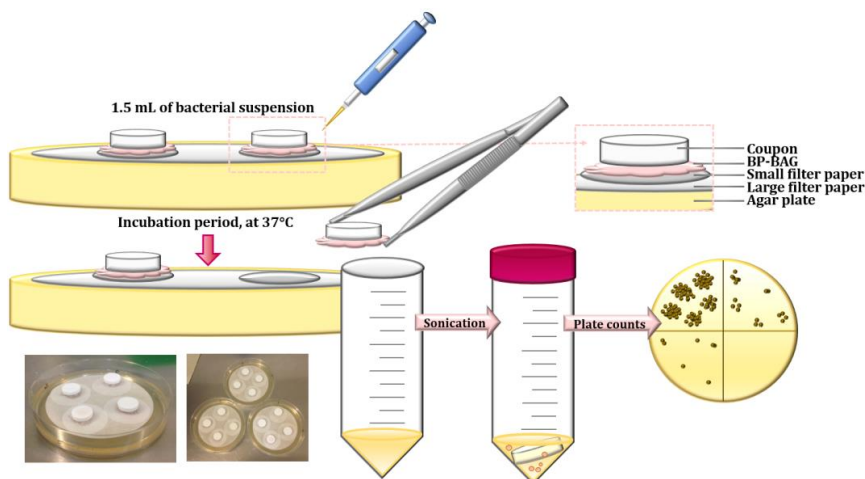


**Figure 5.** The protocol for assaying the bisphosphonate-bioactive glass (BP-BAG) samples in the prosthetic joint infection (study **II**) and dental biofilm model (**III**). These assemblies were incubated for 24 h on tryptic soy agar plates (**II**) or for 48 h on blood agar plates (**III**). Figure adapted from publication **II**, with permission from Elsevier.

#### 4.2.3.4 Quantification of the biofilms (studies II-III)

The disaggregation of the biofilms grown on coupons was performed as described in 4.2.2.3. The anti-biofilm effect of the test compounds is indicated as a logarithmic reduction ( $\log R$ ) of the bacterial burden (Equation 2) as in (Pitts et al. 2003), where  $\langle \cdot \rangle$  depicts averaging over the samples.

$$\log R = \log_{10} \langle (CFU/mL)_{control} \rangle - \log_{10} \langle (CFU/mL)_{compound} \rangle \quad (2)$$

#### 4.2.4 Chemotolerance assays (studies I and III)

In study **I**, chemotolerance of *S. aureus* ATCC 25923 biofilms formed on HA and TI coupons on 12-WPs, for 18 and 66 h (the conditions are described in 4.2.2.1) were studied. In study **III**, chemotolerance of different aged *A. actinomycetemcomitans* ATCC 33384 biofilms were studied. Biofilms were grown on HA coupons in humidified microaerophilic conditions at 37°C for 2, 24, and 48 h, utilizing the Static Biofilm method as in 4.2.3.1.

After the incubation steps, the coupons were first immersed into TSB (**I**) or TSB-YE/Glc (**III**) to remove planktonic and loosely attached cells and then transferred onto 12-WPs containing 2.5 mL of 4.0  $\mu$ M doxycycline (1.92  $\mu$ g/mL), 90.0  $\mu$ M levofloxacin (32.5  $\mu$ g/mL), 2.0  $\mu$ M penicillin G (0.71  $\mu$ g/mL), or 5.0  $\mu$ M vancomycin (7.43  $\mu$ g/mL) or TSB (as a negative control) (**I**) or CHX solution (25 or 50  $\mu$ M; 14.5 or 28.9  $\mu$ g/mL) or TSB-YE/Glc (as a negative control) (**III**) and exposed to the indicated antimicrobials under aerobic conditions at 37 °C 150 rpm for 2 or 24 h (**I**) or in microaerophilic conditions at 37°C for 2 h (**III**). After the incubation periods, formed biofilms were quantified as described in 4.2.2.3.

Additional chemotolerance assay was performed (**I**), where a combination treatment involving trypsin (51.9 ng· $\mu$ L<sup>-1</sup>) and 90  $\mu$ M levofloxacin was tested on 18- and 66-h-old *S. aureus* ATCC 25923 biofilms formed on HA. As previously, the coupons were soaked into TSB after the incubation period. Next, the coupons were moved onto a 24-WP and exposed to trypsin in the buffer (35  $\mu$ L of trypsin dissolved into 350  $\mu$ L of TEAB<sub>S16</sub>) or only buffer (385  $\mu$ L of TEAB<sub>S16</sub>, as a negative control). The 24-WPs were incubated at 37°C for 15 min, as described in 4.2.2.5. Subsequently, the coupons were immersed into TSB and moved onto a 12-WP containing 2.5 mL of 90  $\mu$ M levofloxacin. The 12-WPs were incubated under aerobic conditions at 37°C 150 rpm for 24 h. As a second control, biofilms were exposed only to TSB under similar conditions (for 24 h and 15 min in total). After the incubation periods, formed biofilms were quantified as described in 4.2.2.3.

#### 4.2.5 Imaging of biofilms (studies I and III)

##### 4.2.5.1 Atomic force microscopy (studies I and III)

For atomic force microscopy (AFM), images were taken from G, PG, HA, TI, and PS surfaces without any attached biofilms (**I**) and HA surfaces with and without *A. actinomycetemcomitans* ATCC 33384 biofilms grown in humidified

## 4. MATERIALS AND METHODS

microaerophilic conditions at 37°C for 24 and 48 h, as described in 4.2.3.1 (III). The topography of the material surfaces with and without attached bacteria was captured with a NTegra Prima AFM (NT-MDT, Moscow, Russia) in an intermittent contact mode by employing Au-coated NSG10 (NT-MDT, Moscow, Russia) probes (a nominal tip curvature radius: 10 nm; a force constant: 3.1–37.6 N/m). Scan rates of 0.3–0.5 (I) and 0.39 Hz (III) were utilized. The image analysis was performed with the Scanning Probe Image Processor software (SPIP, Image Metrology, Hørsholm, Denmark). Gaussian (ISO 11562) filtering was used on the captured topographs.

### 4.2.5.2 Fluorescence microscopy (study I)

These images were taken from *S. aureus* ATCC 25923 biofilms formed on G coupons (as described in 4.2.2.1) and stained with WGA (as in 4.2.2.4). After 2 h of incubation in the darkness (4°C), the unbound dye was removed, and the images of the coupons placed on Petri dishes were obtained with an Invitrogen™ EVOS® FL Imaging System (Thermo Scientific, Eugene, US) using the GFP light cube ( $\lambda_{\text{excitation}} = 470/22$  nm;  $\lambda_{\text{emission}} = 510/42$  nm) and a 20x objective.

### 4.2.6 pH measurements (study III)

The pH values were measured from the following combinations: <sup>(1)</sup> 50 mg of BP (alendronate, clodronate, etidronate, risedronate, or zoledronate) and 500 mg of IG in 450  $\mu$ L of 0.9% (w/v) saline; <sup>(2)</sup> 550 mg of IG in 450  $\mu$ L of 0.9% (w/v) saline; <sup>(3)</sup> 50 mg of BP/IG and 500 mg of BAG in 450  $\mu$ L of 0.9% (w/v) saline. These combinations were used to mimic the conditions encountered by *A. actinomycetemcomitans* ATCC 33384 in the dental biofilm model. The pH values were measured (744 pH Meter  $\Omega$ , Metrohm AG, Herisau, Switzerland) at several time points (0, 30, 60, 90 min, 2, 4, 6, 8, 24, and 48 h) as in Rosenqvist et al. (2013). Furthermore, the pH of the used medium (0.9% (w/v) saline) was also measured at 0, 24, and 48 h.

### 4.2.7 Data processing and statistical analysis (studies I-III)

In paired comparisons, the unpaired t-test with Welch's correction was used (GraphPad Software, Prism, La Jolla, US, version 7.0 for Windows) (I-III). One-way analysis of variance comparisons with Games-Howell (for unequal variances) or Tukey (for equal variances) post-tests were implemented (IBM SPSS Statistics, SPSS Inc., Chicago, US, version 24.0 for Windows) (I).

In a multivariate statistical analysis, log<sub>2</sub>-converted averages of the protein relative intensity values (from the proteins that were identified in both biological replicates) were implemented in a principal component analysis (PCA; based on the correlation matrix) (SPSS, Oblimin rotation, Kaiser Normalization) (I).

Throughout all the studies,  $p < 0.05$  was considered statistically significant and  $p < 0.001$  highly significant.

## 5. RESULTS AND DISCUSSION

### 5.1 Characteristics and dynamical changes of *Staphylococcus aureus* biofilms on clinically relevant materials (study I)

#### 5.1.1 Surface roughness analysis of tested substrate materials (study I)

The recent focus of research has been on different approaches for incorporating antimicrobial agents on implantation materials (e.g. Reigada et al. 2020a; 2020b; Sankar et al. 2017; Jennings et al. 2015; Tran et al. 2015; Drago et al. 2014b). In turn, systematic studies concentrating on the correlations between the biomaterial and biofilm properties are rare. Furthermore, the most commonly utilized *in vitro* biofilm assays are performed on well plates (polystyrene), and this material cannot be considered a relevant material to reflect *in vivo* biofilm formation conditions. For this study, four clinically pertinent materials were included: borosilicate glass (G), plexiglass (PG), hydroxyapatite (HA), and titanium (TI) coupons along with the control material polystyrene (PS; 96-well plate). PJs are commonly constituted of TI alloys owing to their corrosion resistance and biocompatibility. In turn, HA represents the mineral component of bones, and it is utilized to coat medical devices in order to enhance the integration of the implant with the freshly formed bone (Kelly et al. 2015). On the other hand, G has been traditionally utilized in PJs, bone cement materials, dental composites, prosthetic eyes, and breast implants (Hench et al. 2010; Peters and Fornasier 2009). Finally, PG is typically employed in bone cement or used to fixate medical devices onto bone (Winkler 2012).

First, the structural features of the biofilm substrate materials were investigated. Therein, AFM topographical images were captured (**Figure 6**). Based on the AFM-images, the smoothest materials seemed to be G, PS, and TI, while PG and HA appeared more heterogeneous and porous surfaces. Performed roughness analysis of the AFM images (**Table 9; Figure S2**) revealed that the surfaces of HA and PG had indeed the largest roughness and porosity values, while the smoothest surface was G.

**Table 9.** Selected roughness parameters of the substrate materials.  $S_{dr}$ , the relative increase in the surface area compared to the flat surface;  $V_v$ , void volume, the surface porosity or openness of the surface. Table adapted from publication I, with permission from MDPI, to keep consistency of this document.

Material	$S_{dr}$ (%)	$V_v$ ( $\mu\text{m}^3/\mu\text{m}^2$ )
Borosilicate glass (G)	$0.3 \pm 0.1$	$0.0048 \pm 0.001$
Plexiglass (PG)	$123 \pm 20$	$0.62 \pm 0.07$
Hydroxyapatite (HA)	$58 \pm 10$	$0.75 \pm 0.08$
Titanium (TI)	$9.0 \pm 1.1$	$0.19 \pm 0.02$
Polystyrene (PS)	$3.0 \pm 0.4$	$0.012 \pm 0.002$

5. RESULTS AND DISCUSSION

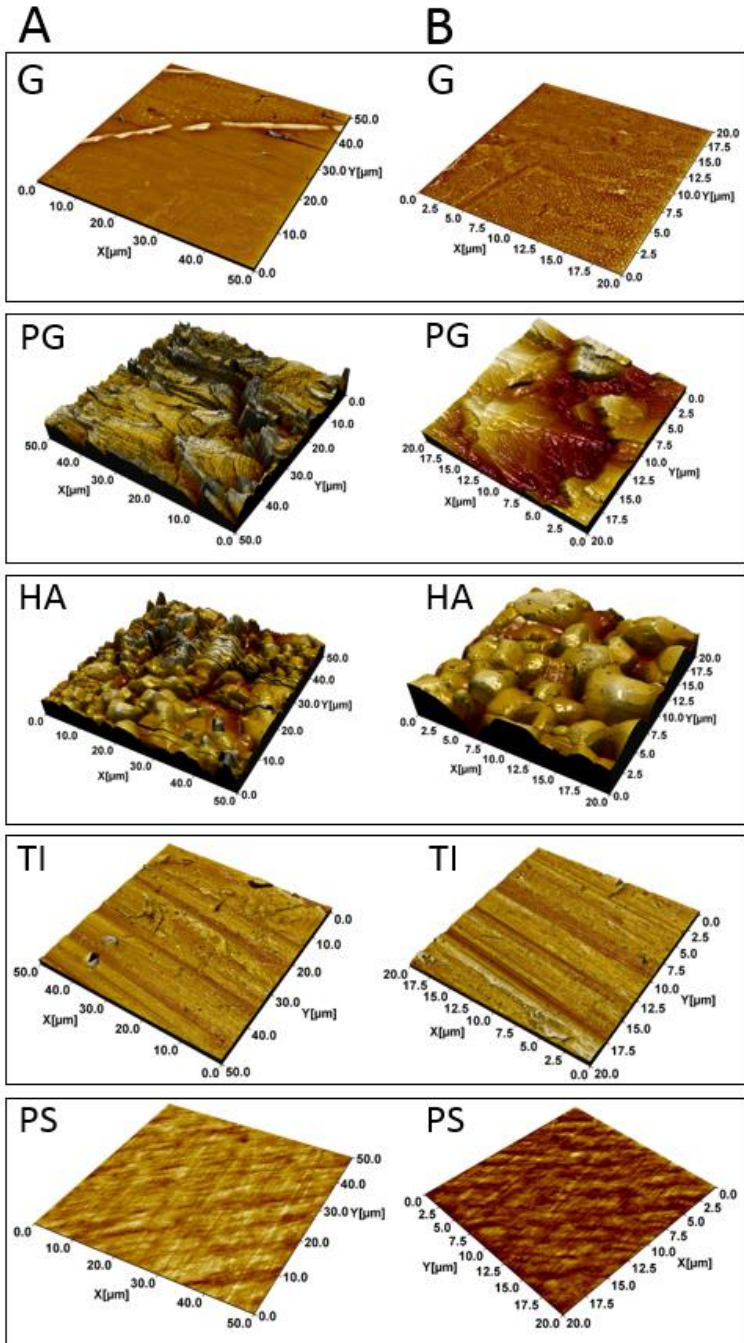


**Figure 6.** The AFM topographical images of borosilicate glass, G; plexiglass, PG; hydroxyapatite, HA; titanium, TI; polystyrene, PS (image size: 50 × 50 μm) (A). Zoomed images (image size: 20 × 20 μm) (B). Figure originally included in publication I and reproduced with permission from MDPI.



### 5.1.2 Bacterial attachment on the materials (study I)

The bacterial attachment of *S. aureus* ATCC 25923 was assessed on all five materials at 18, 42, and 66 h. In the assay conditions, the temporal increase of viable colonies expressed as  $\log_{10}$  of viable CFU·(mL·cm<sup>2</sup>)<sup>-1</sup>, was observed solely in two situations (HA and PG; from 18 to 42 h) ( $p < 0.05$ ) (**Figure 7**). In contrast, a non-statistically significant temporal decrease in viable colonies was observed with G and TI. While biofilm formation on different materials (at identical time points) was compared, it was found that *S. aureus* ATCC 25923 was more prone to establishing biofilms on PS than on the other substrate materials ( $p < 0.05$ ). Furthermore, biofilm formation on PS was equally high at 18, 42, and 66 h.

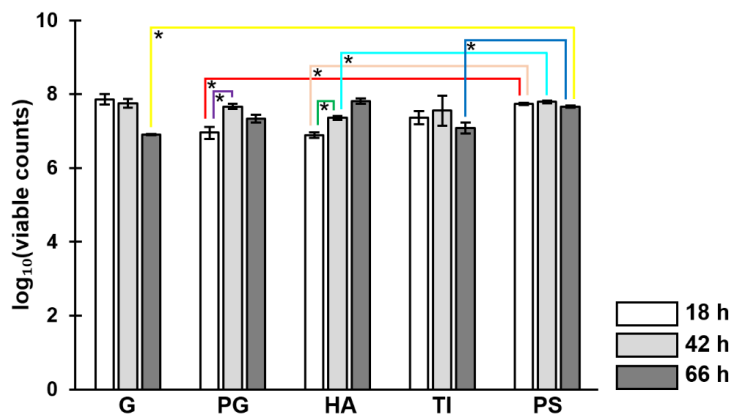


**Figure 7.** Biofilm formation of *S. aureus* ATCC 25923 on five substrate materials (expressed as  $\log_{10}$  values of CFU·(mL·cm<sup>2</sup>)<sup>-1</sup>). Differences in bacterial attachment were compared with a single material between different time points, and at a fixed time point between different materials, employing one-way ANOVA with Games–Howell post-test. \*, significant difference ( $p < 0.05$ ). Error bars indicate the standard error of the mean (SEM) ( $n=3$ ). G, borosilicate glass; PG, plexiglass; HA, hydroxyapatite; TI, titanium; PS, polystyrene. Figure adapted from publication I, with permission from MDPI, to keep consistency of this document.

Based on several previous studies, it could have been assumed that surface roughness would have had a positive correlation with bacterial adhesion due to the increase in surface area (e.g. Carlén et al. 2001; Kawai et al. 2000). However, at the initial stage (at 18 h), it appeared that *S. aureus* ATCC 25923 was more prone to form biofilms on PS and G (the smoothest materials). Instead, the attachment was significantly lower on the rougher HA and PG compared to PS ( $p < 0.05$ ). It would therefore appear that biofilm formation was at first more difficult on rougher materials, but the differences leveled off at 66 h. Of course, other physicochemical factors (such as surface charge and/or surface

hydrophobicity/hydrophilicity) may have had more influence on the biofilm formation. *S. aureus* (as the majority of bacteria) has a modestly negatively charged cell surface at neutral pH, possibly due to the overpowering amount of negatively charged phosphate groups in relation to positively charged *D*-alanine residues of teichoic acids (Gross et al. 2001). Therefore, positively charged materials promote colonization of *S. aureus*. PS, the material with the highest attachment, is known to be slightly charged in an aqueous solution and generates a contact angle to water of ca. 85° (Thormann et al. 2008) (0-90° are regarded as hydrophilic surfaces). *S. aureus* can also attach to slightly negatively charged surfaces such as glass because van der Waals forces can overcome interionic repulsion (Gross et al. 2001). Altogether, hydrophilic (Lee et al. 2015; Määttänen et al. 2014) as well as highly polar surfaces (Määttänen et al. 2014) seem to stimulate colonization of *S. aureus*, while hydrophobic surfaces hinder it (Määttänen et al. 2014).

### 5.1.3 Quantification of polysaccharide intercellular adhesin/poly-N-acetyl- $\beta$ -(1-6)-glucosamine (study I)

The main staphylococcal biofilm matrix polysaccharide is polysaccharide intercellular adhesin/poly-N-acetyl- $\beta$ -(1-6)-glucosamine (PIA/PNAG) (Nguyen et al. 2020; Cramton et al. 1999). The PIA/PNAG is acknowledged to contribute to the attachment of staphylococcal biofilms (Costa et al. 2009), pathogenesis (Lin et al. 2015), antibiotic tolerance (Costa et al. 2009), and resistance to neutrophilic phagocytosis and AMPs (Vuong et al. 2004).

In this study, PIA/PNAG was quantified by employing a Wheat germ agglutinin Alexa Fluor® 488 (WGA) conjugate. *S. aureus* ATCC 25923 biofilms were formed on the five substrate materials for 18, 42, and 66 h, and exposed to WGA conjugate with the optimized staining conditions, described in 4.2.2.4. Biofilms formed on PS contained more PIA/PNAG-fraction than biofilms on G, PG or TI ( $p < 0.05$ ) (**Figure 8**). The PIA/PNAG-fraction was observed to decline temporally (from 18 to 66 h) on all materials, and the deepest decrease was found with TI-associated biofilms ( $p < 0.05$ ).

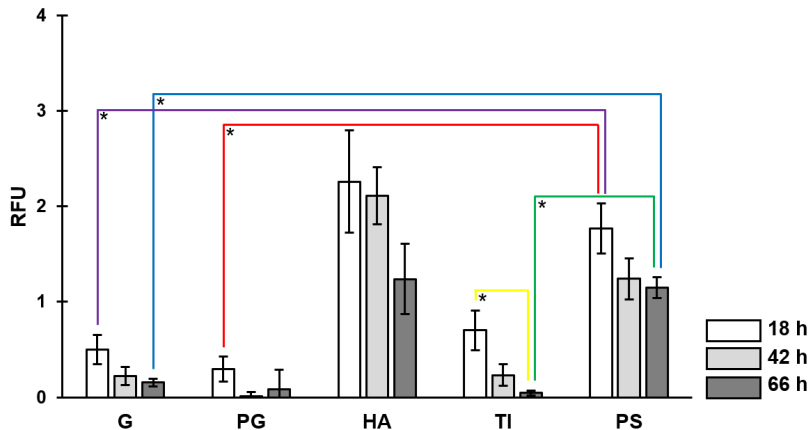


**Figure 8.** Quantification of PIA/PNAG (polysaccharide intercellular adhesin/poly-N-acetyl- $\beta$ -(1-6)-glucosamine) in *S. aureus* ATCC 25923 biofilms utilizing Wheat germ agglutinin Alexa Fluor® 488 conjugate (expressed as relative fluorescence units (RFUs)). Differences in PIA/PNAG amounts were compared for a particular material between different time points, and for a fixed time point between different materials, employing one-way ANOVA comparisons and Games–Howell post-tests for blank-corrected data points. \*, significant difference ( $p < 0.05$ ). Error bars depict the standard error of the mean (SEM) ( $n \geq 2$ ). G, borosilicate glass; PG, plexiglass; HA, hydroxyapatite; TI, titanium; PS, polystyrene. Figure adapted from publication I, with permission from MDPI, to keep consistency of this document.

This decreasing trend in PIA/PNAG-content as *in vitro* biofilm matures differs from the results of Oja et al. (2014): in their study the PIA/PNAG production of *S. aureus* ATCC 25923 seemed to be very pronounced from 4 to 24 h, while between 24–48 h PIA/PNAG-amount still increased but at a slower pace. However, in that study, the biofilms were grown in the Static Biofilm method without any shear stress, which may have affected the outcome. However, to the best of our knowledge, there are no reports comparing the amounts of PIA/PNAG of differently aged *S. aureus* biofilms grown in different *in vitro* methods. Nevertheless, it is known that the biofilm formation method has a large effect on, for example, antibiotic tolerance (Manner et al. 2017; Buckingham-Meyer et al. 2007). One possible explanation may be that in the Static Biofilm method, biofilms are grown in drier conditions compared to well plates where biofilms are submerged into the liquid. Thus, biofilms formed in the Static Biofilm method may try to protect themselves against potential desiccation by promoting the production of PIA/PNAG. On the other hand, the last measuring point of Oja et al. (2014) was at 48 h so it cannot be predicted what would have happened to the amount of PIA/PNAG after that point. In any case, in study I, this declining trend of PIA/PNAG was also observed with the fluorescence microscopy images of biofilms formed on G coupons (**Figure 9**). These images illustrate the macrostructural temporal progression from thick, irregular regions (**Figure 9A**; 18 h) to a thinner, more cohesive PIA/PNAG network (**Figure 9B**; 42 h).

## 5. RESULTS AND DISCUSSION

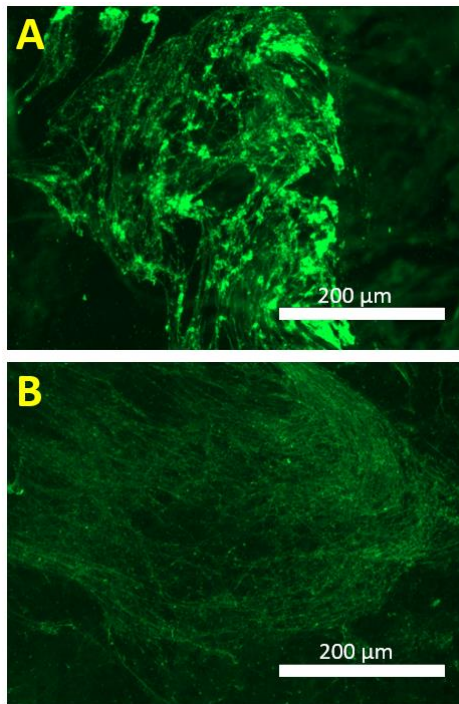


**Figure 9.** Fluorescence microscopy images of 18- (A) and 42-h-old (B) *S. aureus* ATCC 25923 biofilm matrix on borosilicate glass coupons stained with the WGA-Alexa Fluor® 488 fluorescent conjugate. The images were taken with Invitrogen™ EVOS® FL Imaging System. Figure originally included in publication I and reproduced with permission from MDPI.

These findings can potentially indicate that PIA/PNAG has a more vital role than proteins in managing the initial phase of the biofilm formation during the first 18 h. As PIA/PNAG is partially deacetylated by *icaB*, it has a positive net charge (Nguyen et al. 2020). This may contribute to intercellular attachment formation by binding to the negatively charged parts of adjacent cells. Moreover, the positive charge can also promote adherence to negatively charged surfaces. Furthermore, changes in the extracellular pH caused by metabolic fluctuations (*i.e.* accumulation of acidic fermentation products) may also have affected the PIA/PNAG-content. Indeed, it has been reported in the literature that pH <7 decreases the mechanical stability of *S. aureus* SH1000 biofilm matrix because the PIA/PNAG is much less charged at low pH (Stewart et al. 2015). In the same study, the *S. aureus* SH1000 biofilm matrix was in its most stable form within the pH range of 7–9. Among the materials explored here, it seems that PS and HA represent the materials where PIA/PNAG content of the biofilm matrix is higher.

### 5.1.4 Quantification of the protein fraction in the biofilm matrix (study I)

*S. aureus* biofilm matrix has been observed to contain a great number of proteins – however, the exact composition of the matrix protein fraction is not fully understood (Lei et al. 2017; Paharik and Horswill 2016; Speziale et al. 2014). Hence, in this study, the protein fraction of biofilm matrix was of interest. The total protein concentration, as well as the number of identified proteins of the biofilm matrix from biofilms formed on the five materials at 18, 42, and 66 h, were quantified. The clearest temporal elevation in the total protein concentration was detected with G- and HA-associated biofilms (**Figure 10A**). Biofilms formed on PS and PG had the highest protein concentration already at 42 h, and it declined at 66 h in both cases.

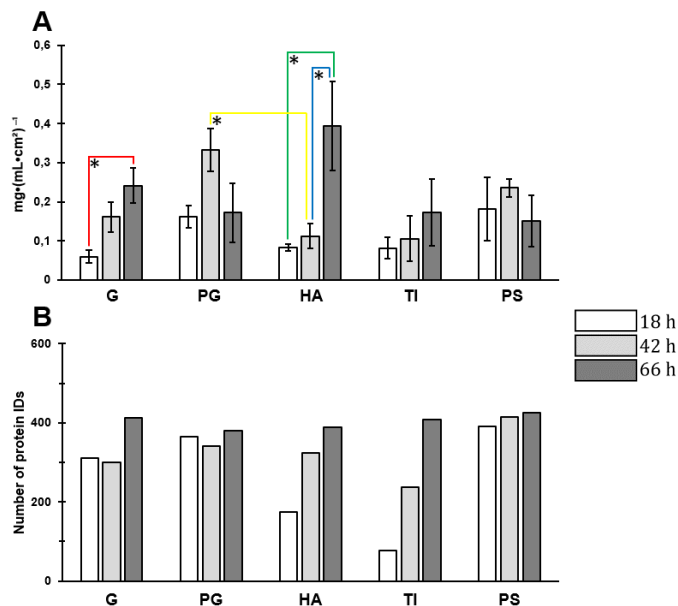


**Figure 10.** Protein concentrations  $\text{mg}\cdot(\text{mL}\cdot\text{cm}^2)^{-1}$  (**A**) and the number of the identified (detected in both replicates) biofilm matrix-associated proteins (**B**) of the *S. aureus* ATCC 25923 biofilms. Differences in protein concentrations were evaluated for a particular material between different time points, and for a fixed time point between the different materials, employing one-way ANOVA comparisons and Tukey post-tests for blank-corrected data points. \*, significant difference ( $p < 0.05$ ). Error bars denote the standard error of the mean (SEM) ( $n \geq 2$ ). G, borosilicate glass; PG, plexiglass; HA, hydroxyapatite; TI, titanium; PS, polystyrene. Figure adapted from publication I, with permission from MDPI, to keep consistency of this document.

## 5. RESULTS AND DISCUSSION

In contrast to the temporally declining PIA/PNAG-content, the protein role seemed to be more pivotal at the later stages of biofilm formation. Owing to the large material-dependent fluctuations in the amounts of exopolysaccharides (PIA/PNAG-fraction) and proteins, it seems plausible to assume that physicochemical factors, such as surface charge or hydrophilicity/hydrophobicity, might have contributed to the biofilm-substrate interactions.

Subsequently, trypsin shaving and LC-MS/MS analyses were carried out to identify all the individual proteins from the proteosurfaceomes. “Proteosurfaceome” refers to cell surface-exposed proteins that are either (i) associated with the plasma membrane (integral or anchored), (ii) anchored to the cell wall (via covalent or weak interactions), (iii) released in the extracellular milieu (*i.e.* exoproteins or extracellular proteins) or (iv) part of high molecular weight protein structures, such as pili or flagella (Desvaux et al. 2018). Based on our results, combined *S. aureus* proteosurfaceome catalogs were built. In total, 460 proteins were identified from all the samples, including all materials and time points. The highest temporal elevation in the number of proteins was observed with HA- and TI-associated biofilms (**Figure 10B**). At 18 h, the uppermost and the lowermost number of proteins were detected from PS- (390 proteins) and TI-associated biofilms (76 proteins), respectively. The number of common proteins at fixed time points (present on every material) were 67, 220, and 347 for 18-, 42-, and 66-h-old biofilms, respectively (**Figure 11A**). The core proteosurfaceome, that is the number of proteins that were common to all biofilms (*i.e.* detected on all materials at every time point), was 66 (**Figure 11B**).

The highest and lowest number of proteins, shared by all time points on a given material, was found with PS- (383 proteins) and TI-associated biofilms (74 proteins), respectively (**Figure 11D**). The quantities of uniquely identified proteins at different time points were analyzed and it was seen that the largest differences were with HA- and TI-related proteosurfaceomes (**Figure 11D**). While these proteosurfaceomes exhibited a moderately high number of specific proteins at 66 h (HA, 74 proteins; TI, 169 proteins), the high number of proteins shared by 42 and 66 h time points (HA, 142 proteins; TI, 164 proteins) could not be detected in the samples of other time points. Notably, TI-associated biofilms (at 18 h) lacked numerous proteins that were present on other materials.

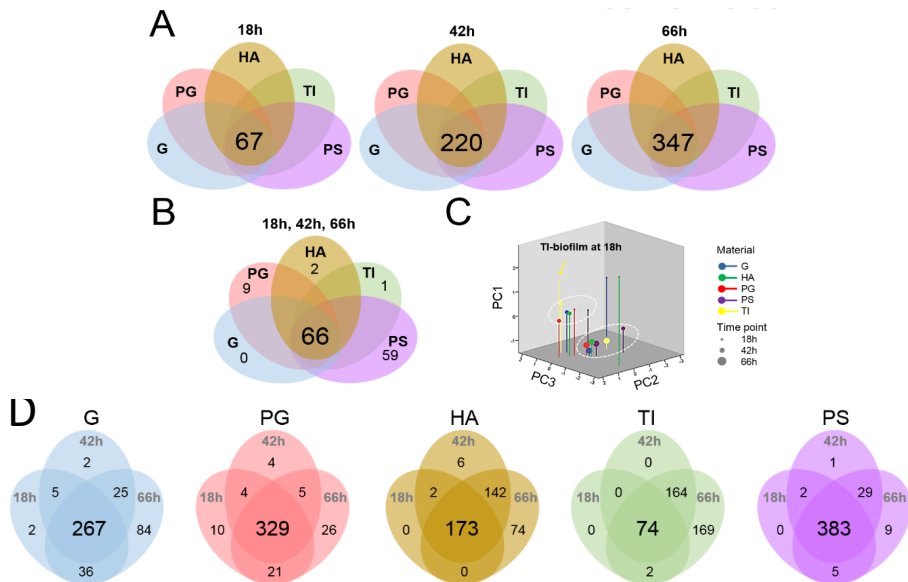


**Figure 11.** Venn diagrams denoting the number of proteosurfaceome proteins present on all materials at fixed time points (**A**) and the number of proteosurfaceome proteins that were present on all materials and time points (**B**). Outliers and clusters (circled) from a three-dimensional principal component analysis (3D PCA) performed on the material- and time point-dependent biofilm proteosurfaceomes (**C**). The number of specific and shared proteins of biofilms formed on different materials (at 18, 42, and 66 h) presented with Venn diagrams (**D**). G, borosilicate glass; PG, plexiglass; HA, hydroxyapatite; TI, titanium; PS, polystyrene. Figure adapted from publication **I** with permission from MDPI.

Finally, the dynamics of relative protein abundance changes were studied with a 3D PCA. **Figure 11C** shows two major clusters; <sup>(1)</sup> 66 h: all materials, 42 h: PS; <sup>(2)</sup> 42 h: G, HA, PG, and TI, 18 h: PG and PS. A third group “outliers” (TI-, G- and HA-associated biofilms at 18 h) was unconnected from the two main clusters. This suggests that TI, G, and HA promote specific proteosurfaceome changes during early phases of biofilm formation (*i.e.* attachment, during 18 h).

### 5.1.5 Qualification of the proteins in the biofilm matrix (study I)

Next, trypsin-released proteins/peptides of the proteosurfaceomes were identified with LC-MS/MS. In **Table 10**, changes in protein quantities in relation to the biofilm age and the used substrate material are presented. The following key clusters were recognized: virulence factors (5.1.5.1), regulatory proteins (5.1.5.2), Clp family proteins (5.1.5.3), and oxidoreductase enzymes (5.1.5.4). In addition, cytoplasmic moonlighting proteins with a described primary function in protein synthesis (5.1.5.5.1), glycolysis (5.1.5.5.2), or responses to stress (5.1.5.5.3) were identified. Known or potential moonlighting proteins

## *5. RESULTS AND DISCUSSION*

represented the greatest portion of the core proteosurfaceome. Among the moonlighting proteins, the ribosomal proteins (r-proteins) represented the most predominant group.



**Table 10.** Intensity values ( $\log_{10}$ ) of elected proteins on a heatmap illustrating the temporal changes in the protein abundances on different substrate materials. N/A = not available. Table adapted from publication I with permission from MDPI.

Protein name	Acc. No. <sup>(a)</sup>	Biological process	Location	18 h			42 h			66 h									
				PS	G	HA	PG	TI	PS	G	HA	PG	TI	PS	G	HA	PG	TI	
Bone sialoprotein-binding protein - Bbp	Q6GI46	Cell adhesion, virulence	Cell wall, secreted																
Clumping factor A - Cifa	Q6GIK4	Cell adhesion, virulence	Cell wall, secreted																
Clumping factor B - CifB	Q6GDH2	Cell adhesion, virulence	Cell wall, secreted																
Fibronectin-binding protein A - FnbPA	Q6GDU5	Cell adhesion, virulence	Cell wall, secreted																
Ser-Asp repeat-containing protein C - SdrC	Q6GJ47	Cell adhesion	Cell wall, secreted																
Ser-Asp repeat-containing protein D - SdrD	Q8NXX6	Cell adhesion	Cell wall, secreted																
Iron-reg. surface determinant prot. B - IsdB	Q6GHV7	Heme acquisition, virulence	Cell wall, secreted																
Bifunctional autolysin - Atl	Q6GI31	Cell wall biogenesis/degradation	Extracellular, secreted																
Elastin-binding protein Ebps	Q6GGT1	Cell adhesion, virulence	Plasma membrane																
Fibrinogen-binding protein - FbnBP	Q6GHS9	Complement binding, cell adhesion, virulence	Extracellular, secreted																
Conserved virulence factor B - CvfB	Q99U93	Virulence	N/A																
Ess extracellular protein A - EssxA	Q99WU4	Virulence	Extracellular, secreted																
Immunoglobulin-binding protein Sbi	Q6GE15	Virulence	Plasma membr., secreted																
Immunoglobulin G-binding protein A - Spa	P38507	IgG-binding, virulence	Cell wall, secreted																
Immunodominant staph. antigen A - IsaA	Q6GDN1	Glycosidase, hydrolase	Extracellular, secreted																
Immunodominant staph. antigen B - IsaB	Q6GDG4	Virulence	Extracellular, secreted																
Staphylococcal secretory antigen - SsaA2	Q99RX4	Immunogenic protein, virulence	Extracellular, secreted																
Phospholipase C - Hlb	Q5HEI1	Cytolysis, hemolysis, virulence	Extracellular																
Delta-hemolysin - Hld	Q6GF37	Cytolysis, hemolysis, virulence	Extracellular, secreted																
Gamma-hemolysin component B - HlgB	Q6GE12	Cytolysis, hemolysis, virulence	Extracellular																
Leukocidin-like protein 1 - Luk1	Q6GF50	Cytolysis	Extracellular																
Leukocidin-like protein 2 - Luk2	Q6GF49	Cytolysis	Extracellular																
Staphylocoagulase - Coa	P17855	Prothrombin activator	Extracellular																
Staphopain A - SspA	Q6GFE8	Hydrolase, protease, virulence	Extracellular, secreted																
Aminoacyltransferase FemA	Q99U47	Cell wall biogenesis/degradation, resistance	Cytoplasm																
Aminoacyltransferase FemB	Q6GH30	Cell wall biogenesis/degradation, resistance	Cytoplasm																
Lyxostaphin resistance protein A - LyrA	Q6GEA0	N/A	Plasma membrane																
Telcholic acid D-alanine hydrolase - FmtA	Q6GI27	Cell wall biogenesis/degradation, resistance	Plasma membrane																
Catabolite control protein A - CcpA	Q6GFX2	Transcription regulation	N/A																
Response regulator Cody	Q6GH0	Transcription regulation	Cytoplasm																
Response regulator SarA	Q7A732	Transcription regulation	Cytoplasm																
Response regulator Rot	Q9RF16	Transcription regulation	N/A																
Response regulator SarR	Q9FOR1	Transcription regulation	Cytoplasm																
Response regulator SarS	Q7A872	Transcription regulation	Cytoplasm																
Response regulator VraR	Q7A4R9	Transcription regulation	Cytoplasm																
Response regulator SaeR	Q99VR7	Transcription regulation	Cytoplasm																
Response regulator MsrR	Q99Q02	Transcription regulation	Cytoplasm																
Response regulator MraZ	Q6GHQ7	Transcription regulation	Plasma membrane																
Response regulator LytR	P52078	Transcription regulation	Nucleoid, cytoplasm																
Response regulator NrdR	Q6G20	Transcription regulation	N/A																
Response regulator GraR	Q6GI11	Transcription regulation	Cytoplasm																
Response regulator MgrA	Q99VT5	Transcription regulation	Cytoplasm																
Redox-sensing transcriptional repressor Rex	Q6GF26	Transcription regulation	Cytoplasm																

## 5. RESULTS AND DISCUSSION

Oxygen regulatory protein NreC	Q99RN8	Transcription regulation	Cytoplasm
Regulatory protein Spx	Q6GI88	Transcription regulation	Cytoplasm
RNA polymerase sigma factor SigA	Q99TT5	Transcription initiation/regulation	Cytoplasm
SOS response repressor LexA	Q9L4P1	DNA replication, SOS response, transcription reg.	N/A
Histidine protein kinase SaeS	Q99VR8	Two-component regulatory system, virulence	Plasma membrane
<b>ATP-dependent protease ATPase HslU</b>	Q6GH1	Protein unfolding, chaperone	Cytoplasm
Clp ATPase ClpC	Q99W78	Stress response, chaperone	N/A
Clp ATPase ClpL	Q6GD00	Stress response, chaperone	N/A
Chaperone protein ClpB	Q6GIB2	Stress response, chaperone	Cytoplasm
Endopeptidase Clp – ClpP	Q6GIM3	Hydrolase, protease	Cytoplasm
Thiol peroxidase – Tpx	Q6GFZ4	Response to oxidative stress, oxidoreductase	N/A
Uncharacterized oxidoreductase SAR2567	Q6GDV6	Oxidoreductase	N/A
Peptide methionine sulfoxide reductase MsrB	Q6GGY4	Oxidoreductase, protein repair	N/A
Putative heme-dependent peroxidase SAV0587	Q99WZ4	Oxidoreductase, heme biosynthesis	N/A
Thioredoxin reductase – TrxB	Q6GB66	Removal of superoxide radicals	Cytoplasm
NADPH-dependent oxidoreductase – NfrA	Q6GIR6	Oxidoreductase	N/A
Multicopper oxidase mco	Q6GIX3	Response to oxidative stress	Cytoplasm
Nitric oxide synthase oxygenase – Nos	Q6GFE2	Oxidoreductase	N/A
Putative NAD(P)H nitroreductase SAV2523	Q99RB2	Oxidoreductase	N/A
FMN-dependent NADPH-azoreductase – Azo1	Q99W49	Oxidoreductase	N/A
Thioredoxin – Trx	Q6GHU0	Electron transport	N/A
Malate:quinone oxidoreductase 2 – Mqo 2	Q6GDJ6	Krebs cycle	N/A
F-ATPase subunit delta – AtpH	Q6GEW9	Proton-transporting ATP synthase activity	Plasma membrane
F-ATPase subunit epsilon – AtpC	Q6GEX3	Proton-transporting ATP synthase activity	Plasma membrane
F-ATPase subunit gamma – AtpG	Q99SF4	Proton-transporting ATP synthase activity	Plasma membrane
<b>Non-heme ferritin – FtnA</b>	Q99SZ3	Iron storage	Cytoplasm
Ferrochelatase – HemH	Q6G8A3	Heme biosynthetic process	Cytoplasm
Foldase protein PrsA	Q6GFL5	Protein folding	Plasma membrane
ATP-dependent protease subunit HslV	Q6GH12	Hydrolase, protease	Cytoplasm
Prob. CtpA-like serine protease – SAR1432	Q6GGY8	Hydrolase, protease	Plasma membrane
Serine protease HtrA-like – SAR0992	Q6G162	Hydrolase, protease	Plasma membrane
Putative dipeptidase SAR1836	Q6GFV0	Hydrolase, protease	N/A
Protein RecA	Q6GHF0	DNA repair, SOS response	Cytoplasm
Anti-sigma-B factor antagonist – RsbV	Q6GF07	Anti-sigma factor antagonist activity	N/A
DegV domain-containing protein SAR1438	Q6GGY2	Possible in lipid transport/fatty acid metabolism	N/A
Signal transduction protein TRAP	Q6GFM2	Virulence, agr-system activation	Membrane
Probable cell wall amidase LytH	Q7A588	Cell wall biogenesis/degradation	Extracellular, secreted
Iron-sulfur cluster repair protein ScaA	Q6GK53	Stress response	Cytoplasm
Hydrolase in agr operon – ORF5	P55177	Stress response	Cytoplasm
Urease accessory protein UreG	Q99RX9	Nitrogen compound metabolic process	N/A
<b>Potential moonlighting proteins</b>			
30S ribosomal protein S1 – RpsA	Q6GGT5	Translation	Ribosome
30S ribosomal protein S10 – RpsI	Q931G5	Translation	Ribosome
30S ribosomal protein S11 – RpsK	Q6GEK8	Translation	Ribosome
30S ribosomal protein S12 – RpsL	Q6GJC3	Translation	Ribosome
30S ribosomal protein S13 – RpsM	Q6GEG7	Translation	Ribosome
30S ribosomal protein S15 – RpsO	Q99UJ9	Translation	Ribosome
30S ribosomal protein S16 – RpsP	Q6GH17	Translation	Ribosome
30S ribosomal protein S17 – RpsQ	Q8NVB4	Translation	Ribosome

5. RESULTS AND DISCUSSION

30S ribosomal protein S18 – RpsR	Q6GV1	Translation	Ribosome	
30S ribosomal protein S19 – RpsS	Q6GE17	Translation	Ribosome	
30S ribosomal protein S2 – RpsB	Q6GHH9	Translation	Ribosome	
30S ribosomal protein S20 – RpsT	Q99FR3	Translation	Ribosome	
30S ribosomal protein S21 – RpsU	Q6GGC5	Translation	Ribosome	
30S ribosomal protein S3 – RpsC	Q6GE19	Translation	Ribosome	
30S ribosomal protein S4 – RpsD	Q6GFY8	Translation	Ribosome	
30S ribosomal protein S5 – RpsE	Q6GEK0	Translation	Ribosome	
30S ribosomal protein S6 – RpsF	Q6GV3	Translation	Ribosome	
30S ribosomal protein S7 – RpsG	Q6GJC2	Translation	Ribosome	
30S ribosomal protein S8 – RpsH	Q6GEJ7	Translation	Ribosome	
30S ribosomal protein S9 – RpsI	Q6GEL8	Translation	Ribosome	
50S ribosomal protein L1 – RplA	Q6GJD0	Translation	Ribosome	
50S ribosomal protein L10 – RplJ	Q6GIC9	Translation	Ribosome	
50S ribosomal protein L11 – RplK	Q6GJD1	Translation	Ribosome	
50S ribosomal protein L13 – RplM	Q99S51	Translation	Ribosome	
50S ribosomal protein L14 – RplN	Q99S31	Translation	Ribosome	
50S ribosomal protein L15 – RplO	Q6GEK2	Translation	Ribosome	
50S ribosomal protein L16 – RplP	Q99S28	Translation	Ribosome	
50S ribosomal protein L17 – RplQ	Q99S46	Translation	Ribosome	
50S ribosomal protein L18 – RplR	Q99S37	Translation	Ribosome	
50S ribosomal protein L2 – RplB	Q6GEI6	Translation	Ribosome	
50S ribosomal protein L20 – RplT	Q6GG27	Translation	Ribosome	
50S ribosomal protein L21 – RplU	Q99TK6	Translation	Ribosome	
50S ribosomal protein L22 – RplV	Q99S26	Translation	Ribosome	
50S ribosomal protein L23 – RplW	Q99S23	Translation	Ribosome	
50S ribosomal protein L24 – RplX	Q6GEJ4	Translation	Ribosome	
50S ribosomal protein L25 – RplY	Q99WA2	Translation	Ribosome	
50S ribosomal protein L27 – RplA	Q93103	Translation	Ribosome	
50S ribosomal protein L28 – RplB	Q6GHL1	Translation	Ribosome	
50S ribosomal protein L29 – RplC	Q6GEJ1	Translation	Ribosome	
50S ribosomal protein L3 – RplC	Q6GEI3	Translation	Ribosome	
50S ribosomal protein L30 – RplD	Q6GEK1	Translation	Ribosome	
50S ribosomal protein L31 type B – RpmE2	Q6GEV5	Translation	Ribosome	
50S ribosomal protein L35 – RpmI	Q6GG26	Translation	Ribosome	
50S ribosomal protein L4 – RplD	Q6GEI4	Translation	Ribosome	
50S ribosomal protein L5 – RplE	Q99S33	Translation	Ribosome	
50S ribosomal protein L6 – RplF	Q99S36	Translation	Ribosome	
50S ribosomal protein L7/L12 – RplL	Q6GIC8	Translation	Ribosome	
50S ribosomal protein L9 – RplI	Q6GKT0	Translation	Ribosome	
Elongation factor G – EF-G	Q6GJCI	Protein biosynthesis	Cytoplasm	
Elongation factor Tu – EF-Tu	Q6GJCO	Protein biosynthesis	Cytoplasm	
Elongation factor P – EF-P	Q6GGH0	Protein biosynthesis	Cytoplasm	
Translation initiation factor IF-2 – InfB	Q6GHG6	Protein biosynthesis	Cytoplasm	
Translation initiation factor IF-3 – InfC	Q6GG25	Protein biosynthesis	Cytoplasm	
Phosphofructokinase – PFK	Q6GG08	Glycolysis	Cytoplasm	
Fructose-bisphosphate aldolase class 1 – FBA	Q6GDJ7	Glycolysis	N/A	
Triosephosphate isomerase – TPI	Q6GIL6	Gluconeogenesis, glycolysis, virulence	Cytoplasm	
Glyceraldehyde-3-phosphate dehydrogenase 1*	Q6GIL8	Glycolysis	Cytoplasm	
Phosphoglycerate kinase – PGK	Q6GIL7	Glycolysis	Cytoplasm	



### 5.1.5.1 Virulence factors

#### 5.1.5.1.1 Adherence factors

Several adherence factors were identified from the proteosurfaceomes of *S. aureus* ATCC 25923. These have traditionally been appealing in the medical context (Otto 2008), as they mediate the initial attachment and invasion of bacteria to host tissues (Foster et al. 2014; Speziale et al. 2014). Detected adherence factors could be roughly divided into two following groups: <sup>(1)</sup> cell wall (peptidoglycan) covalently anchored proteins: MSCRAMMs (**Table 10**; in lilac) and NEAT motif family (**Table 10**; in yellow) and <sup>(2)</sup> non-covalently linked surface proteins (**Table 10**; in brown). Among them, large variations in the expression of adherence factors were observed depending on the used substrate material (at 18 h). This indicates that the type of material determines which adhesins are utilized during the initial biofilm formation phase. Out of MSCRAMMs (**Table 10**; in lilac), bone sialoprotein-binding protein (Bbp) was detected on three materials at 18 h and at later time points (42 and 66 h) it was present on all materials with reasonably high identification scores. This protein Bbp, as the name indicates, binds to bone sialoprotein, which is a pivotal component of bone and dentine ECM. It plays a possible role in localizing the infection to bone tissue and increased IgG levels to Bbp have been associated with osteomyelitis (Persson et al. 2009).

Clumping factors A and B (ClfA/B) promote attachment to nasal epithelial cells (ClfB), bind to fibrinogen, and contribute to immune evasion by degrading neutrophil opsonin C3b (ClfA) (Foster et al. 2014). At 18 h, ClfB was present on four materials, while ClfA was present only on two materials. At later time points (42 and 66 h), both ClfA and ClfB were present on all materials with relatively high identification scores.

Fibronectin-binding protein A (FnBPA) binds to fibronectin, fibrinogen, and elastin and promotes intercellular adhesion (Heilmann 2011). Additionally, fibronectin-binding proteins facilitate the internalization of bacteria by epithelial cells (Dziewanowska et al. 1999), which may contribute to small colony variant formation responsible for persistent and recurrent infections (Otto 2018). FnBPA was detected on two materials (G and PG) at 18 h and on one material (PG) at 42 h. FnBPA was not found on any materials at the last time point (66 h). Therefore, it can be hypothesized that FnBPA could be more important in the initial phase of biofilm formation.

From the serine-aspartate repeat-containing protein family, two members were identified: SdrC and SdrD. Both promote adhesion to nasal epithelial cells (Heilmann 2011). At 18 h, SdrC was present on four materials (at 66 h on all materials), while SdrD adhesin was present only on two materials (HA, G) at every time point. Prevalence of ClfA, ClfB, FnBPA, and SdrC have been associated with strong *S. aureus* biofilm production ability (Chen et al. 2020a).

## 5. RESULTS AND DISCUSSION

Next, out of the NEAT motif family (**Table 10**; in yellow), iron-regulated surface determinant protein B (IsdB) was recognized. IsdB was present at 18 and 42 h on some materials, and it was not observed on any of the materials at 66 h. The NEAT motif proteins are utilized to capture heme from hemoglobin, hence facilitating bacteria to survive in the host where the limited iron amount is available. IsdB also contributes to invasion into non-phagocytic cells (Foster et al. 2014).

Finally, a group of non-covalently linked adherence factors was recognized (**Table 10**; in brown). Elastin-binding protein (EbpS), which is a membrane-spanning protein binding to elastin of ECM (Heilmann 2011), was identified merely on certain materials; EbpS was not present on HA or PG at any of the time points. Another non-covalently linked adherence factor, fibrinogen-binding protein (FbnBP) belongs to a group of SERAM proteins. FbnBP attaches to fibrinogen and impairs C3b opsonization. Furthermore, as FbnBP attracts fibrinogen to the bacterial surface, FbnBP has been hypothesized to assist the coagulase-dependent fibrin shield formation around the bacteria. This in turn would protect from phagocytosis (Ko et al. 2013). This protein, FbnBP, was detected on most of the materials at 18 h. In comparison to FbnBP, FbnBP was detected on all materials at later time points (42 and 66 h) with reasonably high identification scores, implying its crucial role also in the biofilm maturation.

Lastly, bifunctional autolysin (Atl) that participates in the initial attachment phase of biofilm formation by binding to fibrinogen, fibronectin, vitronectin, human endothelial cells, and polystyrene (Heilmann 2011), was extremely abundant on all materials at every time point and reached the highest level at 66 h. This autolysin, Atl, is the key peptidoglycan hydrolase in staphylococci that maintains the equilibrium of peptidoglycan synthesis/degradation and contributes to the separation of the daughter cells during cell division (Porayath et al. 2018). Furthermore, Atl seems to participate in the excretion of moonlighting cytoplasmic proteins to the cell surface (see 2.4.2) (Pasztor et al. 2010). Indeed, Atl has been shown to be strongly upregulated in modestly aged *S. aureus*, and contributing to the excretion and accumulation of intracellular cytoplasmic proteins in the biofilm matrix (Graf et al. 2019).

### 5.1.5.1.2 Proteins contributing to immunoevasion

Several proteins contributing to immunoevasion with various mechanisms were also observed (**Table 10**; in light blue). A novel virulence-associated protein, conserved virulence factor B (CvfB), was detected on every material at 66 h. CvfB controls the production of hemolysins, DNases, and proteases (Liang et al. 2017). Ess extracellular protein A (EsxA) is also an essential virulence factor promoting the establishment of infection in the host. First, EsxA is responsible for delaying apoptosis of *S. aureus*-infected host cells allowing intracellular bacterial replication. Moreover, after intracellular replication, EsxA contributes to the release of *S. aureus* from the host cells to spread the infection to other

locations (Korea et al. 2014). It was found in moderate amounts on all materials at 42 and 66 h.

Ig-binding protein Sbi and IgG-binding protein A (Spa), which bind IgG in a wrong orientation hindering complement fixation by the classical pathway and opsonophagocytosis (Atkins et al. 2008), were identified with high identification scores on every material at every time point. IgG is the most common antibody in the human serum (accounts for 80% of the serum antibodies), and responsible for enhancing phagocytosis, neutralizing toxins, and activating the complement system (Tortora et al. 2014, p. 503). The Spa has also been observed to act as a B-cell superantigen, stimulating proliferation and depletion of the B-cell repertory (Atkins et al. 2008). Moreover, it has been observed to induce bacterial aggregation and biofilm formation (Merino et al. 2009).

Several antigens were also detected. One of them, immunodominant staphylococcal antigen (IsaA) is a major antigen of *S. aureus* and highly immunogenic, and therefore, a potential target for immunization. In addition, it is reported to contribute to biofilm stability, peptidoglycan turnover, and cell division (Koedijk et al. 2017). Immunodominant staphylococcal antigen B (IsaB) is an immunodominant antigen and has been observed to promote the virulence and persistence of MRSA by decreasing host autophagic flux (Liu et al. 2015). Both (IsaA, IsaB) were highly expressed on all materials at every time point.

Finally, staphylococcal secretory antigen (SsaA2) was detected on all materials (except on TI) at every time point. Elevated antibody levels against SsaA2 have been associated specifically with endocarditis (in the case of *S. epidermidis*) (Lang et al. 2000). Altogether, these observations suggest that *S. aureus* can actively control the host immune system, even sheltered within the biofilm.

#### 5.1.5.1.3 Host-damaging proteins

A few immunoevasive proteins with direct cytolytic properties over erythrocytes and leukocytes were identified (**Table 10**; in red). Among these, beta-hemolysin (phospholipase C; Hlb), which is sphingomyelinase that degrades the sphingomyelin component of host cell surfaces (Otto 2014b), was detected on all materials at later time points (42 and 66 h). The delta-hemolysin (Hld), which belongs to a PSM peptide family with erythrocyte- and neutrophil-lytic activity (Cheung et al. 2015), was mostly detected on PS. The gamma-hemolysin component B (HlgB), which is a component of the bi-component gamma-hemolysins HlgAB or HlgCB, was detected with moderate levels on all materials at every time point. These HlgAB and HlgCB have been shown to contribute to the lysis of erythrocytes, neutrophils, and monocytes/macrophages (Spaan et al. 2017). Leukocidin-like proteins (Luk1 and Luk2) were detected on every material and time point, and their abundances reached the highest level at 66 h. For example, the LukAB and HlgAB have been observed to be efficiently secreted *in vivo* in the chronic animal infection model (Lei et al. 2017). Graf et al. (2019) have demonstrated leukocidins and hemolysins to play a crucial role in

## 5. RESULTS AND DISCUSSION

the biofilm lifestyle as they were more abundant in the *S. aureus* HG001 biofilm matrix compared to its planktonic counterpart. Moreover, especially leukocidin and gamma hemolysin genes have been observed to be significantly higher expressed when *Staphylococcus aureus* USA300 was growing *in vivo* compared to its *in vitro* grown counterpart (Xu et al. 2016).

### 5.1.5.1.4 Exoenzymes

A handful of enzymes contributing to immunoevasion were also identified (**Table 10**; in orange). With the aid of a clotting factor, staphylocoagulase (Coa), the infection site can be coated with fibrin clots (Thomer et al. 2013). This provides a barrier against the host immune system, such as phagocytosis, and promotes abscess formation (Cheng et al. 2010). Furthermore, Coa contributes to the adhesion of *S. aureus* on indwelling medical devices (Vanassche et al. 2013). This protein, Coa, was detected only at later time points (42 and/or 66 h) on certain materials (PS, G, HA). By contrast, another exoenzyme (staphylokinase) that contributes to fibrin clot degradation and spreading of the infection (Tortora et al. 2014, p. 450), was not detected on any of the samples.

Another major *S. aureus* exoenzyme, staphopain A (SspP), was identified here in all biofilms (except on HA, at 18 h). The SspP is a cysteine protease that blocks neutrophil chemokine receptors and therefore, hampers phagocytosis (Laarman et al. 2012). Furthermore, SspP promotes vascular leakage causing septic shock-related hypotension (Imamura et al. 2005). Additionally, another staphopain (B) has been observed to disturb host defenses and enhance biofilm persistence by degrading AMP (LL-37) (Sonesson et al. 2017). Finally, thermonuclease (Nuc) that evades from killing strategies of neutrophils by degrading neutrophil extracellular traps (NETs) (Sultan et al. 2019), was detected on all materials at every time point (except on HA) (**Table 10**; in turquoise).

### 5.1.5.1.5 Antimicrobial resistance factors

As a last group of virulence factors presented here, some antimicrobial resistance factors were identified on certain materials (**Table 10**; in pink). Herein, potentially, PG and PS could trigger enzyme-related antibiotic resistance, since aminoacyltransferases (FemA and FemB), lysostaphin resistance protein A (LyrA), and teichoic acid *D*-alanine hydrolase (FmtA) were detected on those materials already at 18 h. Therefore, biofilms formed on other materials may potentially be more susceptible to certain antibiotics. The aminoacyltransferases FemA and FemB affect  $\beta$ -lactam antibiotic resistance indirectly via cell wall development by catalyzing the formation of interpeptide bridges in peptidoglycan (Henze et al. 1993; Maidhof et al. 1991). The LyrA is associated with increased resistance to a bacteriocin, lysostaphin (Gründling et al. 2006). Finally, FmtA removes *D*-alanine groups from the teichoic acid, thus regulating the electrical charge of the bacterial surface, and increases also greatly methicillin resistance (Rahman et al. 2016).



### 5.1.5.2 Regulatory proteins

Transcriptional regulators control the rate of gene transcription by inducing (inducer) or inhibiting (repressor) RNA polymerase binding to DNA (Tortora et al. 2014, p. 221). Therefore, these regulatory proteins control various activities such as biofilm formation, pathogenesis, and drug resistance (Richardson et al. 2015). Many regulatory proteins were already present at 18 h at least on one of the materials (**Table 10**; in burgundy). The relative abundances of most of the regulators increased over time achieving the highest degree at 66 h. At least regulatory proteins CcpA, CodY, and VraR have been observed playing a role and in host-pathogen interaction *in vivo* (Michalik et al. 2017; Richardson et al. 2015). Furthermore, regulatory proteins CcpA, CodY, MgrA, Rot, SaeR, SaeS, SarA, Spx, and LytR have been detected to contribute to biofilm formation (Graf et al. 2019).

### 5.1.5.3 Clp family proteins

The abundances of the Clp family proteins (ClpC, ClpL, ClpB, and ClpP) had material-dependent variation and increased temporally on all materials (**Table 10**; in lime green). The Clp proteolytic complexes have a suggested role in adaptation to stress conditions by degrading misfolded proteins. In addition, they are employed as chaperones refolding proteins denatured by stress (Michel et al. 2006; Squires and Squires 1992). Furthermore, they have been reported to be important in biofilm formation, virulence (Frees et al. 2004) and abundant in host-pathogen interaction *in vivo* (ClpC, ClpL, ClpB; Michalik et al. 2017). Interestingly, the Clp proteins were not detected on TI at 18 h.

### 5.1.5.4 Cellular oxido-redox state-maintaining enzymes

Several oxidoreductase enzymes were also identified during the protein analysis (**Table 10**; in grey). They catalyze the transfer of electrons from the electron donor (reductant) to the electron acceptor (oxidant) (Tortora et al. 2014, pp. 110–111). Several of such enzymes were present only on some materials at 18 h but reached the highest abundance or prevalence at 66 h.

### 5.1.5.5 Cytoplasmic proteins as moonlighters

Traditionally, classical surface proteins have been considered as one of the most attractive targets in drug development against bacterial pathogens. However, in this context, assaying non-classical moonlighting proteins should also be included, as many of their moonlighting functions include actions that aid in infection establishment. As previously indicated, the moonlighting proteins refer to proteins, which have two or more separate and physiologically relevant functions (Kainulainen and Korhonen 2014). MoonProt, a database for moonlighting proteins (MoonProt: A Database for Moonlighting Proteins 2020; Chen et al. 2018), includes over 500 proteins with reported canonical and moonlighting activities. Moonlighting proteins are not restricted to only bacteria: they have also been identified in protists, fungi, plants, and animals (Chen et al.

## 5. RESULTS AND DISCUSSION

2018). Very recently, a collection of moonlighting proteins was suggested to be responsible for a novel molecular mechanism for offering improved stability to *S. aureus* biofilms (Graf et al. 2019). Indeed, reutilizing cytoplasmic proteins as moonlighting components may benefit the biofilm population. Therein, proteins switch between the functions depending on which function currently benefits the cell, e.g. in the cytoplasm in energy metabolism and later on the cell surface increasing the cell virulence, stability, immunoevasion, and attachment on host tissues (Kainulainen and Korhonen 2014).

Overall, understanding the mechanism of how moonlighters are directed to the cell surface could provide novel antibacterial drug targets that would block the secretion or association of moonlighters with the cell surface (Jeffery 2018). However, whether the moonlighters participate in the development of *S. aureus* biofilms on various prosthetic materials, has not been evident.

### 5.1.5.5.1 Protein synthesis-associated adhesins

In study I, the cytoplasmic proteins with suggested moonlighting functions (Chen et al. 2018; Franco-Serrano et al. 2018) formed a substantial group among all identified proteins. Furthermore, e.g. 37 proteins of the core proteosurfaceome (out of the 66 proteins) were moonlighting proteins. This is aligned with *in vivo* results by Lei et al. (2017), where substantial amounts of *S. aureus* cytoplasmic proteins compared to extracellular/cell surface-associated proteins were observed in a rat PJI model. The abundances of the moonlighters were not dependent on the used substrate material. The largest identified protein group overall and the most massive group among the moonlighting proteins included r-proteins (**Table 10**; in dark blue). They are employed as proteins forming the prokaryotic 70S ribosomes together with ribosomal RNA. The 70S ribosomes are composed of two subunits: small 30S and large 50S subunits, and both 30S- and 50S-associated r-proteins were identified on all materials. Typically, their abundances increased towards the 66-h time point. In ribosomes the translation of messenger RNA (mRNA) into proteins by transfer RNA (tRNA) molecules takes place. Bacterial cytoplasm includes thousands of such ribosomes (Tortora et al. 2014, p. 88). It has been suggested that r-proteins also play an important role in the cohesivity of the *S. aureus* biofilm matrix. Herein, oxygen limitation in biofilms causes the release of fermentation end-products (formate, lactate, and acetate) generating acidic conditions. Therefore, alkaline r-proteins and virulence factors get positively charged and form electrostatic interactions with anionic cell wall components, eDNA, and metabolites. This high affinity between the components mediates the stabilization of the biofilm matrix (Graf et al. 2019). It has been implied that besides the tasks of r-proteins in the cytoplasm, they could have an extra-ribosomal role associating with the cell surfaces and operate as a shielding mechanism to external threats caused by e.g. antibiotics, the host immune system, or changing environmental conditions (Alreshidi et al. 2016). Indeed, in

one proteomic study, it was observed that the production of r-proteins increased as a response to exposure to an antibacterial agent (Voigt et al. 2016).

Elongation factors (EF-TU, EF-G, and EF-P) that are responsible for chain elongation during protein synthesis at the ribosome, were identified with high identification scores on all materials at every time point (**Table 10**; in light lilac). At least elongation factors (EF-Tu and EF-G) have been suggested to have moonlighting roles: their moonlighting functions are presented in **Table 11**.

#### 5.1.5.5.2 Glycolytic adhesins

In carbohydrate catabolism, the chemical energy of glucose is released and stored in ATP via cellular respiration or fermentation. Cellular respiration of glucose is composed of three steps: glycolysis, the Krebs cycle, and the electron transport chain (Tortora et al. 2014, p. 118). Herein, most of the enzymes participating in a glycolytic metabolic pathway were identified, forming another large group within moonlighting proteins (**Table 10**; in green). Their moonlighting functions are presented in **Table 11**. All of them (excluding phosphoglyceromutase, PGAM) were remarkably abundant on all the materials at every time point, and their abundances reached the highest level at 66 h. The abundances of these proteins generally exceeded the levels of the r-proteins.

**Table 11.** Selected moonlighting proteins: their canonical and moonlighting functions. References in this table are listed below.

Protein	Function 1	Function 2	Species
<b>Ribosomal proteins (r-proteins)</b>	Translation	Translational repressors <sub>1, 2, 3</sub>	<i>E. coli</i> <sup>1, 2, 3</sup>
<b>Elongation factor G, EF-G</b>	Elongation factor activity in translation	Binds to mucin <sup>4</sup>	<i>Streptococcus gordonii</i> <sup>4</sup>
<b>Elongation factor Tu, EF-Tu</b>	Elongation factor activity in translation	Attaches to human cells, mucins <sup>5</sup> , fibronectin <sup>6</sup> , and plasminogen <sup>7</sup>	<i>Lactobacillus johnsonii</i> <sup>5</sup> ; <i>Mycoplasma pneumoniae</i> <sup>6</sup> ; <i>P. aeruginosa</i> <sup>7</sup>
<b>Phosphofruktokinase, PFK</b>	Glycolysis	Binds plasminogen <sup>8</sup>	<i>Streptococcus oralis</i> <sup>8</sup>
<b>Fructose-bisphosphate aldolase class 1, FBA</b>	Glycolysis	Attaches to human cells <sup>9</sup>	<i>Neisseria meningitidis</i> <sup>9</sup>
<b>Triosephosphate isomerase, TPI</b>	Glycolysis	Adhesin, the contact-mediated killing of <i>Cryptococcus</i> <sup>10</sup> binds to plasminogen <sup>11</sup>	<i>S. aureus</i> <sup>10, 11</sup>
<b>Glyceraldehyde-3-phosphate dehydrogenase 1, GAPDH 1</b>	Glycolysis	Binds transferrin in iron acquisition <sup>12</sup> , binds mucin, Caco-2 cells <sup>13</sup> , fibronectin, laminin, type I collagen <sup>14</sup> , and plasminogen <sup>8, 12</sup>	<i>S. aureus</i> , <i>S. epidermidis</i> <sup>12</sup> ; <i>Lactobacillus plantarum</i> <sup>13</sup> ; <i>Paracoccidioides brasiliensis</i> <sup>14</sup> ; <i>Streptococcus anginosus</i> , <i>S. oralis</i> <sup>8</sup>
<b>Phosphoglycerate kinase, PGK</b>	Glycolysis	Binds plasminogen <sup>8</sup>	<i>S. anginosus</i> , <i>S. oralis</i> <sup>8</sup>

## 5. RESULTS AND DISCUSSION

<b>Phosphoglyceromutase, PGAM</b>	Glycolysis	Binds plasminogen <sup>8, 15</sup>	<i>S. anginosus</i> , <i>S. oralis</i> <sup>8</sup> ; <i>Bifidobacterium lactis</i> , <i>Bifidobacterium bifidum</i> , <i>Bifidobacterium longum</i> <sup>15</sup>
<b>Enolase, ENO</b>	Glycolysis	Binds plasminogen <sup>8, 16</sup> and laminin <sup>16, 17</sup>	<i>S. anginosus</i> , <i>S. oralis</i> <sup>8</sup> ; <i>Lactobacillus crispatus</i> , <i>L. johnsonii</i> <sup>16</sup> ; <i>S. aureus</i> <sup>16, 17</sup>
<b>Pyruvate kinase, PYK</b>	Glycolysis	Binds to invertase <sup>18</sup>	<i>Lactococcus lactis</i> <sup>18</sup>
<b>Pyruvate dehydrogenase E1 subunit <math>\beta</math>, PDHB</b>	The link between glycolysis and Krebs cycle	Binds fibrinogen <sup>6</sup>	<i>M. pneumoniae</i> <sup>6</sup>
<b>Aconitase, Acn</b>	Krebs cycle	Iron homeostasis <sup>19</sup>	<i>Mycobacterium tuberculosis</i> <sup>19</sup>
<b>Alcohol dehydrogenase, ADH</b>	Oxidoreductase	Binds plasminogen <sup>20</sup> , fibronectin, laminin, type II collagen <sup>21</sup> , and ribosomes affecting translation <sup>22</sup>	<i>C. albicans</i> <sup>20</sup> ; <i>Entamoeba histolytica</i> <sup>21</sup> ; <i>E. coli</i> <sup>22</sup>
<b>Chaperone protein GroEL</b>	Chaperone	Binds to human cells <sup>23</sup> , binds to mucins and epithelial cells <sup>24</sup>	<i>Chlamydia pneumoniae</i> <sup>23</sup> ; <i>L. johnsonii</i> <sup>24</sup>
<b>Chaperone protein DnaK</b>	Chaperone	Binds plasminogen <sup>15, 25, 26</sup>	<i>B. lactis</i> , <i>B. bifidum</i> , <i>B. longum</i> <sup>15</sup> ; <i>M. tuberculosis</i> <sup>25</sup> ; <i>N. meningitidis</i> <sup>26</sup>
<b>Superoxide dismutase [Mn/Fe] 1 - SodA (S)</b>	Neutralizes ROS	Binds to epithelial cells <sup>27</sup>	<i>Mycobacterium avium</i> <sup>27</sup>
<b>RNA polymerase subunit <math>\beta</math> - RpoC</b>	RNA-polymerase	Binds to salivary mucin <sup>4</sup>	<i>S. gordonii</i> <sup>4</sup>
<b>Glutamine synthetase, GS</b>	Glutamine synthesis	Binds to a transcription regulator <sup>28</sup> , fibronectin, collagen I, laminin <sup>29</sup> , and plasminogen <sup>29, 25</sup>	<i>M. tuberculosis</i> <sup>25</sup> ; <i>Bacillus subtilis</i> <sup>28</sup> ; <i>L. crispatus</i> <sup>29</sup>
<b>N-acetylmuramoyl-L-alanine amidase, Sle1</b>	Autolysin, cell division, peptidoglycan hydrolase	Binds fibronectin <sup>30, 31</sup>	<i>S. aureus</i> <sup>30</sup>

<sup>1</sup> Dean et al. 1981; <sup>2</sup> Brot et al. 1980; <sup>3</sup> Yates et al. 1980; <sup>4</sup> Kesimer et al. 2009; <sup>5</sup> Granato et al. 2004; <sup>6</sup> Dallo et al. 2002; <sup>7</sup> Kunert et al. 2007; <sup>8</sup> Kinby et al. 2008; <sup>9</sup> Tunio et al. 2010; <sup>10</sup> Yamaguchi et al. 2010; <sup>11</sup> Furuya and Ikeda 2011; <sup>12</sup> Modun and Williams 1999; <sup>13</sup> Kinoshita et al. 2008; <sup>14</sup> Barbosa et al. 2006; <sup>15</sup> Candela et al. 2007; <sup>16</sup> Antikainen et al. 2007; <sup>17</sup> Carneiro et al. 2004; <sup>18</sup> Katakura et al. 2010; <sup>19</sup> Banerjee et al. 2007; <sup>20</sup> Crowe et al. 2003; <sup>21</sup> Yang et al. 1994; <sup>22</sup> Shasmal et al. 2016; <sup>23</sup> Wuppermann et al. 2008; <sup>24</sup> Bergonzelli et al. 2006; <sup>25</sup> Xolalpa et al. 2007; <sup>26</sup> Knaust et al. 2007; <sup>27</sup> Reddy and Suleman 2004; <sup>28</sup> Wray et al. 2001; <sup>29</sup> Kainulainen et al. 2012; <sup>30</sup> Heilmann et al. 2005.

### 5.1.5.5.3 Chaperones and other stress proteins

Chaperones (GroEL, DnaK, DnaJ, and GroES) and other stress-associated proteins (universal stress protein SAV1710, Usp; alkaline shock protein 23, Asp23; superoxide dismutase [Mn/Fe] 1, SodA; alkyl hydroperoxide reductases C and F, AhpC and AhpF) were among the potential moonlighting proteins (**Table 10**; in turquoise). The canonical function of chaperones is to contribute to the folding of new proteins and re-folding of misfolded proteins under normal and stress conditions. The Usp belongs to a general stress protein family that contributes to bacterial adaptation and colonization in the human host

environment by facilitating tolerating e.g. oxidative stress, high temperature, low pH, and hypoxia (O'Connor and McClean 2017), while Asp23 provides protection against alkaline pH values (Kuroda et al. 1995). The SodA, AhpC and AhpF provide cellular defense against ROS and oxidative stress. SodA converts superoxide radicals ( $O_2^{\cdot-}$ ) to molecular oxygen ( $O_2$ ) and hydrogen peroxide ( $H_2O_2$ ) (Tortora et al. 2014, p. 157), while AhpC and AhpF catalyze the reduction of hydrogen peroxide to water and alcohols. All of these aforementioned proteins were identified on most of the materials at 18 h and on all materials at 42 and 66 h. Chaperone DnaK and stress proteins (AhpC/F, Usp, SodA) have been observed to participate in host-pathogen interaction *in vivo* (Michalik et al. 2017). On the other hand, glutamine synthetase, a multi-tasking protein responsible for glutamine synthesis, transcription regulation, and chaperone activity, was interestingly identified only in TI-associated biofilms.

### 5.1.6 Chemotolerance assays (study I)

Based on HA and TI being the most clinically significant materials, they were chosen for further chemotolerance assays. Herein, 18- and 66-h-old biofilms on HA and TI were exposed to various antibiotics: 5.0  $\mu$ M vancomycin, 4.0  $\mu$ M doxycycline, 90.0  $\mu$ M levofloxacin, and 2.0  $\mu$ M penicillin G for 2 or 24 h. The antibiotics in this study were selected to cover a wide spectrum of mechanisms of action.

Levofloxacin, vancomycin, and doxycycline are frequently used as a part of the treatment regimen in managing staphylococcal PJIs. Usually, vancomycin is *iv.*-administered for 2 weeks after the operation (if methicillin-, oxacillin- or rifampicin-resistance has been detected). As previously indicated, vancomycin is a bactericidal glycopeptide antibiotic that inhibits the cell wall synthesis (Terveysportti: Lääkkeet ja hinnat -database 2021; Tortora et al. 2014, p. 595). Doxycycline or levofloxacin are administered *p.o.* as continuation therapy to achieve a total duration of antibiotic treatment of 12 weeks (Li et al. 2018). Doxycycline is a semi-synthetic, bacteriostatic broad-spectrum tetracycline-derivative, which prevents protein synthesis by interfering with the attachment of amino acid-carrying tRNA to the mRNA-70S ribosome complex. Levofloxacin is a bactericidal synthetic fluoroquinolone antibiotic, which inhibits bacterial DNA gyrase enzyme preventing DNA replication. Lastly, penicillin G (benzylpenicillin) is a bactericidal beta-lactam antibiotic that inhibits cross-linking of peptidoglycan, and therefore, the construction of cell walls (Terveysportti: Lääkkeet ja hinnat -database 2021; Tortora et al. 2014, pp. 593–598).

All of the antibiotics decreased the viable cell counts (CFUs) in a statistically significant manner ( $p < 0.05$  and  $p < 0.001$ ) with the 24-h-long exposure (in comparison to the TSB-treated control biofilms (**Figure 12**)). From the tested antibiotics, levofloxacin (90  $\mu$ M) was observed to be the most competent in decreasing the biofilms developed on both materials. The most successful treatment outcome was obtained when 18-h-old biofilms were exposed to

## 5. RESULTS AND DISCUSSION

levofloxacin for 24 h. After levofloxacin, the second most active was penicillin G or doxycycline, depending on the used substrate material. The least effective compound was vancomycin.

These results are in accordance with Manner et al. (2017): in their study against *S. aureus* ATCC 25923, levofloxacin was the most efficient, followed by doxycycline, penicillin G, and vancomycin. Similarly, in Mandell et al. (2019), doxycycline was more effective than vancomycin against different *S. aureus* clinical isolates.

The biofilm formation material had an impact on the biofilm chemotolerance; 66-h-old biofilms on HA were more susceptible than TI-associated biofilms to all of the antibiotics when exposed to antibiotics for 2 h (**Table 12**). In most of the cases (in 8 out of 11), HA-associated biofilms were more susceptible to antibiotics than TI-associated biofilms.

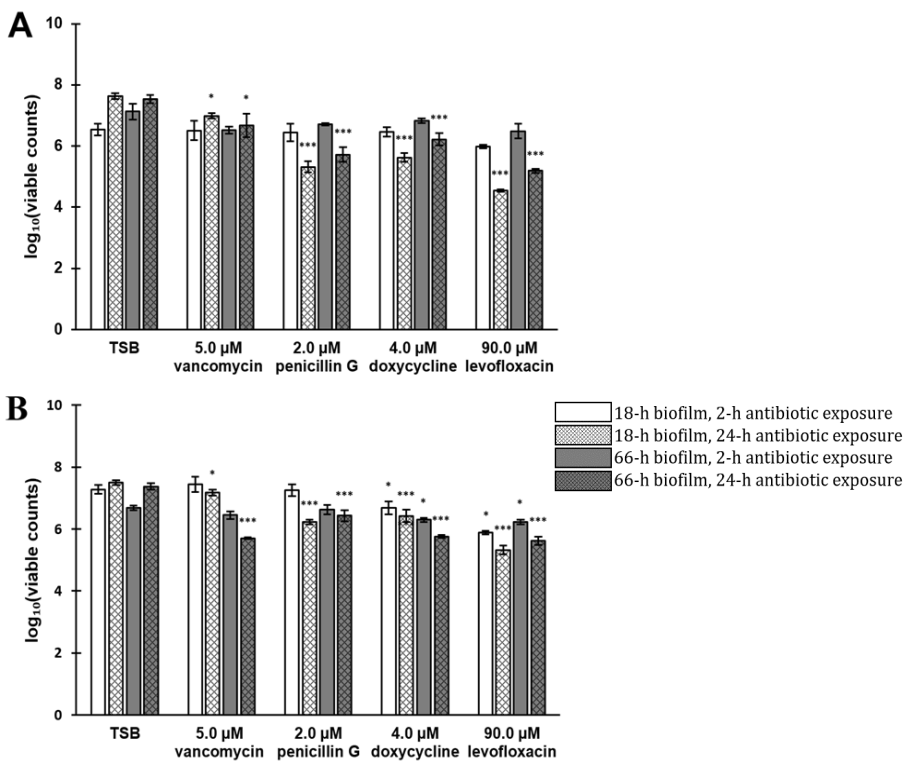


**Figure 12.** Chemotolerance of 18- and 66-h-old *S. aureus* ATCC 25923 biofilms formed on hydroxyapatite (**A**) and titanium (**B**) when treated with diverse antibiotics for 2 or 24 h (expressed as  $\log_{10}$  values of  $\text{CFU} \cdot (\text{mL} \cdot \text{cm}^2)^{-1}$ ). The statistical analysis was conducted by employing unpaired t-tests with Welch's correction by comparing the antibiotic-treated biofilms to TSB-treated biofilms. \*, significant difference ( $p < 0.05$ ); \*\*\*, highly significant difference ( $p < 0.001$ ). Error bars signify the standard error of the mean (SEM) ( $n \geq 2$ ). Figure adapted from publication I, with permission from MDPI, to keep consistency of this document.

It is generally expected the chemotolerance changes as the biofilm matures (Chen et al. 2020b). Therefore, the effect of the biofilm age on chemotolerance was assayed next. Interestingly, a direct correlation between the biofilm age and the measured chemotolerance was not consistently seen. In 3 out of 10 cases, the older (66 h) biofilms were more susceptible than the younger (18 h) biofilms. In the remaining cases (7 out of 10), the 18-h-old biofilms were however more susceptible than the 66-h-old biofilms. Of course, the situation could have been quite different if, for example, 18-h biofilms had been compared to e.g. 2-week-old biofilms. Unsurprisingly, the increased antibiotic exposure time (from 2 to 24 h) reduced chemotolerance regardless of the biofilm age or material.

**Table 12.** The chemotolerance of 18- and 66-h-old *S. aureus* ATCC 25923 biofilms on hydroxyapatite (HA) and titanium (TI) when exposed to several antibiotics. Quantification was performed employing the log reduction of viable counts. Table adapted from publication I, with permission from MDPI, to keep consistency of this document.

Biofilm Age	Biofilm Formed on	Exposure Time	Penicillin G (2.0 $\mu\text{M}$ ) <sup>a</sup>	Levofloxacin (90.0 $\mu\text{M}$ ) <sup>a</sup>	Doxycycline (4.0 $\mu\text{M}$ ) <sup>a</sup>	Vancomycin (5.0 $\mu\text{M}$ ) <sup>a</sup>
18 h	HA	2 h	0.10 $\pm$ 0.28	0.56 $\pm$ 0.06	0.08 $\pm$ 0.15	0.03 $\pm$ 0.31
18 h	TI	2 h	0.01 $\pm$ 0.19	1.39 $\pm$ 0.05 ***, †††	0.59 $\pm$ 0.21 *, †	-0.17 $\pm$ 0.25
18 h	HA	24 h	2.32 $\pm$ 0.18 ***, †††, $\Omega$	3.09 $\pm$ 0.04 ***, †††, $\Omega$ $\Omega$	2.00 $\pm$ 0.14 *, †, $\Omega$ $\Omega$ $\Omega$	0.65 $\pm$ 0.09 $\Omega$
18 h	TI	24 h	1.28 $\pm$ 0.08 †	2.18 $\pm$ 0.15 †††, $\Omega$ $\Omega$ $\Omega$	1.08 $\pm$ 0.20 $\Omega$	0.33 $\pm$ 0.09
66 h	HA	2 h	0.42 $\pm$ 0.04 *	0.64 $\pm$ 0.24 *, †	0.31 $\pm$ 0.08	0.61 $\pm$ 0.11 *, †
66 h	TI	2 h	0.07 $\pm$ 0.15	0.46 $\pm$ 0.08	0.39 $\pm$ 0.06	0.24 $\pm$ 0.12
66 h	HA	24 h	1.82 $\pm$ 0.24 *, $\Omega$ $\Omega$ $\Omega$	2.35 $\pm$ 0.07 ***, $\Omega$	1.32 $\pm$ 0.20 $\Omega$	0.88 $\pm$ 0.38
66 h	TI	24 h	0.94 $\pm$ 0.18 $\Omega$	1.76 $\pm$ 0.14 $\Omega$ $\Omega$ $\Omega$	1.62 $\pm$ 0.04 *, †, $\Omega$ $\Omega$ $\Omega$	1.67 $\pm$ 0.03 $\Omega$

<sup>a</sup> The values denote logR values demonstrating the difference between medium- and antibiotic-treated biofilms. \*,  $p < 0.05$  and \*\*\*,  $p < 0.001$ ; differences between the HA- and TI-associated biofilms (when the biofilm age and exposure time are constant). †,  $p < 0.05$  and †††,  $p < 0.001$ ; differences between the 18- and 66-h-old biofilms (when the exposure times and the materials are constant).  $\Omega$ ,  $p < 0.05$  and  $\Omega$   $\Omega$   $\Omega$ ,  $p < 0.001$ ; differences between the exposure times: 2 and 24 h (when the biofilm ages and the materials are constant). The statistical analyses were executed employing unpaired t-tests with Welch's correction.

Finally, it was tested whether trypsin has an additional beneficial effect supporting levofloxacin therapy. For that purpose, 18- and 66-h-old biofilms formed on HA were treated with <sup>(1)</sup> trypsin (51.9 ng· $\mu\text{L}^{-1}$ ) followed by 90  $\mu\text{M}$  levofloxacin, <sup>(2)</sup> 100 mM TEAB followed by 90  $\mu\text{M}$  levofloxacin or <sup>(3)</sup> TSB (**Figure 13**). The results revealed that trypsin did not offer an additional eradication effect on levofloxacin. In addition, there was no difference between the 18- and 66-h-old trypsin- and levofloxacin-treated biofilms, thus it seemed that the protein content of the biofilm matrix was already well-established at the 18 h, at least from the perspective of tolerating enzymatic treatment. As the protein fractions increased in a statistically significant manner from 18 to 66 h in HA-associated *S. aureus* biofilms (**Figure 10A**), it could have been assumed that the

protection provided by the 66-h biofilm matrix would have been better than that provided by the 18-h biofilm matrix. On the other hand, the penetration of levofloxacin through the biofilm matrix seemed to occur without problems, so that pre-treatment with trypsin may not necessarily provide an additional eradication benefit for levofloxacin. This seemed to be in alignment with the report by Singh et al. (2016), where the penetration of antibiotics from several mechanistic groups through *S. aureus* ATCC 25923 biofilm was assayed. The antibiotic with the best penetrating capabilities was tetracycline followed by ciprofloxacin (which belongs to the same fluoroquinolone group as levofloxacin). In retrospect, our results could have been different e.g. with vancomycin, which had the worst penetration capability through the *S. aureus* ATCC 25923 biofilm matrix (Singh et al. 2016).

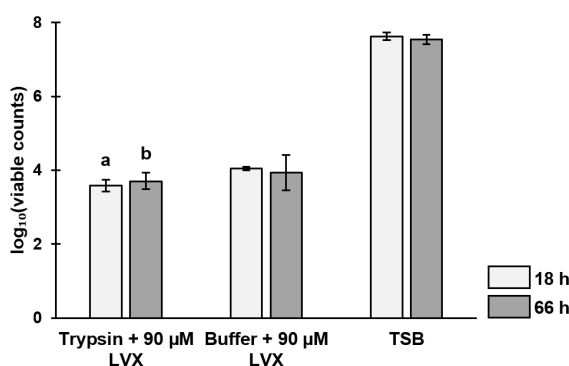


**Figure 13.** Viability of 18- and 66-h-old *S. aureus* ATCC 25923 biofilms on hydroxyapatite coupons exposed to (1) trypsin and 90 µM levofloxacin (LVX); (2) triethylammonium bicarbonate buffer (TEAB) (trypsin buffer) and 90 µM LVX; (3) tryptic soy broth (TSB), expressed as log<sub>10</sub> values of CFU (mL·cm<sup>2</sup>)<sup>-1</sup>. A highly significant difference in viability ( $p < 0.001$ , using unpaired *t*-tests with Welch's correction) was observed only when compared to (a) TSB at 18 h and (b) TSB at 66 h. Error bars denote the standard error of the mean (SEM) ( $n \geq 2$ ). Figure adapted from publication I, with permission from MDPI, to keep consistency of this document.

## 5.2 Anti-biofilm effect of bisphosphonate-bioactive glass combinations against staphylococcal biofilms in the prosthetic joint infection biofilm model (study II)

### 5.2.1 Optimization of the prosthetic joint infection biofilm model (study II)

In this study, testing a novel therapeutical alternative in the treatment of prosthetic joint infection (PJI) was of interest. For that purpose, constructing an *in vitro* PJI biofilm model was required. Bacterial strains *S. aureus* (ATCC 25923 and Newman) and *S. epidermidis* RP62A (ATCC 35984) were chosen for this



study, as these are very common biofilm-forming pathogens in PJIs (Li et al. 2018). To the best of our knowledge, there are no standardized biofilm testing methods available for PJIs. The only existing validated biofilm methods have been generated by ASTM and tailored for *P. aeruginosa*. Furthermore, most of these ASTM-validated biofilm methods utilize biofilm reactors (such as CDC Biofilm Reactor and Rotating Disk Reactor) where biofilms are formed in large growth medium volumes under high shear stress. These would not simulate well the PJI conditions. Moreover, such systems require large amounts of the test compounds or formulations (Coenye and Nelis 2010) and are not compatible with testing semisolid two-component formulations.

In staphylococcal biofilm research, the most typical approach is to grow biofilms directly in 96-well plates. However, polystyrene cannot be regarded as a relevant material to reflect *in vivo* conditions of PJI. To mimic *in vivo* conditions more appropriately, implementation of clinically relevant surfaces is required. For that purpose, a user-friendly approach is to grow biofilms on discs made of various materials inserted into well plates, as in study I. However, this assembly cannot be considered ideal for this study II where semisolid samples composed of BPs and BAG were tested. Therefore, a better-suited biofilm model that more correctly mimics the conditions encountered by bacteria in a PJI (minor quantity of liquid, low shear stress), needed to be introduced. To meet these requirements, the Static Biofilm method was chosen. This method has also been used by Shaqour et al. (2020) to study anti-biofilm effects of 3D-printed materials against *S. aureus* ATCC 25923, which is one of the strains tested here in study II. The advantages of the Static Biofilm are its robustness, simplicity, price-friendliness, and the absence of requirements for sophisticated instrumentation. It allows the testing of versatile substrate materials, as well as liquid and solid test compounds (Oja et al. 2014).

First, suitable biofilm-forming conditions were optimized by comparing four substrate materials and two incubation times. Herein, three clinically relevant materials (plexiglass, PG; titanium, TI; hydroxyapatite, HA) were involved using the reference material and time point by Buckingham-Meyer et al. (2007) (borosilicate glass, G; 48 h). The clinical relevance of the materials is described in section 5.1.1. The AFM topographical images and roughness parameters of those materials are presented in **Figure 6**, **Table 9**, and **Figure S2**.

Bacterial attachment of *S. aureus* ATCC 25923, *S. aureus* Newman, and *S. epidermidis* RP62A (ATCC 35984) on the three materials was compared to the biofilm control, 48-h-old biofilms on G, as used in a crucial publication that introduced the optimized Static Biofilm method (Buckingham-Meyer et al. 2007). Bacteria were incubated under humidified aerobic conditions at 37°C for 24 and 48 h and quantified as log<sub>10</sub> of viable counts (CFU·mL<sup>-1</sup>). The bacterial attachment of all strains was significantly higher on HA (24 h) (**Figure 14**) when compared to the control material (G, 48 h) ( $p < 0.05$ ). As a comparison to study I, where biofilms were grown in liquid cultures, the viable colonies of HA-associated *S. aureus* ATCC 25923 biofilms increased from 18 to 42 h. In contrast, here in study

## 5. RESULTS AND DISCUSSION

**II**, where *S. aureus* ATCC 25923 biofilms were grown in static cultures, the viable colonies on HA seemed to slightly decrease from 24 to 48 h.

This biologically most relevant material (HA), with a convenient biofilm formation time (24 h), was chosen for the susceptibility trials for all the strains.

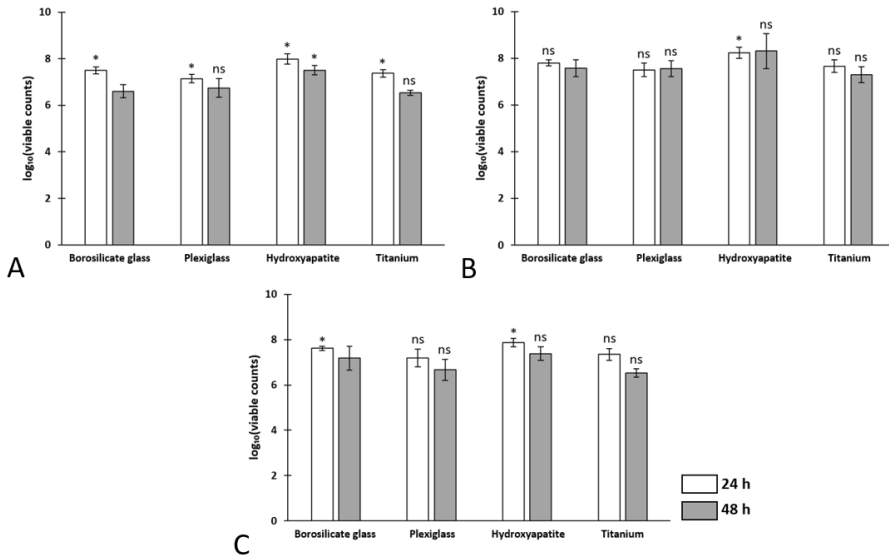


**Figure 14.** Biofilm formation of *S. aureus* ATCC 25923 (A), *S. aureus* Newman (B), and *S. epidermidis* RP62A (ATCC 35984) (C) for 24 and 48 h on the materials (expressed as log<sub>10</sub> values of CFU·mL<sup>-1</sup>). The bacterial attachment was assessed against the control material (borosilicate glass, 48 h) utilizing unpaired t-tests with Welch's correction. \*, statistically significant ( $p < 0.05$ ); ns, not significant difference. Error bars denote standard deviations (SD) (n=6). Figure adapted from publication II, with permission from Elsevier, to keep consistency of this document.

### 5.2.2 Examination of bisphosphonates in combination with inert glass and bioactive glass against staphylococcal biofilms (study II)

At first, anti-biofilm effects of five BPs (alendronate, clodronate, etidronate, risedronate, and zoledronate) combined with BAG were tested against *S. aureus* ATCC 25923, *S. aureus* Newman, and *S. epidermidis* RP62A (ATCC 35984) biofilms (incubated under humidified aerobic conditions at 37°C for 24 h) using a negative control (IG-BAG) (Figure 15; Table 13).

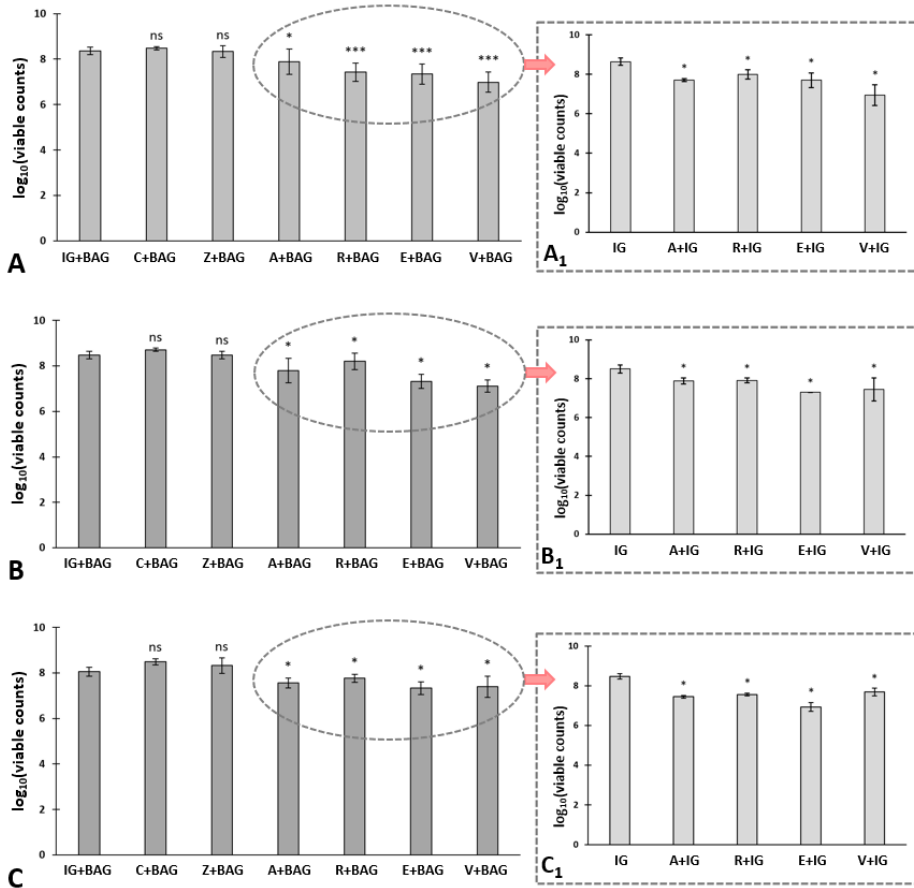


**Figure 15.** Biofilm formation of *S. aureus* ATCC 25923 (**A**), *S. aureus* Newman (**B**), and *S. epidermidis* RP62A (ATCC 35984) (**C**) (presented as  $\log_{10}$  values) on hydroxyapatite coupons covered with BP-BAG samples ( $n \geq 4$ ). The elected BPs were mixed with IG to examine their genuine anti-biofilm effect (**A<sub>1</sub>**, **B<sub>1</sub>**, and **C<sub>1</sub>**) ( $n \geq 2$ ). An unpaired *t*-test with Welch's correction was used. \*\*\*, highly significant difference ( $p < 0.001$ ); \*, significant difference ( $p < 0.05$ ); ns, not significant difference. Error bars denote standard deviations (SD). A, alendronate; C, clodronate; E, etidronate; R, risedronate; Z, zoledronate; V, vancomycin; IG, inert glass; BAG, bioactive glass. Figure adapted from publication II, with permission from Elsevier, to keep consistency of this document.

The positive control used here, vancomycin-BAG, was shown to reduce viable counts of the two *S. aureus* strains and *S. epidermidis* ( $p < 0.05$  or  $p < 0.001$ ) in a statistically significant manner. Vancomycin is a bactericidal glycopeptide antibiotic that inhibits cell wall synthesis (Terveysportti: Lääkkeet ja hinnat -database 2021; Tortora et al. 2014, p. 595). The combinations of risedronate-BAG, etidronate-BAG, and alendronate-BAG significantly reduced viable counts

## 5. RESULTS AND DISCUSSION

of all tested bacterial samples ( $p < 0.05$  or  $p < 0.001$ ). By contrast, zoledronate- and clodronate-BAG were not effective against any of the bacterial strains.

**Table 13.** The logR-values (expressing the difference between the control and the test compound samples) of the BP-BAG and BP-IG combinations. Vancomycin-IG and -BAG were included as positive controls. N/A = not available. Table adapted from publication II, with permission from Elsevier, to keep consistency of this document.

Bisphosphonate (BP)	logR (BP-IG)	logR (BP-BAG)
<i>Staphylococcus aureus</i> ATCC 25923		
Etidronate	1.00 ± 0.07	1.10 ± 0.08
Risedronate	0.67 ± 0.02	1.00 ± 0.06
Alendronate	0.93 ± 0.002	0.61 ± 0.13
Zoledronate	N/A	0.06 ± 0.03
Clodronate	N/A	-0.12 ± 0.01
Vancomycin	1.77 ± 0.07	1.44 ± 0.07
<i>Staphylococcus aureus</i> Newman		
Etidronate	1.20 ± 0.001	1.21 ± 0.05
Risedronate	0.59 ± 0.005	0.32 ± 0.05
Alendronate	0.62 ± 0.007	0.81 ± 0.13
Zoledronate	N/A	0.01 ± 0.01
Clodronate	N/A	-0.23 ± 0.01
Vancomycin	1.14 ± 0.09	1.39 ± 0.03
<i>Staphylococcus epidermidis</i> RP62A (ATCC 35984)		
Etidronate	1.55 ± 0.01	0.75 ± 0.03
Risedronate	0.91 ± 0.001	0.31 ± 0.01
Alendronate	1.02 ± 0.001	0.51 ± 0.02
Zoledronate	N/A	-0.23 ± 0.04
Clodronate	N/A	-0.44 ± 0.01
Vancomycin	0.79 ± 0.01	0.74 ± 0.08

Second, the BPs of the three most active combinations were analyzed in terms of their intrinsic anti-biofilm effect. Etidronate, risedronate, and alendronate were combined with inert glass (IG) to physically mimic the two-component semisolid paste with the BAG (inserts **A1**, **B1**, and **C1** in **Figure 15**; **Table 13**) and compared to mere IG (negative control). The positive control (vancomycin-IG) reduced viable counts in a significant manner when compared to the negative control ( $p < 0.05$ ). Alendronate-, etidronate- and risedronate-IG combinations reduced viable counts of all the tested *Staphylococcus* spp. significantly ( $p < 0.05$ ). Antimicrobial effects of risedronate against *P. aeruginosa* and *E. coli* (minimal inhibitory concentration, MIC = 1.4 mg/mL for both species; Kruszewska et al. 2012), and the biofilm inhibitory effect of risedronate against *E. coli* and *Salmonella pullorum* (>60 %, at 300 µM) (Reshamwala et al. 2016) have been reported in the literature. The antimicrobial activities of alendronate against *E. coli*, *P. aeruginosa*, and *C. albicans* (MIC = 5, 10, and 5 mg/mL, respectively; Kruszewska et al. 2002) have also been described. Moreover, clodronate has a reported antibacterial effect against planktonic *P. aeruginosa* with a MIC of 63 mg/mL (Kruszewska et al. 2002). However, in our study clodronate was not effective, at least not against biofilms. In contrast,

antimicrobial activity for etidronate has not been earlier reported in the literature. Mechanistic insight into the actions of BP-BAGs will be further discussed in section 5.4.

### 5.3 Anti-biofilm effect of bisphosphonate-bioactive glass combinations against *Aggregatibacter actinomycetemcomitans* biofilms in the periodontal biofilm model (study III)

#### 5.3.1 Optimization of the dental biofilm model (study III)

In this study, similar combinations of BPs and BAG (as those used in study II) were tested as a therapeutical alternative against periodontitis. From this perspective, periodontitis is a more novel and less studied target disease than PJI: only one BP-BAG has been tested against periodontitis in a pilot clinical trial (Rosenqvist et al. 2017), to the best of our knowledge. Moreover, the anti-biofilm effects of BP-BAGs have not yet been studied in that application.

In this study III, a periodontal pathogen and late colonizer in dental biofilms *Aggregatibacter actinomycetemcomitans* ATCC 33384 was chosen to simulate periodontal biofilms. This particular organism was selected due to its extensively documented role in periodontal tissue damage (e.g. Arirachakaran et al. 2012). There are also no standardized biofilm testing methods available for periodontal biofilms. For mimicking periodontal biofilms, a number of experimental models have been used, such as growing oral biofilms on well plates (Oettinger-Barak et al. 2013) or discs made of various materials inserted into well plates (Park et al. 2014; Sánchez et al. 2011). However, as previously indicated, these commonly utilized well plates are not suitable for semisolid sample testing (herein, a combination of BPs and BAG). Therefore, a better-suited biofilm model that more accurately reflects oral cavity conditions (*i.e.* a small fluid volume in the absence of fluid shear stress) (Lagerlöf and Dawes 1984) needed to be introduced. To meet these requirements, the Static Biofilm method was also chosen, as in the previous study II.

Before the anti-biofilm testing was initiated, pertinent substrate material and a suitable biofilm formation time were correspondingly determined. For that purpose, three clinically relevant materials for dental applications (plexiglass, PG; titanium, TI; hydroxyapatite, HA) were compared to the reference material used by Buckingham-Meyer et al. (2007) (borosilicate glass, G). HA is the mineral component of bones and dentine (Kelly et al. 2015), and the three selected materials (HA, in addition to PG and TI) are all used as dental implant materials. The AFM topographical images and roughness parameters of the materials are represented in **Figure 6**, **Table 9**, and **Figure S2**.

Bacteria were incubated under humidified microaerophilic conditions at 37°C for 24 and 48 h and quantified as log<sub>10</sub> of viable counts (CFU·mL<sup>-1</sup>). In the conditions of the assay, bacteria attached on all four surfaces after 24 and 48 h without significant statistical differences when compared to the control material

## 5. RESULTS AND DISCUSSION

(G) (**Figure 16**). Hence, the most clinically relevant substrate material for dental applications – HA – was chosen for further assays.

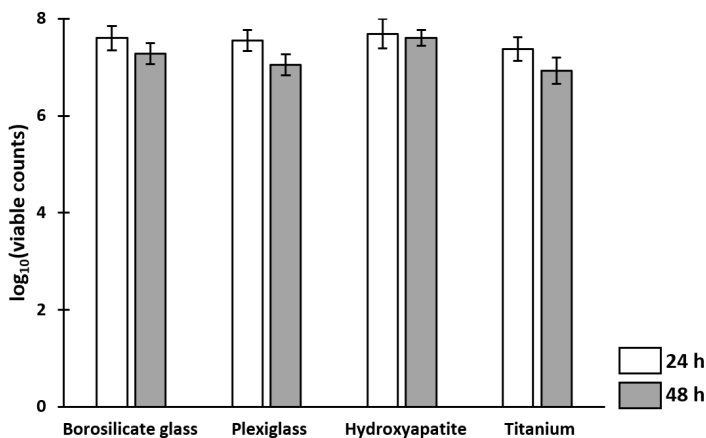


**Figure 16.** Bacterial attachment of *A. actinomycetemcomitans* ATCC 33384 on four substrate materials after 24 and 48 h of incubation (depicted as  $\log_{10}$  values of CFU·mL<sup>-1</sup>). Bacterial attachment of each material was compared to the control material (borosilicate glass) at fixed time points using unpaired t-tests with Welch's correction. The differences were not statistically significant ( $p < 0.05$  was considered statistically significant). Error bars denote standard deviations (SD) ( $n=6$ ). Figure adapted from publication III, with permission from Elsevier, to keep consistency of this document.

Next, the presence of *A. actinomycetemcomitans* ATCC 33384 biofilms on the HA surface was confirmed with imaging. Topographical images taken with AFM of HA coupons before and after the bacterial attachment are shown in **Figure 17A** and **Figure 17B**, respectively. Relatively high roughness values were measured on the HA surface ( $S_{dr} = 63 \pm 6\%$ ;  $S_q = 2200 \pm 320$  nm). The surface area ratio ( $S_{dr}$ ) expresses the roughness-induced increase of the interfacial surface area relative to the area of the projected flat plane. The root-mean-square roughness ( $S_q$ ) indicates the standard deviation of height values. The  $S_{dr}$  value was in correspondence to the value measured in study I (**Table 9**). The AFM topographs show the existence of attached bacteria on the HA surface already at 24 h (**Figure 17B** and **Figure 17C**) after the incubation in humidified microaerophilic conditions at 37°C. Local clusters of bacteria were observed on the surface (blue square; **Figure 17B**), but also single planktonic bacteria were distinguishable (red circle; **Figure 17B**). The average dimensions of the observed rod-shaped bacteria were  $1.1 \pm 0.2$   $\mu\text{m}$  (length) and  $0.590 \pm 0.035$  nm (width), and these were in correspondence to the AFM images of *A. actinomycetemcomitans* D7S that were more recently published by Bao et al. (2018).

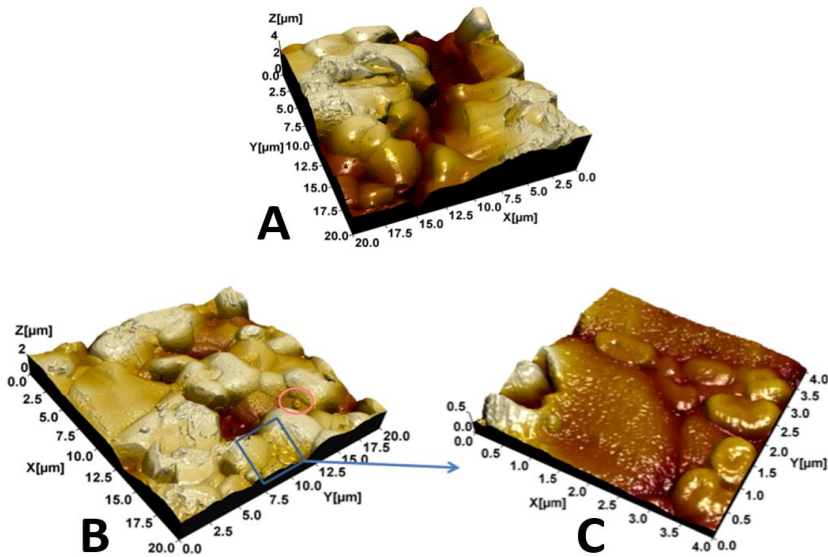


**Figure 17.** AFM topographical image of a hydroxyapatite coupon surface (image size: 20 x 20  $\mu\text{m}$ ) (A), 24-h-old *A. actinomycetemcomitans* ATCC 33384 biofilm growing on the hydroxyapatite (image size: 20 x 20  $\mu\text{m}$ ) (B), and a zoomed cluster of *A. actinomycetemcomitans* ATCC 33384 cells (image size: 4 x 4  $\mu\text{m}$ ) (C). A local bacterial cluster and a planktonic bacterium are indicated with the blue square and red circle, respectively. Figure adapted from publication III with permission from Elsevier.

The chemotolerance of 24- and 48-h-old *A. actinomycetemcomitans* ATCC 33384 biofilms on HA were compared. The biofilms were first allowed to form in humidified microaerophilic conditions at 37°C for 2, 24, and 48 h. Samples with bacteria attached for 2 h were used here as a reference for young biofilms, to assess the kinetic course of development of the biofilm tolerance. Next, the biofilms were exposed to 25  $\mu\text{M}$  (0.0015% (w/v)) or 50  $\mu\text{M}$  (0.003%) (w/v) CHX, or medium (TSB-YE/Glc, as a negative control) in microaerophilic conditions at 37°C for 2 h. The selected CHX concentrations were based on Wood et al. (2015). The compound CHX is a cationic antimicrobial agent that interacts with the negatively charged plasma membrane and causes a subsequent leakage of cytoplasmic components (Gilbert and Moore 2005). This agent is widely applied in mouth rinses in the treatment of gingivitis, caries, and mouth infections at concentrations within the range of 0.06–0.2% (Terveysportti: Lääkkeet ja hinnat -database 2021).

The bacterial attachment on coupons (expressed as  $\log_{10}$  values of CFU·mL<sup>-1</sup>) and logR-values (denoting the bacterial burden reduction after the CHX treatments), are shown **Figure 18** and **Table 14**. In the case of bacteria attached for 2 h, the differences in bacterial viability were statistically significant in samples exposed to both 25 and 50  $\mu\text{M}$  CHX, when compared to untreated

## 5. RESULTS AND DISCUSSION

bacteria. The logR values were over 4 for both CHX concentrations (25 and 50  $\mu\text{M}$ ).

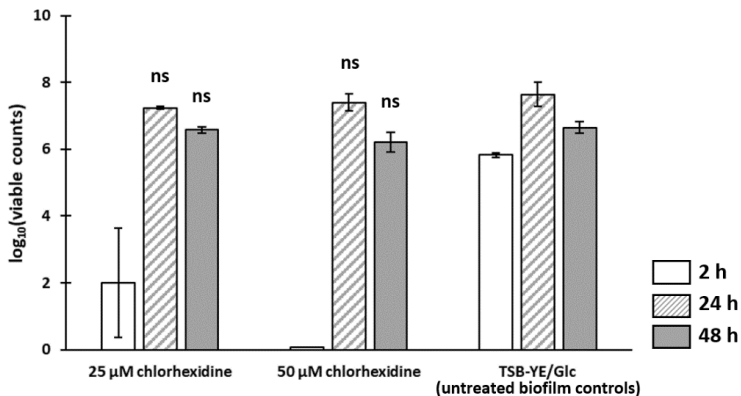


**Figure 18.** The bacterial attachment (expressed as  $\log_{10}$  values of  $\text{CFU}\cdot\text{mL}^{-1}$ ) of 2-, 24- and 48-h-incubated *A. actinomycetemcomitans* ATCC 33384 on hydroxyapatite coupons, when exposed to chlorhexidine (25 or 50  $\mu\text{M}$ ) or medium (TSB-YE/Glc). The chlorhexidine (25 and 50  $\mu\text{M}$ ) -treated biofilms were compared to TSB-YE/Glc-treated biofilms, using an unpaired t-test with Welch's correction ( $p < 0.05$ ). ns, not significant difference. Error bars denote standard deviations (SD) ( $n \geq 2$ ). Figure adapted from publication III, with permission from Elsevier, to keep consistency of this document.

The effect was more significant with the 50  $\mu\text{M}$  CHX concentration, where the viable bacteria were completely eradicated. This situation reflects the known fact that 2 h incubated bacteria can be regarded as being rather surface-attached proliferating planktonic bacteria than biofilms and that the cells are not yet sealed within the protective biofilm matrix.

**Table 14.** The chemotolerance of different aged biofilms (expressed as logR-values, representing the difference between chlorhexidine- (CHX) and medium-treated coupons). Table adapted from publication III, with permission from Elsevier, to keep consistency of this document.

Incubation time	logR (25 $\mu\text{M}$ CHX)	logR(50 $\mu\text{M}$ CHX)
2 h	$4.25 \pm 0.42$	$5.83 \pm 0$
24 h	$0.40 \pm 0.0005$	$0.26 \pm 0.02$
48 h	$0.07 \pm 0.003$	$0.47 \pm 0.024$

The differences between CHX (25 and 50  $\mu\text{M}$ ) treated 24- and 48-h-old biofilms were not statistically significant when compared to untreated (TSB-YE/Glc-exposed) biofilms. The logR values of 24- and 48-h-old biofilms were under 0.5 for both CHX concentrations. This indicates that both 24- and 48-h-old biofilms can withstand exposure to relatively high CHX concentrations and therefore, have already reached a chemotolerant state. This is in agreement with results obtained by Park et al. (2014). In their study, 24-h-old *A.*



*actinomycescomitans* ATCC 33384 biofilms were capable to tolerate even CHX concentrations of 1110  $\mu$ M. In the study of Takahashi et al. (2007), 48-h-old *A. actinomycescomitans* 310a biofilms were observed to be more tolerant to several antibiotics when compared to 24-h-old biofilms. Therefore, the longer incubation time (48 h) was chosen for further susceptibility assays.

### 5.3.2 Examination of bisphosphonates in combination with inert glass and bioactive glass against periodontal biofilms (study III)

After the optimal material (HA) and incubation time (48 h) were established, the compounds were assayed in terms of their anti-biofilm activity. To the best of our knowledge, BAG and BPs have not been studied against *A. actinomycescomitans* ATCC 33384 biofilms. The BPs alone (*i.e.* combined with inert glass) (**Figure 19; Table 15**) and combined with BAG (**Figure 20; Table 15**) were tested against *A. actinomycescomitans* ATCC 33384 biofilms in humidified microaerophilic conditions, at 37°C, for 48 h. As shown in **Figure 19**, biofilms treated with the positive control (CHX-IG) had significantly fewer viable counts ( $p < 0.001$ ) than IG-treated biofilms (negative control). In terms of the intrinsic effects of the BPs, risedronate-IG was the only BP-IG combination that displayed anti-biofilm activity ( $p < 0.05$ ). In line with that finding, risedronate has proven antimicrobial and anti-biofilm effect against some gram-negative strains (Reshamwala et al. 2016; Kruszewska et al. 2012). On the contrary, the reported antimicrobial activities of alendronate and clodronate against some gram-negative strains (Kruszewska et al. 2002) were not observed with *A. actinomycescomitans* ATCC 33384, at least not against biofilms.

## 5. RESULTS AND DISCUSSION

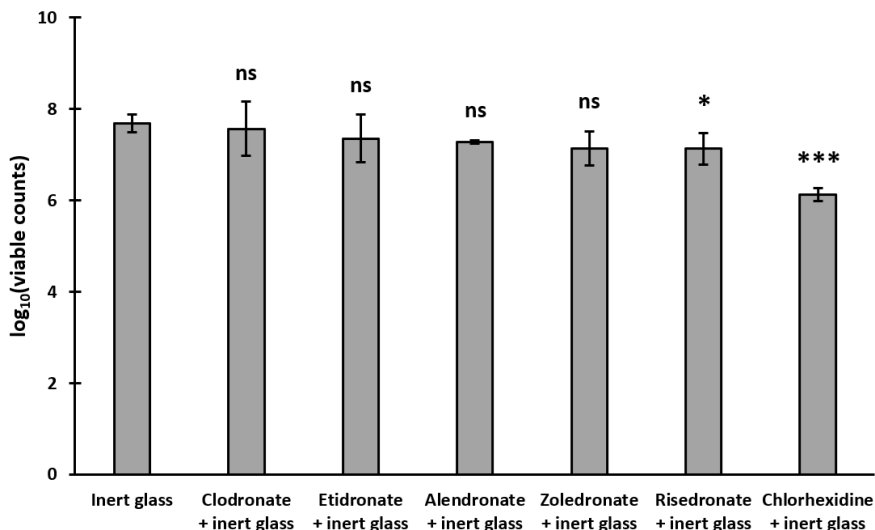


**Figure 19.** The bacterial attachment (expressed as  $\log_{10}$  values of CFU·mL<sup>-1</sup>) of *A. actinomycetemcomitans* ATCC 33384 on hydroxyapatite coupons coated with BP-IG samples (composed of 50 mg of BP/CHX and 500 mg of IG). The results were compared to the negative control (composed of 550 mg IG), using an unpaired t-test with Welch's correction. \*\*\*, statistically highly significant difference ( $p < 0.001$ ); \*, statistically significant difference ( $p < 0.05$ ); ns, not significant difference. Error bars denote standard deviations (SD) ( $n \geq 2$ ). Figure originally included in publication **III** and reproduced with permission from Elsevier.

Next, the BP-BAG combinations were assayed (**Figure 20; Table 15**). Both the positive control (CHX-BAG) and all the BP-BAG combinations (except clodronate-BAG) significantly reduced biofilm formation ( $p < 0.001$ ). These findings are in agreement with the results of study **II** obtained with *S. aureus* ATCC 25923, *S. aureus* Newman, and *S. epidermidis* RP62A (ATCC 35984) biofilms, where etidronate-BAG, alendronate-BAG, and risedronate-BAG had anti-biofilm activity (**Table 13**). Clodronate-BAG was similarly non-effective in both studies (**II** and **III**). However, in contrast to the results of study **III**, zoledronate-BAG was not effective in study **II**.

The bacterial attachment was similar on IG-BAG- and IG-coated coupons (**Figure 19; Figure 20**) indicating that BAG alone does not have an inherent anti-biofilm effect in these assay conditions. The advantageous impact of adding BAG on BP was particularly observed with risedronate (**Table 15**), as its logR increased from  $0.59 \pm 0.03$  (risedronate-IG) to  $2.25 \pm 0.37$  (risedronate-BAG). Interestingly, this synergistic interaction was not observed with CHX-BAG when compared to CHX-IG (**Table 15**), suggesting that this interaction may be somewhat specific to BPs. In next section 5.4, the potential effect of mechanism of BP-BAGs and BP-IGs will be discussed based on the data obtained from the pH measurements of such combinations.

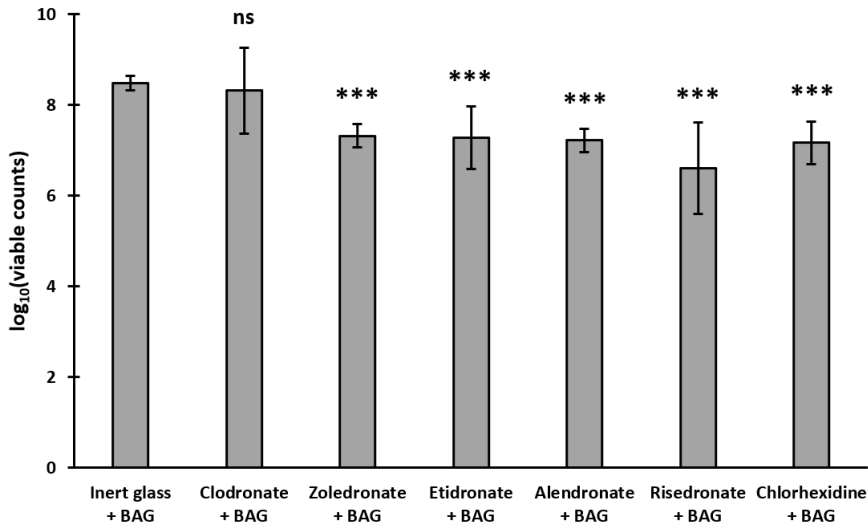


**Figure 20.** The bacterial attachment (expressed as  $\log_{10}$  values of  $\text{CFU}\cdot\text{mL}^{-1}$ ) of *A. actinomycetemcomitans* ATCC 33384 on hydroxyapatite coupons coated with BP-BAG samples (composed of 50 mg of BP/CHX/IG and 500 mg of BAG). The results were compared to the negative control (50 mg of IG and 500 mg of BAG), using an unpaired t-test with Welch's correction. \*\*\*, statistically highly significant difference ( $p < 0.001$ ); ns, not significant difference. Error bars denote standard deviations (SD) ( $n \geq 4$ ). Figure originally included in publication III and reproduced with permission from Elsevier.

**Table 15.** The logR-values of BP-IG and BP-BAG combinations, expressing the difference between the control and the test samples. Chlorhexidine-IG and chlorhexidine-BAG were included as positive controls. Table adapted from publication III, with permission from Elsevier, to keep consistency of this document.

Bisphosphonate (BP)	logR (BP-IG)	logR (BP-BAG)
Risedronate	$0.59 \pm 0.03$	$2.25 \pm 0.37$
Etidronate	$0.40 \pm 0.07$	$1.42 \pm 0.21$
Alendronate	$0.41 \pm 0.0003$	$1.29 \pm 0.03$
Zoledronate	$0.59 \pm 0.04$	$1.19 \pm 0.03$
Clodronate	$0.21 \pm 0.09$	$0.43 \pm 0.27$
Chlorhexidine	$1.57 \pm 0.006$	$1.38 \pm 0.06$

#### 5.4 Mechanistic insight and possible targets of bisphosphonates and bisphosphonate-bioactive glass combinations on bacterial biofilms (studies I-III)

The changes in pH may hamper bacterial growth and therefore be one explanation for the antimicrobial effects of the studied materials. For example, drastic pH changes can induce cellular damage in several ways. Both acidic and

## 5. RESULTS AND DISCUSSION

alkalic conditions may cause protein denaturation, impaired activity of enzymes, DNA damage, and malfunctioning of the electron transport chain in cellular respiration, which leads to accumulation of ROS (Zhou and Fey 2020; Konermann 2012). To survive in such unfavorable pH conditions, bacteria have developed different coping strategies. For example, *S. aureus* can protect itself against alkaline pH values with alkaline shock protein 23 (Kuroda et al. 1995) and against low pH e.g. with enzymatic pathways that produce pH-increasing products or systems that pump protons out of the cytoplasm, contribute to ROS detoxification, DNA repair, or operate as chaperones (Zhou and Fey 2020). Even though *S. aureus* can protect itself with the aforementioned methods, it is known that such protection is effective until pH gets below <2-5 or over 10, as these strategies require the optimal functioning of enzymes/proteins (Zhou and Fey 2020; Konermann 2012). Moreover, decreased initial adhesion has been observed to happen with *S. aureus* and *S. epidermidis* already in mildly alkaline pH (8.5). This is probably the result of the reduced *D*-alanylation degree of teichoic acids, which leads to teichoic acids having more anionic character (Nostro et al. 2012). Furthermore, the ability of *S. aureus* to form biofilms has been observed to be inhibited at pH levels 3 and 12 (Zmantar et al. 2010).

Therefore, pH measurements were carried out on tested combinations mimicking the conditions encountered by bacteria in the *in vitro* biofilm models. First, pH values of 50 mg of BPs combined with 500 mg of IG in 450  $\mu$ L of 0.9% (w/v) saline were measured (**Figure 21**). As a control, 550 mg of IG in 450  $\mu$ L of saline was used, and it showed a tendency to elevate the medium pH. All the BP-IG combinations behaved in an intrinsically acidic manner, which remained relatively steady during the whole measurement. The pH values collected with clodronate were similar to Rosenqvist et al. (2014). The pH of the media (0.9% (w/v) saline) stayed near the pH value of 7 throughout the entire measurement period (**Figure 21**; **Figure 22**).

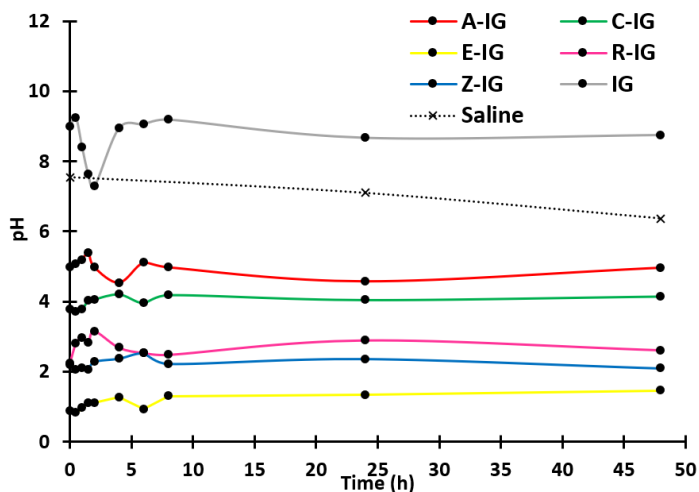


**Figure 21.** Kinetic measurements of pH taken on BP-IG combinations. A-IG, C-IG, E-IG, R-IG, Z-IG: 50 mg of BP and 500 mg of IG in 450  $\mu$ L 0.9% (w/v) saline; IG: 550 mg of IG in 450  $\mu$ L 0.9% (w/v) saline; saline: 0.9% (w/v) saline. The coefficient of variations of the pH values on replicate samples was below 11% (n=2). A, alendronate; C, clodronate; E, etidronate; R, risedronate; Z, zoledronate; IG, inert glass. Figure adapted from publication **III** with permission from Elsevier.

After that, the pH values of 50 mg of BPs/IG combined with 500 mg of BAG in 450  $\mu$ L of 0.9% (w/v) saline were determined (**Figure 22**). Additionally, the pH of BAG as a stand-alone compound in saline was measured. The BAG displayed (in the same way as IG) an inherent propensity to raise the pH of saline, as similarly reported by Rosenqvist et al. (2014; 2013). Nevertheless, BPs seemed to influence this alkaline trend with a distinguishable and transient pH decline. After the dive, the climbing pH was observed, and according to Rosenqvist et al. (2014; 2013), that indicates the rapid ion exchange taking place. Next, a stabilized pH can be detected, which in turn implies hydroxyapatite formation.

## 5. RESULTS AND DISCUSSION

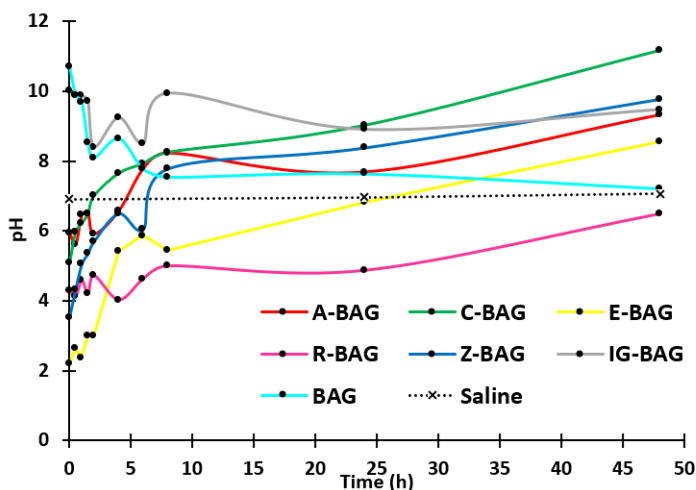


**Figure 22.** Kinetic measurements of pH taken on BP-BAG combinations. A-BAG, C-BAG, E-BAG, R-BAG, Z-BAG: 50 mg of BP and 500 mg of BAG in 450  $\mu$ L 0.9% (w/v) saline; IG-BAG: 50 mg of IG and 500 mg BAG in 450  $\mu$ L 0.9% (w/v) saline; BAG: 500 mg BAG in 450  $\mu$ L 0.9% (w/v) saline; saline: 0.9% (w/v) saline. The coefficient of variations of the pH values on replicate samples was below 16% ( $n=2$ ). A, alendronate; C, clodronate; E, etidronate; R, risedronate; Z, zoledronate; IG, inert glass; BAG, bioactive glass S53P4. Figure adapted from publication **III** with permission from Elsevier.

The described initial pH decline, however, was found strongly to be compound-specific: while the pH drop of etidronate was a short-lived but drastic, risedronate produced a modest but much longer-lasting dive. These BP-BAG combinations of etidronate-BAG and risedronate-BAG also produced the most significant reductions in biofilm viability in studies **II** and **III**, respectively. Especially, the vulnerability of *A. actinomycetemcomitans* to acidity has been reported in the literature. In one study even a mild reduction of medium pH (from 7 to 6) decreased bacterial viability with a logR of 2 (Bhattacharjee et al. 2011). *S. aureus* and *S. epidermidis*, in turn, are more tolerant to acidic pH values presumably because their typical growth environment (skin) is naturally acidic (ca. pH 4–6) (Zhou and Fey 2020; Störmer et al. 2008). This may have been one reason contributing as to why BP-BAGs were less effective against staphylococci than *A. actinomycetemcomitans*. Furthermore, accordingly, the least effective combination (clodronate-BAG), caused only a mild and a very short-lived (<2 h) decrease in pH.

It can be hypothesized that with such radically acidic pH values, of etidronate-BAG and risedronate-BAG, the detrimental effects of the BP-BAGs may extend beyond the bacterial cells to the biofilm matrix. For example, as previously indicated, low extracellular pH (<7) has been observed to reduce the PIA/PNAG charge of *S. aureus* SH1000, thereby weakening its matrix stabilizing interactions (Stewart et al. 2015). The same study found that the *S. aureus*

SH1000 matrix was most stable at pH 7–9 (Stewart et al. 2015) as PIA/PNAG is positively charged in neutral and basic pH (Nguyen et al. 2020). On this basis, when reflecting on **Figure 22**, it can be seen that the pH generated by clodronate-BAG (the least efficient combination) was most of the time within this pH range. Instead, the pH values of the most effective combinations were a majority of the time below pH 7: risedronate-BAG (for the whole measurement period) and etidronate-BAG (reached neutral pH at 25 hours). With respect to biofilm matrix, denaturation of proteins may happen already < pH 5 (Koneremann 2012), so it can be assumed that negative changes have also occurred in the protein fraction, at least in the cases of the most acidic etidronate-BAG and risedronate-BAG. Moreover, acidic stress also probably affects eDNA via the protonation of nitrogenous bases (Zhou and Fey 2020).

However, if the anti-biofilm effect would be completely pH-dependent, the logR-values of BP-IGs could be assumed to be drastically higher (**Table 13**; **Table 15**) as the pH values of BP-IGs were even lower than with BP-BAGs (**Figure 21**; **Figure 22**). Therefore, acidity-activity-relationship cannot alone explain the measured logR values of BP-BAGs. Thus, it can be hypothesized that other mechanisms, e.g. the increased osmotic pressure, may be responsible for the detected anti-biofilm effects of BPs and BP-BAG combinations. Of note, the upregulation of bacterial proteins that provide protection against acidity can be a mechanism possibly compensating the pH changes caused by BP-BAG combinations. That would for instance include e.g. urease enzymatic pathways (which convert urea to ammonia that can be further protonated to pH-increasing ammonium), arginine deiminase pathways (that produce ammonia), F-ATPases (which pump out protons from the cytoplasm), ROS detoxification, Clp proteases (ClpB, ClpC, ClpP), and DNA repair systems (Zhou and Fey 2020).

Interactions between BPs and BAG have not been widely explored in the literature. However, it has been observed that the combination of clodronate and BAG leads to extended and longer-lasting ion exchange, compared to the level that BAG would yield alone. According to the hypothesis of Rosenqvist et al. (2013), this boosted ion exchange for clodronate-BAG was caused by higher calcium ion release from BAG, which occurs in the acidic conditions created by clodronate in water solution. This in turn could result in an anti-biofilm effect via increased osmotic pressure causing bacterial plasmolysis. Even though clodronate-BAG did not have an anti-biofilm effect against any of the strains (studies **II** and **III**), it could be speculated that this reported accelerated ion exchange may also take place in other BP-BAG combinations. This would support the results of study **III**, where more pronounced anti-biofilm effects were observed with BP-BAGs than with BP-IGs. In contrast, in study **II** (**Table 13**), there was no improvement in the anti-biofilm activity of the BP-BAG over BP-IG. It can be hypothesized that more dramatic differences in logR values between BP-BAGs and BP-IGs would have been obtained in study **II** if a longer exposure time (48 h) would have been used, as in study **III**. Hence, the delayed onset of this accelerated osmotic pressure with BP-BAGs (for which this 24-h-long period is too short to take place) might explain the results of this study **II**. Indeed,

## 5. RESULTS AND DISCUSSION

according to a recent article (Cunha et al. 2018), BAG needs more time than 24 h to convey its effect: inhibition of bacterial growth started only after 48 h of incubation and reached zero CFU·mL<sup>-1</sup> after 120–168 h of incubations. Therefore, it could be claimed that in study II, with this short incubation time, the intrinsic anti-biofilm effects of alendronate, etidronate, and risedronate were possibly responsible for the detected anti-biofilm effects of alendronate-, etidronate- and risedronate-BAG combinations.

Furthermore, if increased osmotic pressure would be the predominant mechanism, it could explain (along with a longer incubation time) why BP-BAGs were more effective against *A. actinomycetemcomitans* ATCC 33384 than staphylococcal strains. The osmotolerance has been found to be a very species-specific property, and this cannot be attributed to, for example, a particular species type (e.g. gram-positive versus gram-negative) (Mille et al. 2005). For example, *S. aureus* is notorious for tolerating high osmotic pressure, likely associated with the fact that *S. aureus* lives in nasal passages where salt levels are naturally high (Tortora et al. 2014, p. 163). There is also a specific protein channel called the large-conductance mechanosensitive channel (MscL) that opens when stretch forces in the plasma membrane are encountered. Therefore, MscL likely participates in the regulation of osmotic pressure changes within the cell (Carniello et al. 2020). Interestingly, MscL is an integral protein of the plasma membrane, and it is likely the reason why it was not detected in any of the samples in study I. Integral proteins require a rigid disruption of phospholipids (e.g. with a detergent) in order to be assayed in proteomic analysis. Whether bacteria would up-regulate MscL, would be an interesting topic for future studies. Moreover, *S. aureus* transport compatible solutes (such as proline, glycine betaine, choline, taurine, and glutamic acid) into the intracellular milieu to create high intracellular pressure enabling survival in high osmotic environments. *S. aureus* is only capable to synthesize glutamic acid out of these compatible solutes, while the rest have to be imported from the external environment via osmolyte transporters (Schwan and Wetzels 2016). Assaying the levels of osmolyte transporters (e.g. sodium/proline symporter) and enzymes contributing to glutamic acid synthesis as a response to BP-BAG exposure, are therefore of interest. Likewise, as it is known that *S. aureus* responds to increased osmotic pressure via shortening peptidoglycan interpeptide bridges (Vijaranakul et al. 1995), analysis of protein levels involved in the synthesis of peptidoglycan interpeptide bridges (e.g. aminoacyltransferases FemA and FemB) would be of interest.

Finally, a third possible mechanism could be considered as risedronate has been hypothesized to target catabolite repressor/activator protein (Cra), and in this fashion, disturb the biofilm formation of *E. coli*, as proposed by Reshamwala et al. (2016). This mechanism may have possibly mediated anti-biofilm activity against *A. actinomycetemcomitans* ATCC 33384, which also possesses this Cra-protein. Reflecting on study I, *S. aureus* does not have exactly the same Cra-protein, but instead it produces a protein called catabolite control protein A (CcpA) that is responsible for mediating similar activities. The interactions



between risedronate and CcpA have not been studied, to the best of our knowledge, and could be a focus of work for future studies. This protein, CcpA, was not present in HA-associated *S. aureus* ATCC 25923 biofilms at 18 h, but it was detected at the later time points of 42 and 66 h (**Table 10**). The later onset of CcpA could be one hypothetical explanation as to why BP-BAGs were not as active with the 24 h incubation (study **II**). This possibility further encourages the investigation of longer incubation times (at least 48 h) with BP-BAGs in future studies.

Altogether, etidronate-BAG was the most effective combination in study **II** against gram-positive staphylococci, while risedronate-BAG was the most active combination in study **III** against gram-negative *A. actinomycetemcomitans* ATCC 33384. Based on the similar logR values of etidronate-BAG and vancomycin-IG (commonly employed to resolve PJIs) (study **II**), etidronate-BAG can be considered as an interesting treatment option for vancomycin owing to its additional bone constructing properties. On the other hand, based on the higher anti-biofilm activity of risedronate-BAG compared to chlorhexidine-IG (study **III**), risedronate-BAG can be considered as a potential therapeutic approach for periodontitis, displaying bone-constructing and anti-biofilm actions. In conclusion, this data suggests that risedronate-BAG and etidronate-BAG are the most promising BP-BAG combinations to be used in future studies.

## 6. CONCLUSIONS AND FUTURE PERSPECTIVES

Biofilms are responsible for chronic and severe infections, which are recalcitrant to the currently available antibiotic approaches. Particularly challenging are biofilms infecting indwelling medical devices that have been permanently inserted into the human body. Such biofilms cannot be removed with antibiotics alone – some kind of invasive surgery is always necessary. What makes this issue even more difficult to tackle, is the dauntingly rapid development of resistance towards conventional antibiotics. It is clear that there is a great need for novel, non-antibiotic-based and truly effective strategies to combat biofilms. Here, the overall aims were to contribute to the understanding of biofilm features on different biomaterials used in medical devices and to protect these biomaterials from biofilm colonization with a novel non-antibiotic-based combination strategy.

With better material-specific understanding, biofilm formation could potentially be prevented e.g. by targeted immunotherapy already at the time of device installation. We aimed for this understanding with a multidimensional orthogonal approach to characterize (i) biofilm dynamics covering biomaterial surface properties (correlated with material susceptibility to biofilm formation), (ii) biofilm structures (via proteosurfaceomics and exopolysaccharide/protein contents), and (iii) biofilm functionality (antimicrobial tolerance studies) (study I). This was done in a way that allowed side-by-side comparisons of *Staphylococcus aureus* biofilms formed on different biomaterials (borosilicate glass, plexiglass, hydroxyapatite, titanium, and polystyrene) as well as at different maturation time points (18, 42, and 66 h).

The biofilm matrix-associated polysaccharide content seemed to be important in the initial stages of biofilm formation, decreasing towards the end of the observation period. In turn, the matrix protein content was rising throughout the observation period. The core proteosurfaceome was identified, which can be used as a platform for future studies related to e.g. immunotherapy development. Generally, the classical surface proteins have been deemed as the most appealing targets in drug development against bacterial pathogens. However, in this study, classical surface proteins demonstrated high biomaterial-dependent variability in their amounts. In turn, the non-classical surface proteins “moonlighters” comprised the major portion of the core proteosurfaceome. It is known that reutilization of cytoplasmic proteins as moonlighting constituents benefits the biofilm inhabitants via enhanced attachment, virulence, and drug tolerance. Consequently, recognizing mechanisms that coordinate the moonlighting activity would help offering insight into novel strategies for anti-biofilm agent/material development. The last part of the study shed light on the effect of biomaterial and biofilm age on antibiotic tolerance. Biofilms formed on titanium were in many cases more tolerant to antibiotics than biofilms on hydroxyapatite. The older, more mature (66 h) biofilms were not always more tolerant than the younger (18 h) ones.

All this creates more understanding of the fact that material choices in medical devices need to be carefully considered. While it is clear the e.g. biocompatibility and mechanical durability are key factors in such selections, it could also be beneficial to consider biomaterial-dependent properties of biofilms. One such example could be biofilm prevention via targeted immunotherapy at the time of device installation. An evident next step for the present research context would be to assay biofilm and biomaterial interactions in the presence of a serum medium. The most fascinating extension for study **I** would undeniably be to examine the actual removed *S. aureus*-infected medical devices made of different biomaterials and subject them to proteomic analysis.

In the second part of the thesis (studies **II** and **III**), it was studied whether one of these biomaterials, hydroxyapatite, could be actually protected from biofilm colonization utilizing a novel non-antibiotic combination therapy consisting of bisphosphates (BPs) and bioactive glass (S53P4; BAG). From the perspective of both studies, etidronate-BAG and risedronate-BAG were the most promising combinations. Additionally, it was observed that an improved anti-biofilm effect was systemically obtained in study **III**, probably due to the longer treatment period (48 h) compared to the one used in study **II** (24 h).

While the observations of studies (**II** and **III**) present aspects of the functionality of BP-BAG-combinations in two pertinent clinical applications, further investigation on the anti-biofilm mechanism would be of value. The anti-biofilm effects could not be explained alone with lowered pH values. Increased osmotic pressure or another, yet-unknown, mechanism seems to contribute to the observed anti-biofilm effect. Hence, studying staphylococcal biofilms and/or *Aggregatibacter actinomycetemcomitans* biofilms from the proteomic perspective represents an interesting expansion: this could especially entail BPs *per se* (etidronate and risedronate), mere BAG, and the combinations (etidronate-BAG and risedronate-BAG). Therein, the proteomic profiles compared to each other would offer a more pinpointed view on the mechanism of action of BP-BAGs. Moreover, as mono-species biofilms were used in study **III**; multi-species dental biofilms (comprising pioneer, early, intermediate, and late colonizers) could be introduced in future studies to reflect periodontal status more realistically. Furthermore, it could be also explored whether the acidic pH changes caused by BP-BAG-combinations are not detrimental to oral tissues. Finally, since all studies were based on a limited number of bacterial strains, in future studies several different clinical strains should be involved.

In conclusion, the used biomaterial and biofilm age greatly influence the characteristics of the biofilm and its antibiotic tolerance. These aspects should be taken into account when designing new anti-biofilm strategies/immunotherapeutic solutions (study **I**). The results of studies **II** and **III** further support the use of the most effective BP-BAG combinations in protecting biomaterials from biofilm infections in PJI and dental applications.

## 7. REFERENCES

- Adachi H, Igarashi K, Mitani H, Shinoda H: Effects of topical administration of a bisphosphonate (risedronate) on orthodontic tooth movements in rats. *J Dent Res* 73: 1478–1486, 1994
- Aggarwal VK, Bakhshi H, Ecker NU, Parvizi J, Gehrke T, Kendoff D: Organism profile in periprosthetic joint infection: Pathogens differ at two arthroplasty infection referral centers in Europe and in the United States. *J Knee Surg* 27: 399–406, 2014
- Alav I, Sutton JM, Rahman KM: Role of bacterial efflux pumps in biofilm formation. *J Antimicrob Chemother* 73: 2003–2020, 2018
- Alencar VB, Bezerra MM, Lima V, Abreu AL, Brito GA, Rocha FA, Ribeiro RA: Disodium chlodronate prevents bone resorption in experimental periodontitis in rats. *J Periodontol* 73: 251–256, 2002
- Alhede M, Alhede M, Qvortrup K, Kragh KN, Jensen PØ, Stewart PS, Bjarnsholt T: The origin of extracellular DNA in bacterial biofilm infections *in vivo*. *Pathog Dis* 78: ftaa018, 2020
- Alhede M, Bjarnsholt T, Givskov M, Alhede M: *Pseudomonas aeruginosa* biofilms: Mechanisms of immune evasion. *Adv Appl Microbiol* 86: 1–40, 2014
- Alreshidi MM, Dunstan RH, Gottfries J, Macdonald MM, Crompton MJ, Ang CS, Williamson NA, Roberts TK: Changes in the cytoplasmic composition of amino acids and proteins observed in *Staphylococcus aureus* during growth under variable growth conditions representative of the human wound site. *PLoS One* 11: e0159662, 2016
- Antikainen J, Kuparinen V, Lähteenmäki K, Korhonen TK: Enolases from gram-positive bacterial pathogens and commensal lactobacilli share functional similarity in virulence-associated traits. *FEMS Immunol Med Microbiol* 51: 526–534, 2007
- Arciola CR, Campoccia D, Montanaro L: Implant infections: Adhesion, biofilm formation and immune evasion. *Nat Rev Microbiol* 16: 397–409, 2018
- Arirachakaran P, Apinhasmit W, Paungmalit P, Jeramethakul P, Rerkyen P, Mahanonda R: Infection of human gingival fibroblasts with *Aggregatibacter actinomycetemcomitans*: An *in vitro* study. *Arch Oral Biol* 57: 964–972, 2012
- Askarian F, Wagner T, Johannessen M, Nizet V: *Staphylococcus aureus* modulation of innate immune responses through Toll-like (TLR), (NOD)-like (NLR) and C-type lectin (CLR) receptors. *FEMS Microbiol Rev* 42: 656–671, 2018
- ASTM International Websites (Online). Available online: [www.astm.org](http://www.astm.org). Accessed: December 18<sup>th</sup>, 2020
- ASTM International: Standard test method for quantification of *Pseudomonas aeruginosa* biofilm grown using Drip Flow Biofilm Reactor with low shear and continuous flow (E2647-13), 2013
- ASTM International: Standard test method for quantification of *Pseudomonas aeruginosa* biofilm grown with high shear and continuous flow using CDC Biofilm Reactor (E2562-12), 2012
- ASTM International: Standard test method for quantification of *Pseudomonas aeruginosa* biofilm grown with medium shear and continuous flow using Rotating Disk Reactor (E2196-12), 2012
- ASTM International: Standard test method for testing disinfectant efficacy against *Pseudomonas aeruginosa* biofilm using the MBEC Assay (E2799-12), 2012

- Atkins KL, Burman JD, Chamberlain ES, Cooper JE, Poutrel B, Bagby S, Jenkins AT, Feil EJ, van den Elsen JM: *S. aureus* IgG-binding proteins SpA and Sbi: Host specificity and mechanisms of immune complex formation. *Mol Immunol* 45: 1600–1611, 2008
- Bahekar AA, Singh S, Saha S, Molnar J, Arora R: The prevalence and incidence of coronary heart disease is significantly increased in periodontitis: A meta-analysis. *Am Heart J* 154: 830–837, 2007
- Baker B, McKernan PA, Marsik F: Clinical and regulatory development of antibiofilm drugs: The need, the potential, and the challenges. In the book: *Antibiofilm agents: From diagnosis to treatment and prevention*, pp. 469–486. Eds. Rumbaugh K, Ahmad I. Springer, Berlin, Heidelberg, Germany, 2014
- Banerjee S, Nandyala AK, Raviprasad P, Ahmed N, Hasnain SE: Iron-dependent RNA-binding activity of *Mycobacterium tuberculosis* aconitase. *J Bacteriol* 189: 4046–4052, 2007
- Bao K, Bostanci N, Thurnheer T, Grossmann J, Wolski WE, Thay B, Belibasakis GN, Oscarsson J: *Aggregatibacter actinomycetemcomitans* H-NS promotes biofilm formation and alters protein dynamics of other species within a polymicrobial oral biofilm. *NPJ Biofilms Microbiomes* 4: 12, 2018
- Barbosa MS, B ao SN, Andreotti PF, de Faria FP, Felipe MS, dos Santos Feitosa L, Mendes-Giannini MJ, Soares CM: Glyceraldehyde-3-phosphate dehydrogenase of *Paracoccidioides brasiliensis* is a cell surface protein involved in fungal adhesion to extracellular matrix proteins and interaction with cells. *Infect Immun* 74: 382–389, 2006
- Bergonzelli GE, Granato D, Pridmore RD, Marvin-Guy LF, Donnicola D, Corth esy-Theulaz IE: GroEL of *Lactobacillus johnsonii* La1 (NCC 533) is cell surface associated: Potential role in interactions with the host and the gastric pathogen *Helicobacter pylori*. *Infect Immun* 74: 425–434, 2006
- Bhattacharjee MK, Childs CB, Ali E: Sensitivity of the periodontal pathogen *Aggregatibacter actinomycetemcomitans* at mildly acidic pH. *J Periodontol* 82: 917–925, 2011
- Binderman I, Adut M, Yaffe A: Effectiveness of local delivery of alendronate in reducing alveolar bone loss following periodontal surgery in rats. *J Periodontol* 71: 1236–1240, 2000
- Bjarnsholt T, Alhede M, Alhede M, Eickhardt-S orensen SR, Moser C, K uhl M, Jensen P , H oiby N: The *in vivo* biofilm. *Trends Microbiol* 21: 466–474, 2013a
- Bjarnsholt T, Ciofu O, Molin S, Givskov M, H oiby N: Applying insights from biofilm biology to drug development – Can a new approach be developed? *Nat Rev Drug Discov* 12: 791–808, 2013b
- Bjarnsholt T, Jensen P , Fiandaca MJ, Pedersen J, Hansen CR, Andersen CB, Pressler T, Givskov M, H oiby N: *Pseudomonas aeruginosa* biofilms in the respiratory tract of cystic fibrosis patients. *Pediatr Pulmonol* 44: 547–558, 2009
- Bjarnsholt T: The role of bacterial biofilms in chronic infections. *APMIS Suppl* 136: 1–51, 2013
- Blomqvist BEC: Optimization and characterization of the Static Biofilm method for antibiofilm studies. Master’s thesis, Åbo Akademi University, Turku, Finland, 2014
- Bonalive® Biomaterials Ltd. Available online: [www.bonalive.com](http://www.bonalive.com). Accessed: January 19<sup>th</sup>, 2021

## 7. REFERENCES

- Bortolin M, De Vecchi E, Romanò CL, Toscano M, Mattina R, Drago L: Antibiofilm agents against MDR bacterial strains: Is bioactive glass BAG-S53P4 also effective? *J Antimicrob Chemother* 71: 123–127, 2016
- Brot N, Caldwell P, Weissbach H: Autogenous control of *Escherichia coli* ribosomal protein L10 synthesis *in vitro*. *Proc Natl Acad Sci U S A* 77: 2592–2595, 1980
- Brunsvold MA, Chaves ES, Kornman KS, Aufdemorte TB, Wood R: Effects of a bisphosphonate on experimental periodontitis in monkeys. *J Periodontol* 63: 825–830, 1992
- Buckingham-Meyer K, Goeres DM, Hamilton MA: Comparative evaluation of biofilm disinfectant efficacy tests. *J Microbiol Methods* 70: 236–244, 2007
- Candela M, Bergmann S, Vici M, Vitali B, Turrone S, Eikmanns BJ, Hammerschmidt S, Brigidi P: Binding of human plasminogen to *Bifidobacterium*. *J Bacteriol* 189: 5929–5936, 2007
- Carlén A, Nikdel K, Wennerberg A, Holmberg K, Olsson J: Surface characteristics and *in vitro* biofilm formation on glass ionomer and composite resin. *Biomaterials* 22: 481–487, 2001
- Carneiro CR, Postol E, Nomizo R, Reis LF, Brentani RR: Identification of enolase as a laminin-binding protein on the surface of *Staphylococcus aureus*. *Microbes Infect* 6: 604–608, 2004
- Carniello V, Peterson BW, van der Mei HC, Busscher HJ: Role of adhesion forces in mechanosensitive channel gating in *Staphylococcus aureus* adhering to surfaces. *NPJ Biofilms Microbiomes* 6: 31, 2020
- Cerca N, Jefferson KK, Oliveira R, Pier GB, Azeredo J: Comparative antibody-mediated phagocytosis of *Staphylococcus epidermidis* cells grown in a biofilm or in the planktonic state. *Infect Immun* 74: 4849–4855, 2006
- Chacko NL, Abraham S, Rao HN, Sridhar N, Moon N, Barde DH: A clinical and radiographic evaluation of periodontal regenerative potential of PerioGlas®: A synthetic, resorbable material in treating periodontal infrabony defects. *J Int Oral Health* 6: 20–26, 2014
- Charaf UK, Bakich SC, Falbo DM: A model biofilm for efficacy assessment of antimicrobials versus biofilm bacteria. In the book: *Biofilms: The good, the bad and the ugly*, pp. 171–177. Eds. Walker J, Gilbert P, Wimpenny J, Bioline 1999
- Chen C, Zabad S, Liu H, Wang W, Jeffery C: MoonProt 2.0: An expansion and update of the moonlighting proteins database. *Nucleic Acids Res* 46: D640–D644, 2018
- Chen L, Tang ZY, Cui SY, Ma ZB, Deng H, Kong WL, Yang LW, Lin C, Xiong WG, Zeng ZL: Biofilm production ability, virulence and antimicrobial resistance genes in *Staphylococcus aureus* from various veterinary hospitals. *Pathogens* 9: 1–17, 2020a
- Chen X, Thomsen TR, Winkler H, Xu Y: Influence of biofilm growth age, media, antibiotic concentration and exposure time on *Staphylococcus aureus* and *Pseudomonas aeruginosa* biofilm removal *in vitro*. *BMC Microbiol* 20: 264, 2020b
- Cheng AG, McAdow M, Kim HK, Bae T, Missiakas DM, Schneewind O: Contribution of coagulases towards *Staphylococcus aureus* disease and protective immunity. *PLoS Pathog* 6: e1001036, 2010
- Cheung GY, Yeh AJ, Kretschmer D, Duong AC, Tuffuor K, Fu CL, Joo HS, Diep BA, Li M, Nakamura Y, Nunez G, Peschel A, Otto M: Functional characteristics of the *Staphylococcus aureus*  $\delta$ -toxin allelic variant G10S. *Sci Rep* 5: 18023, 2015

- Chua JD, Wilkoff BL, Lee I, Juratli N, Longworth DL, Gordon SM: Diagnosis and management of infections involving implantable electrophysiologic cardiac devices. *Ann Intern Med* 133: 604–608, 2000
- Ciofu O, Rojo-Molinero E, Macià MD, Oliver A: Antibiotic treatment of biofilm infections. *APMIS* 125: 304–319, 2017
- Clais S: The applicability of virulence inhibitors as a therapy for *Porphyromonas gingivalis* infections. Dissertation, University of Antwerp, Antwerp, Belgium, 2014
- ClinicalTrials.gov. NIH: U.S. National library of medicine. Available online <https://www.clinicaltrials.gov/>, Accessed November 3<sup>rd</sup>, 2020
- Coenye T, Nelis HJ: *In vitro* and *in vivo* model systems to study microbial biofilm formation. *J Microbiol Methods* 83: 89–105, 2010
- Cohen JB, Carroll C, Tenenbaum MM, Myckatyn TM: Breast implant-associated infections: The role of the national surgical quality improvement program and the local microbiome. *Plast Reconstr Surg* 136: 921929, 2015
- Coraça-Huber DC, Fille M, Hausdorfer J, Putzer D, Nogler M: Efficacy of antibacterial bioactive glass S53P4 against *S. aureus* biofilms grown on titanium discs *in vitro*. *J Orthop Res* 32: 175–177, 2014
- Cortese YJ, Wagner VE, Tierney M, Devine D, Fogarty A. Review of catheter-associated urinary tract infections and *in vitro* urinary tract models. *J Healthc Eng* 2018: 2986742, 2018
- Costa AR, Henriques M, Oliveira R, Azeredo J: The role of polysaccharide intercellular adhesin (PIA) in *Staphylococcus epidermidis* adhesion to host tissues and subsequent antibiotic tolerance. *Eur J Clin Microbiol Infect Dis* 28: 623–629, 2009
- Costerton JW, Geesey GG, Cheng KJ: How bacteria stick. *Sci Am* 238: 86–95, 1978
- Costerton JW, Stewart PS, Greenberg EP: Bacterial biofilms: A common cause of persistent infections. *Science* 284: 1318–1322, 1999
- Cox J, Mann M: MaxQuant enables high peptide identification rates, individualized p.p.b.-range mass accuracies and proteome-wide protein quantification. *Nat Biotechnol* 26: 1367–1372, 2008
- Cox J, Neuhauser N, Michalski A, Scheltema RA, Olsen JV, Mann M: Andromeda: A peptide search engine integrated into the MaxQuant environment. *J Proteome Res* 10: 1794–1805, 2011
- Cramton SE, Gerke C, Schnell NF, Nichols WW, Götz F: The intercellular adhesion (*ica*) locus is present in *Staphylococcus aureus* and is required for biofilm formation. *Infect Immun* 67: 5427–5433, 1999
- Crowe JD, Sievwright IK, Auld GC, Moore NR, Gow NA, Booth NA: *Candida albicans* binds human plasminogen: Identification of eight plasminogen-binding proteins. *Mol Microbiol* 47: 1637–1651, 2003
- Cunha MT, Murça MA, Nigro S, Klautau GB, Salles MJC: *In vitro* antibacterial activity of bioactive glass S53P4 on multiresistant pathogens causing osteomyelitis and prosthetic joint infection. *BMC Infect Dis* 18: 157, 2018
- Current Care Guidelines: Periodontitis. Suomalaisen Lääkäriseuran Duodecim ja Suomen Hammaslääkäriseura Apollonia ry:n asettama työryhmä. December 11<sup>st</sup>, 2019. <https://www.kaypahoito.fi/hoi50086?tab=suositus#s7>, Accessed August 27<sup>th</sup>, 2020
- Dallo SF, Kannan TR, Blaylock MW, Baseman JB: Elongation factor Tu and E1 beta subunit of pyruvate dehydrogenase complex act as fibronectin binding proteins in *Mycoplasma pneumoniae*. *Mol Microbiol* 46: 1041–1051, 2002

## 7. REFERENCES

- Darveau RP, Tanner A, Page RC: The microbial challenge in periodontitis. *Periodontol* 2000 14: 12–32, 1997
- Davidson DJ, Spratt D, Liddle AD: Implant materials and prosthetic joint infection: The battle with the biofilm. *EFORT Open Rev* 4: 633–639, 2019
- de Jong NWM, van Kessel KPM, van Strijp JAG: Immune evasion by *Staphylococcus aureus*. *Microbiol Spectr* 7, 2019
- de la Fuente-Núñez C, Reffuveille F, Fernández L, Hancock RE: Bacterial biofilm development as a multicellular adaptation: Antibiotic resistance and new therapeutic strategies. *Curr Opin Microbiol* 16: 580–589, 2013
- de Veij Mestdagh PD, Colnot DR, Borggreven PA, Orelia CC, Quak JJ: Mastoid obliteration with S53P4 bioactive glass in cholesteatoma surgery. *Acta Otolaryngol* 137: 690–694, 2017
- de Vor L, Rooijackers SHM, van Strijp JAG: Staphylococci evade the innate immune response by disarming neutrophils and forming biofilms. *FEBS Lett* 594: 2556–2569, 2020
- Dean D, Yates JL, Nomura M: Identification of ribosomal protein S7 as a repressor of translation within the *str* operon of *E. coli*. *Cell* 24: 413–419, 1981
- Delcaru C, Alexandru I, Podgoreanu P, Grosu M, Stavropoulos E, Chifiriuc MC, Lazar V: Microbial biofilms in urinary tract infections and prostatitis: Etiology, pathogenicity, and combating strategies. *Pathogens* 5: 1–12, 2016
- Demmer RT, Jacobs DR Jr, Singh R, Zuk A, Rosenbaum M, Papapanou PN, Desvarieux M: Periodontal bacteria and prediabetes prevalence in ORIGINS: The oral infections, glucose intolerance, and insulin resistance study. *J Dent Res* 94: 201S–211S, 2015
- Demmer RT, Papapanou PN, Jacobs DR Jr, Desvarieux M: Bleeding on probing differentially relates to bacterial profiles: The oral infections and vascular disease epidemiology study. *J Clin Periodontol* 35: 479–486, 2008
- Desvaux M, Candela T, Serror P: Surfaceome and proteosurfaceome in parietal monoderm bacteria: Focus on protein cell-surface display. *Front Microbiol* 9: 100, 2018
- Díaz-Zúñiga J, Muñoz Y, Melgar-Rodríguez S, More J, Bruna B, Lobos P, Monasterio G, Vernal R, Paula-Lima A: Serotype b of *Aggregatibacter actinomycetemcomitans* triggers pro-inflammatory responses and amyloid beta secretion in hippocampal cells: A novel link between periodontitis and Alzheimer's disease? *J Oral Microbiol* 11: 1586423, 2019
- Donlan RM, Costerton JW: Biofilms: Survival mechanisms of clinically relevant microorganisms. *Clin Microbiol Rev* 15: 167–193, 2002
- Drago L, Boot W, Dimas K, Malizos K, Hänsch GM, Stuyck J, Gawlitta D, Romanò CL: Does implant coating with antibacterial-loaded hydrogel reduce bacterial colonization and biofilm formation *in vitro*? *Clin Orthop Relat Res* 472: 3311–3323, 2014b
- Drago L, Bortolin M, De Vecchi E, Agrappi S, Weinstein RL, Mattina R, Francetti L: Antibiofilm activity of sandblasted and laser-modified titanium against microorganisms isolated from peri-implantitis lesions. *J Chemother* 28: 383–389, 2016
- Drago L, De Vecchi E, Bortolin M, Toscano M, Mattina R, Romanò CL: Antimicrobial activity and resistance selection of different bioglass S53P4 formulations against multidrug resistant strains. *Future Microbiol* 10: 1293–1299, 2015
- Drago L, Romanò D, De Vecchi E, Vassena C, Logoluso N, Mattina R, Romanò CL: Bioactive glass BAG-S53P4 for the adjunctive treatment of chronic



- osteomyelitis of the long bones: An *in vitro* and prospective clinical study. *BMC Infect Dis* 13: 584, 2013
- Drago L, Vassena C, Fenu S, De Vecchi E, Signori V, De Francesco R, Romanò CL: *In vitro* antibiofilm activity of bioactive glass S53P4. *Future Microbiol* 9: 593–601, 2014a
- Dziewanowska K, Patti JM, Deobald CF, Bayles KW, Trumble WR, Bohach GA: Fibronectin binding protein and host cell tyrosine kinase are required for internalization of *Staphylococcus aureus* by epithelial cells. *Infect Immun* 67: 4673–4678, 1999
- Ebner P, Rinker J, Götz F: Excretion of cytoplasmic proteins in *Staphylococcus* is most likely not due to cell lysis. *Curr Genet* 62: 19–23, 2016
- El-Shinnawi UM, El-Tantawy SI: The effect of alendronate sodium on alveolar bone loss in periodontitis (clinical trial). *J Int Acad Periodontol* 5: 5–10, 2003
- Espino E, Koskenniemi K, Mato-Rodriguez L, Nyman TA, Reunanen J, Koponen J, Öhman T, Siljamäki P, Alatossava T, Varmanen P, Savijoki K: Uncovering surface-exposed antigens of *Lactobacillus rhamnosus* by cell shaving proteomics and two-dimensional immunoblotting. *J Proteome Res* 14: 1010–1024, 2015
- European Centre for Disease Prevention and Control: Percentage (%) of invasive isolates resistant to meticillin (MRSA), by country, EU/EEA, 2014. available online: <https://www.ecdc.europa.eu/en/publications-data/percentage-invasive-isolates-resistant-meticillin-mrsa-country-eueea-2014>. Published: November 16<sup>th</sup>, 2015. Accessed: December 4<sup>th</sup>, 2020
- Fitzpatrick F, Humphreys H, O’Gara JP: Evidence for *ica*A/BC-independent biofilm development mechanism in methicillin-resistant *Staphylococcus aureus* clinical isolates. *J Clin Microbiol* 43: 1973–1976, 2005
- Flemming HC, Wingender J: The biofilm matrix. *Nat Rev Microbiol* 8: 623–633, 2010
- Foster TJ, Geoghegan JA, Ganesh VK, Höök M: Adhesion, invasion and evasion: The many functions of the surface proteins of *Staphylococcus aureus*. *Nat Rev Microbiol* 12: 49–62, 2014
- Foulston L, Elsholz AK, DeFrancesco AS, Losick R: The extracellular matrix of *Staphylococcus aureus* biofilms comprises cytoplasmic proteins that associate with the cell surface in response to decreasing pH. *mBio* 5: e01667–14, 2014
- Franco-Serrano L, Hernández S, Calvo A, Severi MA, Ferragut G, Pérez-Pons J, Piñol J, Pich Ò, Mozo-Villarias Á, Amela I, Querol E, Cedano J: MultitaskProtDB-II: An update of a database of multitasking/moonlighting proteins. *Nucleic Acids Res* 46: D645–D648, 2018
- Frees D, Chastanet A, Qazi S, Sørensen K, Hill P, Msadek T, Ingmer H: Clp ATPases are required for stress tolerance, intracellular replication and biofilm formation in *Staphylococcus aureus*. *Mol Microbiol* 54: 1445–1462, 2004
- Furuya H, Ikeda R: Interaction of triosephosphate isomerase from *Staphylococcus aureus* with plasminogen. *Microbiol Immunol* 55: 855–862, 2011
- Geraci J, Neubauer S, Pöllath C, Hansen U, Rizzo F, Krafft C, Westermann M, Hussain M, Peters G, Pletz MW, Löffler B, Makarewicz O, Tuchscher L: The *Staphylococcus aureus* extracellular matrix protein (Emp) has a fibrous structure and binds to different extracellular matrices. *Sci Rep* 7: 13665, 2017

## 7. REFERENCES

- Gergely I, Nagy Ö, Zagyva Ancuța, Zuh SGy, Russu OM, Pop TS: Our short-term experience with the use of S53P4 (BonAlive®) bioactive glass as a bone graft substitute. *Acta Marisiensis Seria Medica* 57: 627–630, 2011
- Gergely I, Zagyva A, Man A, Zuh SG, Pop TS: The *in vitro* antibacterial effect of S53P4 bioactive glass and gentamicin impregnated polymethylmethacrylate beads. *Acta Microbiol Immunol Hung* 61: 145–160, 2014
- Geurts J, van Vugt T, Thijssen E, Arts JJ: Cost-effectiveness study of one-stage treatment of chronic osteomyelitis with bioactive glass S53P4. *Materials (Basel)* 12, 2019
- Gilbert P, Moore LE: Cationic antiseptics: Diversity of action under a common epithet. *J Appl Microbiol* 99: 703–715, 2005
- Gjødsbøl K, Christensen JJ, Karlsmark T, Jørgensen B, Klein BM, Krogfelt KA: Multiple bacterial species reside in chronic wounds: A longitudinal study. *Int Wound J* 3: 225–231, 2006
- Gomes-Filho IS, de Oliveira TF, da Cruz SS, Passos-Soares Jde S, Trindade SC, Oliveira MT, Souza-Machado A, Cruz AA, Barreto ML, Seymour GJ: Influence of periodontitis in the development of nosocomial pneumonia: A case control study. *J Periodontol* 85: e82–e90, 2014
- Graf AC, Leonard A, Schäuble M, Rieckmann LM, Hoyer J, Maass S, Lalk M, Becher D, Pané-Farré J, Riedel K: Virulence factors produced by *Staphylococcus aureus* biofilms have a moonlighting function contributing to biofilm integrity. *Mol Cell Proteomics* 18: 1036–1053, 2019
- Granato D, Bergonzelli GE, Pridmore RD, Marvin L, Rouvet M, Corthésy-Theulaz IE: Cell surface-associated elongation factor Tu mediates the attachment of *Lactobacillus johnsonii* NCC533 (La1) to human intestinal cells and mucins. *Infect Immun* 72: 2160–2169, 2004
- Grønseth T, Vestby LK, Nesse LL, von Unge M, Silvola JT: Bioactive glass S53P4 eradicates *Staphylococcus aureus* in biofilm/planktonic states *in vitro*. *Ups J Med Sci* 125: 217–225, 2020
- Gross M, Cramton SE, Götz F, Peschel A: Key role of teichoic acid net charge in *Staphylococcus aureus* colonization of artificial surfaces. *Infect Immun* 69: 3423–3426, 2001
- Gründling A, Missiakas DM, Schneewind O: *Staphylococcus aureus* mutants with increased lysostaphin resistance. *J Bacteriol* 188: 6286–6297, 2006
- Gubler M, Brunner TJ, Zehnder M, Waltimo T, Sener B, Stark WJ: Do bioactive glasses convey a disinfecting mechanism beyond a mere increase in pH? *Int Endod J* 41: 670–678, 2008
- Günther F, Stroh P, Wagner C, Obst U, Hänsch GM: Phagocytosis of staphylococci biofilms by polymorphonuclear neutrophils: *S. aureus* and *S. epidermidis* differ with regard to their susceptibility towards the host defense. *Int J Artif Organs* 32: 565–573, 2009a
- Günther F, Wabnitz GH, Stroh P, Prior B, Obst U, Samstag Y, Wagner C, Hänsch GM: Host defence against *Staphylococcus aureus* biofilms infection: Phagocytosis of biofilms by polymorphonuclear neutrophils (PMN). *Mol Immunol* 46: 1805–1813, 2009b
- Gupta P, Pruthi PA, Pruthi V: Role of exopolysaccharides in biofilm formation. In the book: Introduction to biofilm engineering, pp. 17–57. Eds. Rathinam NK, Sani RK. American Chemical Society, Washington, D.C, US, 2019
- Gurung M, Moon DC, Choi CW, Lee JH, Bae YC, Kim J, Lee YC, Seol SY, Cho DT, Kim SI, Lee JC: *Staphylococcus aureus* produces membrane-derived vesicles that induce host cell death. *PLoS One* 6: e27958, 2011

- Haghi Ghahremanlou Olia A, Ghahremani M, Ahmadi A, Sharifi Y: Comparison of biofilm production and virulence gene distribution among community- and hospital-acquired *Staphylococcus aureus* isolates from northwestern Iran. *Infect Genet Evol* 81:104262, 2020
- Hall-Stoodley L, Hu FZ, Gieseke A, Nistico L, Nguyen D, Hayes J, Forbes M, Greenberg DP, Dice B, Burrows A, Wackym PA, Stoodley P, Post JC, Ehrlich GD, Kerschner JE: Direct detection of bacterial biofilms on the middle-ear mucosa of children with chronic otitis media. *JAMA* 296: 202–211, 2006
- Heilmann C, Hartleib J, Hussain MS, Peters G: The multifunctional *Staphylococcus aureus* autolysin Aaa mediates adherence to immobilized fibrinogen and fibronectin. *Infect Immun* 73: 4793–4802, 2005
- Heilmann C: Adhesion mechanisms of staphylococci. *Adv Exp Med Biol* 715: 105–123, 2011
- Helwig P, Morlock J, Oberst M, Hauschild O, Hübner J, Borde J, Südkamp NP, Konstantinidis L: Periprosthetic joint infection – Effect on quality of life. *Int Orthop* 38: 1077–1081, 2014
- Hench LL, Day DE, Höland W, Rheinberger VM: Glass and medicine. *Int J Appl Glass Sci* 1: 104–117, 2010
- Henze U, Sidow T, Wecke J, Labischinski H, Berger-Bächi B: Influence of femB on methicillin resistance and peptidoglycan metabolism in *Staphylococcus aureus*. *J Bacteriol* 175: 1612–1620, 1993
- Herant M, Heinrich V, Dembo M: Mechanics of neutrophil phagocytosis: Experiments and quantitative models. *J Cell Sci* 119: 1903–1913, 2006
- Herbert BA, Novince CM, Kirkwood KL: *Aggregatibacter actinomycetemcomitans*, a potent immunoregulator of the periodontal host defense system and alveolar bone homeostasis. *Mol Oral Microbiol* 31: 207–227, 2016
- Hillilä M: Osteoporosisin lääkehoito. In the book: *Farmakologia ja toksikologia*, pp. 765–772. Eds. Koulu M, Tuomisto J. *Medicina*, Kuopio, Finland, 2007
- Hiltunen A, Skogman M, Vuorela PM, Fallarero A: Exploration of microbial communities using the Thermo Scientific Varioskan LUX Multimode Reader and the Invitrogen EVOS FL Cell Imaging System. *Biotechniques* 63: 236–237, 2017
- Hiltunen AK: The anti-biofilm effects of bisphosphonates and bioactive glass on the periodontopathogen *Aggregatibacter actinomycetemcomitans*. Master's thesis, University of Helsinki, Helsinki, Finland, 2015. Available online: <https://helda.helsinki.fi/handle/10138/156237>
- Hoceini A, Khelil NK, Ben-Yelles I, Mesli A, Ziouani S, Ghellai L, Aissaoui N, Nas F, Arab M: Caries-related factors and bacterial composition of supragingival plaques in caries free and caries active Algerian adults. *Asian Pac J Trop Biomed* 6: 720–726, 2016
- Høiby N, Bjarnsholt T, Moser C, Bassi GL, Coenye T, Donelli G, Hall-Stoodley L, Holá V, Imbert C, Kirketerp-Møller K, Lebeaux D, Oliver A, Ullmann AJ, Williams C; ESCMID study group for biofilms and consulting external expert Werner Zimmerli: ESCMID guideline for the diagnosis and treatment of biofilm infections 2014. *Clin Microbiol Infect* 21: S1–25, 2015
- Høiby N, Olling S: *Pseudomonas aeruginosa* infection in cystic fibrosis. Bactericidal effect of serum from normal individuals and patients with cystic fibrosis on *P. aeruginosa* strains from patients with cystic fibrosis or other diseases. *Acta Pathol Microbiol Scand C* 85: 107–114, 1977

## 7. REFERENCES

- Höing B, Kirchhoff L, Arnolds J, Hussain T, Buer J, Lang S, Arweiler-Harbeck D, Steinmann J: Bioactive glass granules inhibit mature bacterial biofilms on the surfaces of cochlear implants. *Otol Neurotol* 39: e985–e991, 2018
- Igarashi K, Adachi H, Mitani H, Shinoda H: Inhibitory effect of the topical administration of a bisphosphonate (risedronate) on root resorption incident to orthodontic tooth movement in rats. *J Dent Res* 75: 1644–1649, 1996
- Imamura T, Tanase S, Szmyd G, Kozik A, Travis J, Potempa J: Induction of vascular leakage through release of bradykinin and a novel kinin by cysteine proteinases from *Staphylococcus aureus*. *J Exp Med* 201: 1669–1676, 2005
- Izakovicova P, Borens O, Trampuz A: Periprosthetic joint infection: Current concepts and outlook. *EFORT Open Rev* 4: 482–494, 2019
- Jamal M, Ahmad W, Andleeb S, Jalil F, Imran M, Nawaz MA, Hussain T, Ali M, Rafiq M, Kamil MA: Bacterial biofilm and associated infections. *J Chin Med Assoc* 81: 7–11, 2018
- Jeffcoat MK, Cizza G, Shih WJ, Genco R, Lombardi A: Efficacy of bisphosphonates for the control of alveolar bone loss in periodontitis. *J Int Acad Periodontol* 9: 70–76, 2007
- Jeffery C: Intracellular proteins moonlighting as bacterial adhesion factors. *AIMS Microbiol* 4: 362–376, 2018
- Jennings JA, Carpenter DP, Troxel KS, Beenken KE, Smeltzer MS, Courtney HS, Haggard WO: Novel antibiotic-loaded point-of-care implant coating inhibits biofilm. *Clin Orthop Relat Res* 473: 2270–2282, 2015
- Jeon H, Oh MH, Jun SH, Kim SI, Choi CW, Kwon HI, Na SH, Kim YJ, Nicholas A, Selasi GN, Lee JC: Variation among *Staphylococcus aureus* membrane vesicle proteomes affects cytotoxicity of host cells. *Microb Pathog* 93: 185–193, 2016
- Joo HS, Otto M: Molecular basis of *in vivo* biofilm formation by bacterial pathogens. *Chem Biol* 19: 1503–1513, 2012
- Kainulainen V, Korhonen TK: Dancing to another tune-adhesive moonlighting proteins in bacteria. *Biology (Basel)* 3: 178–204, 2014
- Kainulainen V, Loimaranta V, Pekkala A, Edelman S, Antikainen J, Kylväjä R, Laaksonen M, Laakkonen L, Finne J, Korhonen TK: Glutamine synthetase and glucose-6-phosphate isomerase are adhesive moonlighting proteins of *Lactobacillus crispatus* released by epithelial cathelicidin LL-37. *J Bacteriol* 194: 2509–2519, 2012
- Kamer AR, Craig RG, Pirraglia E, Dasanayake AP, Norman RG, Boylan RJ, Nehorayoff A, Glodzik L, Brys M, de Leon MJ: TNF-alpha and antibodies to periodontal bacteria discriminate between Alzheimer's disease patients and normal subjects. *J Neuroimmunol* 216: 92–97, 2009
- Kaplan JB: Therapeutic potential of biofilm-dispersing enzymes. *Int J Artif Organs* 32: 545–554, 2009
- Karavolos MH, Horsburgh MJ, Ingham E, Foster SJ: Role and regulation of the superoxide dismutases of *Staphylococcus aureus*. *Microbiology (Reading)* 149: 2749–2758, 2003
- Katakura Y, Sano R, Hashimoto T, Ninomiya K, Shioya S: Lactic acid bacteria display on the cell surface cytosolic proteins that recognize yeast mannan. *Appl Microbiol Biotechnol* 86: 319–326, 2010
- Kavanagh N, Ryan EJ, Widaa A, Sexton G, Fennell J, O'Rourke S, Cahill KC, Kearney CJ, O'Brien FJ, Kerrigan SW: Staphylococcal osteomyelitis: Disease progression, treatment challenges, and future directions. *Clin Microbiol Rev* 31: e00084–17, 2018

- Kawai K, Urano M, Ebisu S: Effect of surface roughness of porcelain on adhesion of bacteria and their synthesizing glucans. *J Prosthet Dent* 83: 664–667, 2000
- Kelly M, Williams R, Aojula A, O'Neill J, Trzińska Z, Grover L, Scott RA, Peacock AF, Logan A, Stamboulis A, de Cogan F: Peptide aptamers: Novel coatings for orthopaedic implants. *Mater Sci Eng C Mater Biol Appl* 54: 84–93, 2015
- Kesimer M, Kiliç N, Mehrotra R, Thornton DJ, Sheehan JK: Identification of salivary mucin MUC7 binding proteins from *Streptococcus gordonii*. *BMC Microbiol* 9: 163, 2009
- Kinnby B, Booth NA, Svensäter G: Plasminogen binding by oral streptococci from dental plaque and inflammatory lesions. *Microbiology* 154: 924–931, 2008
- Kinoshita H, Uchida H, Kawai Y, Kawasaki T, Wakahara N, Matsuo H, Watanabe M, Kitazawa H, Ohnuma S, Miura K, Horii A, Saito T: Cell surface *Lactobacillus plantarum* LA 318 glyceraldehyde-3-phosphate dehydrogenase (GAPDH) adheres to human colonic mucin. *J Appl Microbiol* 104: 1667–1674, 2008
- Knaust A, Weber MV, Hammerschmidt S, Bergmann S, Frosch M, Kurzai O: Cytosolic proteins contribute to surface plasminogen recruitment of *Neisseria meningitidis*. *J Bacteriol* 189: 3246–3255, 2007
- Ko YP, Kuipers A, Freitag CM, Jongerius I, Medina E, van Rooijen WJ, Spaan AN, van Kessel KPM, Höök M, Rooijackers SHM: Phagocytosis escape by a *Staphylococcus aureus* protein that connects complement and coagulation proteins at the bacterial surface. *PLoS Pathog* 9: e1003816, 2013
- Koedijk DGAM, Pastrana FR, Hoekstra H, Berg SVD, Back JW, Kerstholt C, Prins RC, Bakker-Woudenberg IAJM, van Dijk JM, Buist G: Differential epitope recognition in the immunodominant staphylococcal antigen A of *Staphylococcus aureus* by mouse versus human IgG antibodies. *Sci Rep* 7: 8141, 2017
- Konermann L: Protein unfolding and denaturants. *eLS*: 1–7, 2012
- König MF, Abusleme L, Reinholdt J, Palmer RJ, Teles RP, Sampson K, Rosen A, Nigrovic PA, Sokolove J, Giles JT, Moutsopoulos NM, Andrade F: *Aggregatibacter actinomycetemcomitans*-induced hypercitrullination links periodontal infection to autoimmunity in rheumatoid arthritis. *Sci Transl Med* 8: 369ra176, 2016
- Korea CG, Balsamo G, Pezzicoli A, Merakou C, Tavarini S, Bagnoli F, Serruto D, Unnikrishnan M: Staphylococcal Exs proteins modulate apoptosis and release of intracellular *Staphylococcus aureus* during infection in epithelial cells. *Infect Immun* 82: 4144–4153, 2014
- Koseki H, Yonekura A, Shida T, Yoda I, Horiuchi H, Morinaga Y, Yanagihara K, Sakoda H, Osaki M, Tomita M: Early staphylococcal biofilm formation on solid orthopaedic implant materials: *In vitro* study. *PLoS One* 9: e107588, 2014
- Kristian SA, Birkenstock TA, Sauder U, Mack D, Götz F, Landmann R: Biofilm formation induces C3a release and protects *Staphylococcus epidermidis* from IgG and complement deposition and from neutrophil-dependent killing. *J Infect Dis* 197: 1028–1035, 2008
- Kruszewska H, Zareba T, Tyski S: Examination of antimicrobial activity of selected non-antibiotic medicinal preparations. *Acta Pol Pharm* 69: 1368–1371, 2012
- Kruszewska H, Zareba T, Tyski S: Search of antimicrobial activity of selected non-antibiotic drugs. *Acta Pol Pharm* 59: 436–439, 2002
- Kunert A, Losse J, Gruszyn C, Hühn M, Kaendler K, Mikkat S, Volke D, Hoffmann R, Jokiranta TS, Seeberger H, Moellmann U, Hellwege J, Zipfel PF: Immune evasion of the human pathogen *Pseudomonas aeruginosa*: Elongation factor

## 7. REFERENCES

- Tuf is a factor H and plasminogen binding protein. *J Immunol* 179: 2979–2988, 2007
- Kuroda M, Ohta T, Hayashi H: Isolation and the gene cloning of an alkaline shock protein in methicillin resistant *Staphylococcus aureus*. *Biochem Biophys Res Commun* 207: 978–984, 1995
- Kuźnik A, Październiak-Holewa A, Jewula P, Kuźnik N: Bisphosphonates – much more than only drugs for bone diseases. *Eur J Pharmacol* 866: 172773, 2020
- Kwon T, Lamster IB, Levin L: Current concepts in the management of periodontitis. *Int Dent J* 2020. doi: 10.1111/idj.12630. Epub ahead of print.
- Laarman AJ, Mijnheer G, Mootz JM, van Rooijen WJ, Ruyken M, Malone CL, Heezius EC, Ward R, Milligan G, van Strijp JA, de Haas CJ, Horswill AR, van Kessel KP, Rooijackers SH: *Staphylococcus aureus* staphopain A inhibits CXCR2-dependent neutrophil activation and chemotaxis. *EMBO J* 31: 3607–3619, 2012
- Lafon A, Pereira B, Dufour T, Rigouby V, Giroud M, Béjot Y, Tubert-Jeannin S: Periodontal disease and stroke: A meta-analysis of cohort studies. *Eur J Neurol* 21: 1155–1161, 2014
- Lagerlöf F, Dawes C: The volume of saliva in the mouth before and after swallowing. *J Dent Res* 63: 618–621, 1984
- Lang S, Livesley MA, Lambert PA, Littler WA, Elliott TS: Identification of a novel antigen from *Staphylococcus epidermidis*. *FEMS Immunol Med Microbiol* 29: 213–220, 2000
- Lebeaux D, Chauhan A, Rendueles O, Beloin C: From *in vitro* to *in vivo* models of bacterial biofilm-related infections. *Pathogens* 2: 288–356, 2013
- Lee EY, Choi DY, Kim DK, Kim JW, Park JO, Kim S, Kim SH, Desiderio DM, Kim YK, Kim KP, Gho YS: Gram-positive bacteria produce membrane vesicles: Proteomics-based characterization of *Staphylococcus aureus*-derived membrane vesicles. *Proteomics* 9: 5425–5436, 2009
- Lee J, Lee EY, Kim SH, Kim DK, Park KS, Kim KP, Kim YK, Roh TY, Gho YS: *Staphylococcus aureus* extracellular vesicles carry biologically active  $\beta$ -lactamase. *Antimicrob Agents Chemother* 57: 2589–2595, 2013
- Lee JS, Bae YM, Lee SY, Lee SY: Biofilm formation of *Staphylococcus aureus* on various surfaces and their resistance to chlorine sanitizer. *J Food Sci* 80: M2279–M2286, 2015
- Lei MG, Gupta RK, Lee CY: Proteomics of *Staphylococcus aureus* biofilm matrix in a rat model of orthopedic implant-associated infection. *PLoS One* 12: e0187981, 2017
- Leid JG, Cope EK, Parmenter S, Shirtliff ME, Dowd S, Wolcott R, Basaraba DVM R, Hunsaker D, Palmer J, Cohen N: The importance of biofilms in chronic rhinosinusitis. In the book: *Biofilm infections*, pp. 139–160. Eds. Bjarnsholt T, Jensen P, Moser C, Høiby N. Springer, New York, US, 2011
- Lenguerrand E, Whitehouse MR, Beswick AD, Kunutsor SK, Burston B, Porter M, Blom AW: Risk factors associated with revision for prosthetic joint infection after hip replacement: A prospective observational cohort study. *Lancet Infect Dis* 18: 1004–1014, 2018
- Leppäranta O, Vaahtio M, Peltola T, Zhang D, Hupa L, Hupa M, Ylänen H, Salonen JI, Viljanen MK, Eerola E: Antibacterial effect of bioactive glasses on clinically important anaerobic bacteria *in vitro*. *J Mater Sci Mater Med* 19: 547–551, 2008
- Lewis K: Multidrug tolerance of biofilms and persister cells. *Curr Top Microbiol Immunol* 322: 107–131, 2008

- Lewis K: Persister cells. *Annu Rev Microbiol* 64: 357–372, 2010
- Li C, Renz N, Trampuz A: Management of periprosthetic joint infection. *Hip Pelvis* 30: 138–146, 2018
- Liang BS, Huang YM, Chen YS, Dong H, Mai JL, Xie YQ, Zhong HM, Deng QL, Long Y, Yang YY, Gong ST, Zhou ZW: Antimicrobial resistance and prevalence of *CvfB*, *SEK* and *SEQ* genes among *Staphylococcus aureus* isolates from paediatric patients with bloodstream infections. *Exp Ther Med* 14: 5143–5148, 2017
- Liljestrand JM, Paju S, Pietiäinen M, Buhlin K, Persson GR, Nieminen MS, Sinisalo J, Mäntylä P, Pussinen PJ: Immunologic burden links periodontitis to acute coronary syndrome. *Atherosclerosis* 268: 177–184, 2018
- Lin D, Moss K, Beck JD, Hefti A, Offenbacher S: Persistently high levels of periodontal pathogens associated with preterm pregnancy outcome. *J Periodontol* 78: 833–841, 2007
- Lin MH, Shu JC, Lin LP, Chong KY, Cheng YW, Du JF, Liu ST: Elucidating the crucial role of poly N-acetylglucosamine from *Staphylococcus aureus* in cellular adhesion and pathogenesis. *PLoS One* 10: e0124216, 2015
- Liu L, Igarashi K, Haruyama N, Saeki S, Shinoda H, Mitani H: Effects of local administration of clodronate on orthodontic tooth movement and root resorption in rats. *Eur J Orthod* 26: 469–473, 2004
- Liu PF, Cheng JS, Sy CL, Huang WC, Yang HC, Gallo RL, Huang CM, Shu CW: IsaB inhibits autophagic flux to promote host transmission of methicillin-resistant *Staphylococcus aureus*. *J Invest Dermatol* 135: 2714–2722, 2015
- Lorey MB, Rossi K, Eklund KK, Nyman TA, Matikainen S: Global characterization of protein secretion from human macrophages following non-canonical caspase-4/5 inflammasome activation. *Mol Cell Proteomics* 16: S187–S199, 2017
- Löwik CAM, Parvizi J, Jutte PC, Zijlstra WP, Knobben BAS, Xu C, Goswami K, Belden KA, Sousa R, Carvalho A, Martínez-Pastor JC, Soriano A, Wouthuyzen-Bakker M: Debridement, antibiotics, and implant retention is a viable treatment option for early periprosthetic joint infection presenting more than 4 weeks after index arthroplasty. *Clin Infect Dis* 71: 630–636, 2020
- Määttänen A, Fallarero A, Kujala J, Ihalainen P, Vuorela P, Peltonen J: Printed paper-based arrays as substrates for biofilm formation. *AMB Express* 4: 32, 2014
- Maidhof H, Reinicke B, Blümel P, Berger-Bächi B, Labischinski H: FemA, which encodes a factor essential for expression of methicillin resistance, affects glycine content of peptidoglycan in methicillin-resistant and methicillin-susceptible *Staphylococcus aureus* strains. *J Bacteriol* 173: 3507–3513, 1991
- Malat TA, Glombitza M, Dahmen J, Hax PM, Steinhausen E: The use of bioactive glass S53P4 as bone graft substitute in the treatment of chronic osteomyelitis and infected non-unions – A retrospective study of 50 patients. *Z Orthop Unfall* 156: 152–159, 2018
- Mandakhalikar KD, Chua RR, Tambyah PA: New technologies for prevention of catheter associated urinary tract infection. *Curr Treat Options Infect Dis* 8: 24–41, 2016
- Mandakhalikar KD, Rahmat JN, Chiong E, Neoh KG, Shen L, Tambyah PA: Extraction and quantification of biofilm bacteria: Method optimized for urinary catheters. *Sci Rep* 8: 8069, 2018

## 7. REFERENCES

- Mandakhalikar KD: Medical Biofilms. In the book: Introduction to biofilm engineering, pp. 83–99. Eds. Rathinam NK, Sani RK. American Chemical Society, Washington, D.C, US, 2019
- Mandell JB, Orr S, Koch J, Nourie B, Ma D, Bonar DD, Shah N, Urish KL: Large variations in clinical antibiotic activity against *Staphylococcus aureus* biofilms of periprosthetic joint infection isolates. *J Orthop Res* 37: 1604–1609, 2019
- Manner S, Goeres DM, Skogman M, Vuorela P, Fallarero A: Prevention of *Staphylococcus aureus* biofilm formation by antibiotics in 96-microtiter well plates and drip flow reactors: Critical factors influencing outcomes. *Sci Rep* 7: 43854, 2017
- Marshall KC: Interfaces in microbial ecology. Harvard University Press, Cambridge, US, 1976
- Menezes AM, Rocha FA, Chaves HV, Carvalho CB, Ribeiro RA, Brito GA: Effect of sodium alendronate on alveolar bone resorption in experimental periodontitis in rats. *J Periodontol* 76: 1901–1909, 2005
- Mengel R, Schreiber D, Flores-de-Jacoby L: Bioabsorbable membrane and bioactive glass in the treatment of intrabony defects in patients with generalized aggressive periodontitis: Results of a 5-year clinical and radiological study. *J Periodontol* 77: 1781–1787, 2006
- Mengel R, Soffner M, Flores-de-Jacoby L: Bioabsorbable membrane and bioactive glass in the treatment of intrabony defects in patients with generalized aggressive periodontitis: Results of a 12-month clinical and radiological study. *J Periodontol* 74: 899–908, 2003
- Merino N, Toledo-Arana A, Vergara-Irigaray M, Valle J, Solano C, Calvo E, Lopez JA, Foster TJ, Penadés JR, Lasa I: Protein A-mediated multicellular behavior in *Staphylococcus aureus*. *J Bacteriol* 191: 832–843, 2009
- Michalik S, Depke M, Murr A, Gesell Salazar M, Kusebauch U, Sun Z, Meyer TC, Surmann K, Pfortner H, Hildebrandt P, Weiss S, Palma Medina LM, Gutjahr M, Hammer E, Becher D, Pribyl T, Hammerschmidt S, Deutsch EW, Bader SL, Hecker M, Moritz RL, Mäder U, Völker U, Schmidt F: A global *Staphylococcus aureus* proteome resource applied to the *in vivo* characterization of host-pathogen interactions. *Sci Rep* 7: 9718, 2017
- Michaud DS, Fu Z, Shi J, Chung M: Periodontal disease, tooth loss, and cancer risk. *Epidemiol Rev* 39: 49–58, 2017
- Michel A, Agerer F, Hauck CR, Herrmann M, Ullrich J, Hacker J, Ohlsen K: Global regulatory impact of ClpP protease of *Staphylococcus aureus* on regulons involved in virulence, oxidative stress response, autolysis, and DNA repair. *J Bacteriol* 188: 5783–5796, 2006
- Mille Y, Beney L, Gervais P: Compared tolerance to osmotic stress in various microorganisms: Towards a survival prediction test. *Biotechnol Bioeng* 92: 479–484, 2005
- Mitsuta T, Horiuchi H, Shinoda H: Effects of topical administration of clodronate on alveolar bone resorption in rats with experimental periodontitis. *J Periodontol* 73: 479–486, 2002
- Modun B, Williams P: The staphylococcal transferrin-binding protein is a cell wall glyceraldehyde-3-phosphate dehydrogenase. *Infect Immun* 67: 1086–1092, 1999
- MoonProt: A Database for Moonlighting Proteins. Available online: <http://www.moonlightingproteins.org/>. Accessed: December 20<sup>th</sup>, 2020



- Moreira MM, Bradaschia-Correa V, Marques ND, Ferreira LB, Arana-Chavez VE: Ultrastructural and immunohistochemical study of the effect of sodium alendronate in the progression of experimental periodontitis in rats. *Microsc Res Tech* 77: 902–909, 2014
- Munukka E, Leppäranta O, Korkeamäki M, Vaahtio M, Peltola T, Zhang D, Hupa L, Ylänen H, Salonen JI, Viljanen MK, Eerola E: Bactericidal effects of bioactive glasses on clinically important aerobic bacteria. *J Mater Sci Mater Med* 19: 27–32, 2008
- Namvar AE, Bastarahang S, Abbasi N, Ghehi GS, Farhadbakhtarian S, Arezi P, Hosseini M, Baravati SZ, Jokar Z, Chermahin SG: Clinical characteristics of *Staphylococcus epidermidis*: A systematic review. *GMS Hyg Infect Control* 9: Doc23, 2014
- National Institute for Health and Welfare: Finnish Arthroplasty Register 2020. Available online: <https://www.thl.fi/far/#index>. Accessed: November 16<sup>th</sup>, 2020
- Nazir MA: Prevalence of periodontal disease, its association with systemic diseases and prevention. *Int J Health Sci (Qassim)* 11: 72–80, 2017
- Nguyen HTT, Nguyen TH, Otto M: The staphylococcal exopolysaccharide PIA - Biosynthesis and role in biofilm formation, colonization, and infection. *Comput Struct Biotechnol J* 18: 3324–3334, 2020
- Nostro A, Cellini L, Di Giulio M, D'Arrigo M, Marino A, Blanco AR, Favalaro A, Cutroneo G, Bisignano G: Effect of alkaline pH on staphylococcal biofilm formation. *APMIS* 120: 733–742, 2012
- Nymer M, Cope E, Brady R, Shirliff ME, Leid JG: Immune responses to indwelling medical devices. In the book: *The role of biofilms in device-related infections*, pp. 239–264. Eds. Shirliff ME, Leid JG. Springer, Cham, Switzerland, 2008
- O'May GA, Brady RA, Prabhakara R, Leid JG, Calhoun JH, Shirliff ME: Osteomyelitis. In the book: *Biofilm infections*, pp. 111–137. Eds. Bjarnsholt T, Jensen P, Moser C, Høiby N. Springer, New York, US, 2011
- O'Connor A, McClean S: The role of universal stress proteins in bacterial infections. *Curr Med Chem* 24: 3970–3979, 2017
- Oettinger-Barak O, Dashper SG, Catmull DV, Adams GG, Sela MN, Machtei EE, Reynolds EC: Antibiotic susceptibility of *Aggregatibacter actinomycetemcomitans* JP2 in a biofilm. *J Oral Microbiol* 5, 2013
- Oja T, Blomqvist B, Buckingham-Meyer K, Goeres D, Vuorela P, Fallarero A: Revisiting an agar-based plate method: What the static biofilm method can offer for biofilm research. *J Microbiol Methods* 107: 157–160, 2014
- Otto M: Biofilms in disease. In the book: *Antibiofilm agents*, pp. 3–13. Eds. Rumbaugh K, Ahmad I. Springer, Berlin, Heidelberg, Germany, 2014a
- Otto M: Staphylococcal biofilms. *Microbiol Spectr* 6: 1–26, 2018
- Otto M: *Staphylococcus aureus* toxins. *Curr Opin Microbiol* 17: 32–37, 2014b
- Otto M: *Staphylococcus* colonization of the skin and antimicrobial peptides. *Expert Rev Dermatol* 5: 183–195, 2010
- Otto M: Targeted immunotherapy for staphylococcal infections: Focus on anti-MSCRAMM antibodies. *BioDrugs* 22: 27–36, 2008
- Paharik AE, Horswill AR: The staphylococcal biofilm: Adhesins, Regulation, and host response. *Microbiol Spectr* 4, 2016
- Paino A, Tuominen H, Jääskeläinen M, Alanko J, Nuutila J, Asikainen SE, Pelliniemi LJ, Pöllänen MT, Chen C, Ihalin R: Trimeric form of intracellular ATP synthase

## 7. REFERENCES

- subunit  $\beta$  of *Aggregatibacter actinomycetemcomitans* binds human interleukin-1 $\beta$ . PLoS One 6: e18929, 2011
- Palomo L, Bissada NF, Liu J: Periodontal assessment of postmenopausal women receiving risedronate. Menopause 12: 685–690, 2005
- Parameswaran R, Sherchan JB, Varma D M, Mukhopadhyay C, Vidyasagar S: Intravascular catheter-related infections in an Indian tertiary care hospital. J Infect Dev Ctries 5: 452–458, 2011
- Park JH, Lee JK, Um HS, Chang BS, Lee SY: A periodontitis-associated multispecies model of an oral biofilm. J Periodontal Implant Sci 44: 79–84, 2014
- Parsek MR, Fuqua C: Biofilms 2003: Emerging themes and challenges in studies of surface-associated microbial life. J Bacteriol 186: 4427–4440, 2004
- Pasztor L, Ziebandt AK, Nega M, Schlag M, Haase S, Franz-Wachtel M, Madlung J, Nordheim A, Heinrichs DE, Götz F: Staphylococcal major autolysin (Atl) is involved in excretion of cytoplasmic proteins. J Biol Chem 285: 36794–36803, 2010
- Patel SS, Aruni W, Inceoglu S, Akpolat YT, Botimer GD, Cheng WK, Danisa OA: A comparison of *Staphylococcus aureus* biofilm formation on cobalt-chrome and titanium-alloy spinal implants. J Clin Neurosci 31: 219–223, 2016
- Payne DE, Boles BR: Emerging interactions between matrix components during biofilm development. Curr Genet 62: 137–141, 2016
- Periasamy S, Joo HS, Duong AC, Bach TH, Tan VY, Chatterjee SS, Cheung GY, Otto M: How *Staphylococcus aureus* biofilms develop their characteristic structure. Proc Natl Acad Sci U S A 109: 1281–1286, 2012
- Persson L, Johansson C, Rydén C: Antibodies to *Staphylococcus aureus* bone sialoprotein-binding protein indicate infectious osteomyelitis. Clin Vaccine Immunol 16: 949–952, 2009
- Peters W, Fornasier V: Complications from injectable materials used for breast augmentation. Can J Plast Surg 17: 89–96, 2009
- Peterson SB, Irie Y, Borlee BR, Murakami K, Harrison JJ, Colvin KM, Parsek MR: Different methods for culturing biofilms *in vitro*. In the book: Biofilm infections, pp. 251–266. Eds. Bjarnsholt T, Jensen P, Moser C, Høiby N. Springer, New York, US, 2011a
- Peterson SN, Snesrud E, Schork NJ, Bretz WA: Dental caries pathogenicity: A genomic and metagenomic perspective. Int Dent J 61: 11–22, 2011b
- Pitts B, Hamilton MA, Zilver N, Stewart PS: A microtiter-plate screening method for biofilm disinfection and removal. J Microbiol Methods 54: 269–276, 2003
- Podlesek Z, Žgur Bertok D: The DNA damage inducible SOS response is a key player in the generation of bacterial persister cells and population wide tolerance. Front Microbiol 11: 1785, 2020
- Pollitt E J G, Diggle S P. Defining motility in the staphylococci. Cell Mol Life Sci 74: 2943–2958, 2017
- Porayath C, Suresh MK, Biswas R, Nair BG, Mishra N, Pal S: Autolysin mediated adherence of *Staphylococcus aureus* with fibronectin, gelatin and heparin. Int J Biol Macromol 110: 179–184, 2018
- Pradeep AR, Sharma A, Rao NS, Bajaj P, Naik SB, Kumari M: Local drug delivery of alendronate gel for the treatment of patients with chronic periodontitis with diabetes mellitus: A double-masked controlled clinical trial. J Periodontol 83:1322–1328, 2012
- Pye AD, Lockhart DE, Dawson MP, Murray CA, Smith AJ: A review of dental implants and infection. J Hosp Infect 72: 104–110, 2009

- Que YA, Moreillon P: Infective endocarditis. *Nat Rev Cardiol* 8: 322–336, 2011
- Rahamat-Langendoen JC, van Vonderen MG, Engström LJ, Manson WL, van Winkelhoff AJ, Mooi-Kokenberg EA: Brain abscess associated with *Aggregatibacter actinomycetemcomitans*: Case report and review of literature. *J Clin Periodontol* 38: 702–706, 2011
- Rahman MM, Hunter HN, Prova S, Verma V, Qamar A, Golemi-Kotra D: The *Staphylococcus aureus* methicillin resistance factor Fmta is a d-amino esterase that acts on teichoic acids. *mBio* 7: e02070–15, 2016
- Rajan S, Saiman L: Pulmonary infections in patients with cystic fibrosis. *Semin Respir Infect* 17: 47–56, 2002
- Rantakokko J, Frantzén JP, Heinänen J, Kajander S, Kotilainen E, Gullichsen E, Lindfors NC: Posterolateral spondylosis using bioactive glass S53P4 and autogenous bone in instrumented unstable lumbar spine burst fractures. A prospective 10-year follow-up study. *Scand J Surg* 101: 66–71, 2012
- Reddy GT, Kumar TM, Veena: Formulation and evaluation of alendronate sodium gel for the treatment of bone resorptive lesions in periodontitis. *Drug Deliv* 12: 217–222, 2005
- Reddy MS, Weatherford TW 3rd, Smith CA, West BD, Jeffcoat MK, Jacks TM: Alendronate treatment of naturally-occurring periodontitis in beagle dogs. *J Periodontol* 66: 211–217, 1995
- Reddy VM, Suleman FG: *Mycobacterium avium*-superoxide dismutase binds to epithelial cell aldolase, glyceraldehyde-3-phosphate dehydrogenase and cyclophilin A. *Microb Pathog* 36: 67–74, 2004
- Reigada I, Guarch-Pérez C, Patel JZ, Riool M, Savijoki K, Yli-Kauhaluoma J, Zaat SAJ, Fallarero A: Combined effect of naturally-derived biofilm inhibitors and differentiated HL-60 cells in the prevention of *Staphylococcus aureus* biofilm formation. *Microorganisms* 8: 1757, 2020a
- Reigada I, Pérez-Tanoira R, Patel JZ, Savijoki K, Yli-Kauhaluoma J, Kinnari TJ, Fallarero A: Strategies to prevent biofilm infections on biomaterials: Effect of novel naturally-derived biofilm inhibitors on a competitive colonization model of titanium by *Staphylococcus aureus* and SaOS-2 cells. *Microorganisms* 8: 345, 2020b
- Reshamwala SMS, Mamidipally C, Pissurlenkar RRS, Coutinho EC, Noronha S: Evaluation of risedronate as an antibiofilm agent. *J Med Microbiol* 65: 9–18, 2016
- Richardson AR, Somerville GA, Sonenshein AL: Regulating the intersection of metabolism and pathogenesis in gram-positive bacteria. *Microbiol Spectr* 3, 2015
- Rocha M, Nava LE, Vázquez de la Torre C, Sánchez-Márin F, Garay-Sevilla ME, Malacara JM: Clinical and radiological improvement of periodontal disease in patients with type 2 diabetes mellitus treated with alendronate: A randomized, placebo-controlled trial. *J Periodontol* 72: 204–209, 2001
- Rocha ML, Malacara JM, Sánchez-Marin FJ, Vazquez de la Torre CJ, Fajardo ME: Effect of alendronate on periodontal disease in postmenopausal women: A randomized placebo-controlled trial. *J Periodontol* 75: 1579–1585, 2004
- Roehling S, Astasov-Frauenhoffer M, Hauser-Gerspach I, Braissant O, Woelfler H, Waltimo T, Kniha H, Gahlert M: *In vitro* biofilm formation on titanium and zirconia implant surfaces. *J Periodontol* 88: 298–307, 2017
- Rohde H, Burandt EC, Siemssen N, Frommelt L, Burdelski C, Wurster S, Scherpe S, Davies AP, Harris LG, Horstkotte MA, Knobloch JK, Ragunath C, Kaplan JB, Mack D: Polysaccharide intercellular adhesin or protein factors in biofilm

## 7. REFERENCES

- accumulation of *Staphylococcus epidermidis* and *Staphylococcus aureus* isolated from prosthetic hip and knee joint infections. *Biomaterials* 28: 1711–1720, 2007
- Romanò CL, Logoluso N, Meani E, Romanò D, De Vecchi E, Vassena C, Drago L: A comparative study of the use of bioactive glass S53P4 and antibiotic-loaded calcium-based bone substitutes in the treatment of chronic osteomyelitis: A retrospective comparative study. *Bone Joint J* 96-B: 845–850, 2014
- Rosenqvist K, Airaksinen S, Fraser SJ, Gordon KC, Juppo AM: Interaction of bioactive glass with clodronate. *Int J Pharm* 452: 102–107, 2013
- Rosenqvist K, Airaksinen S, Vehkamäki M, Juppo AM: Evaluating optimal combination of clodronate and bioactive glass for dental application. *Int J Pharm* 468: 112–120, 2014
- Rosenqvist K, Gursöy M, Könönen E, Gursöy U, Juppo AM: Comparison between a novel combination of bioactive glass with clodronate and bioactive glass alone as a treatment for chronic periodontitis. *J Biotechnol Biomat* 7: 1000265, 2017
- Rosman M, Rachminov O, Segal O, Segal G: Prolonged patients' in-hospital waiting period after discharge eligibility is associated with increased risk of infection, morbidity and mortality: A retrospective cohort analysis. *BMC Health Serv Res* 15: 246, 2015
- Sánchez MC, Llama-Palacios A, Blanc V, León R, Herrera D, Sanz M: Structure, viability and bacterial kinetics of an *in vitro* biofilm model using six bacteria from the subgingival microbiota. *J Periodontal Res* 46: 252–260, 2011
- Sankar GG, Murthy PS, Das A, Sathya S, Nankar R, Venugopalan VP, Doble M: Polydimethyl siloxane based nanocomposites with antibiofilm properties for biomedical applications. *J Biomed Mater Res B Appl Biomater* 105: 1075–1082, 2017
- Savage VJ, Chopra I, O'Neill AJ: *Staphylococcus aureus* biofilms promote horizontal transfer of antibiotic resistance. *Antimicrob Agents Chemother* 57: 1968–1970, 2013
- Savijoki K, Nyman TA, Kainulainen V, Miettinen I, Siljamäki P, Fallarero A, Sandholm J, Satokari R, Varmanen P: Growth mode and carbon source impact the surfaceome dynamics of *Lactobacillus rhamnosus* GG. *Front Microbiol* 10: 1272, 2019
- Schilcher K, Horswill AR: Staphylococcal biofilm development: Structure, regulation, and treatment strategies. *Microbiol Mol Biol Rev* 84: e00026-19, 2020
- Schwan WR, Wetzel KJ: Osmolyte transport in *Staphylococcus aureus* and the role in pathogenesis. *World J Clin Infect Dis* 6: 22–27, 2016
- Shaqour B, Reigada I, Górecka Ż, Choińska E, Verleije B, Beyers K, Świążkowski W, Fallarero A, Cos P: 3D-printed drug delivery systems: The effects of drug incorporation methods on their release and antibacterial efficiency. *Materials (Basel)* 13: 3364, 2020
- Sharma A, Pradeep AR: Clinical efficacy of 1% alendronate gel as a local drug delivery system in the treatment of chronic periodontitis: A randomized, controlled clinical trial. *J Periodontol* 83: 11–18, 2012a
- Sharma A, Pradeep AR: Clinical efficacy of 1% alendronate gel in adjunct to mechanotherapy in the treatment of aggressive periodontitis: A randomized controlled clinical trial. *J Periodontol* 83: 19–26, 2012b

- Shasmal M, Dey S, Shaikh TR, Bhakta S, Sengupta J: *E. coli* metabolic protein aldehyde-alcohol dehydrogenase-E binds to the ribosome: A unique moonlighting action revealed. *Sci Rep* 6: 19936, 2016
- Shoji K, Horiuchi H, Shinoda H: Inhibitory effects of a bisphosphonate (risedronate) on experimental periodontitis in rats. *J Periodontal Res* 30: 277–284, 1995
- Singh JA, Yu S, Chen L, Cleveland JD: Rates of total joint replacement in the United States: Future projections to 2020–2040 using the national inpatient sample. *J Rheumatol* 46: 1134–1140, 2019
- Singh R, Ray P, Das A, Sharma M: Penetration of antibiotics through *Staphylococcus aureus* and *Staphylococcus epidermidis* biofilms. *J Antimicrob Chemother* 65: 1955–1958, 2010
- Singh R, Sahore S, Kaur P, Rani A, Ray P: Penetration barrier contributes to bacterial biofilm-associated resistance against only select antibiotics, and exhibits genus-, strain- and antibiotic-specific differences. *Pathog Dis* 74: ftw056, 2016
- Skogman M: A Platform for anti-biofilm assays combining biofilm viability, biomass and matrix quantifications in susceptibility assessments of antimicrobials against *Staphylococcus aureus* biofilms. Dissertation, Åbo Akademi University, Turku, Finland, 2012. Available online: <https://www.doria.fi/handle/10024/84809>
- Skogman ME, Vuorela PM, Fallarero A: Combining biofilm matrix measurements with biomass and viability assays in susceptibility assessments of antimicrobials against *Staphylococcus aureus* biofilms. *J Antibiot (Tokyo)* 65: 453–459, 2012
- Slot DE, Dörfer CE, Van der Weijden GA: The efficacy of interdental brushes on plaque and parameters of periodontal inflammation: A systematic review. *Int J Dent Hyg* 6: 253–264, 2008
- Sonesson A, Przybyszewska K, Eriksson S, Mörgelin M, Kjellström S, Davies J, Potempa J, Schmidtchen A: Identification of bacterial biofilm and the *Staphylococcus aureus* derived protease, staphopain, on the skin surface of patients with atopic dermatitis. *Sci Rep* 7: 8689, 2017
- Spaan AN, van Strijp JAG, Torres VJ: Leukocidins: Staphylococcal bi-component pore-forming toxins find their receptors. *Nat Rev Microbiol* 15: 435–447, 2017
- Speziale P, Pietrocola G, Foster TJ, Geoghegan JA: Protein-based biofilm matrices in staphylococci. *Front Cell Infect Microbiol* 4: 171, 2014
- Squires C, Squires CL: The Clp proteins: Proteolysis regulators or molecular chaperones? *J Bacteriol* 174: 1081–1085, 1992
- Srisubut S, Teerakapong A, Vattraphodes T, Taweechaisupapong S: Effect of local delivery of alendronate on bone formation in bioactive glass grafting in rats. *Oral Surg Oral Med Oral Pathol Oral Radiol Endod* 104: e11–e16, 2007
- Stanko P, Izakovicova Holla L: Bidirectional association between diabetes mellitus and inflammatory periodontal disease. A review. *Biomed Pap Med Fac Univ Palacky Olomouc Czech Repub* 158: 35–38, 2014
- Stewart EJ, Ganesan M, Younger JG, Solomon MJ: Artificial biofilms establish the role of matrix interactions in staphylococcal biofilm assembly and disassembly. *Sci Rep* 5: 13081, 2015
- Stewart PS, Bjarnsholt T: Risk factors for chronic biofilm-related infection associated with implanted medical devices. *Clin Microbiol Infect* 26: 1034–1038, 2020

## 7. REFERENCES

- Stoodley P, Lewandowski Z, Boyle JD, Lappin-Scott HM: Oscillation characteristics of biofilm streamers in turbulent flowing water as related to drag and pressure drop. *Biotechnol Bioeng* 57: 536–544, 1998
- Stoor P, Frantzen J: Influence of bioactive glass S53P4 granules and putty on osteomyelitis associated bacteria *in vitro*. *Biomed. Glasses* 3: 79–85, 2017
- Stoor P, Söderling E, Salonen JI: Antibacterial effects of a bioactive glass paste on oral microorganisms. *Acta Odontol Scand* 56: 161–165, 1998
- Störmer M, Kleesiek K, Dreier J: pH value promotes growth of *Staphylococcus epidermidis* in platelet concentrates. *Transfusion* 48: 836–846, 2008
- Sultan AR, Hoppenbrouwers T, Lemmens-den Toom NA, Snijders SV, van Neck JW, Verbon A, de Maat MPM, van Wamel WJB: During the early stages of *Staphylococcus aureus* biofilm formation, induced neutrophil extracellular traps are degraded by autologous thermonuclease. *Infect Immun* 87: e00605-19, 2019
- Syvänen J, Nietosvaara Y, Kohonen I, Koskimies E, Haara M, Korhonen J, Pajulo O, Helenius I: Treatment of aneurysmal bone cysts with bioactive glass in children. *Scand J Surg* 107: 76–81, 2018
- Takahashi N, Ishihara K, Kato T, Okuda K. Susceptibility of *Actinobacillus actinomycetemcomitans* to six antibiotics decreases as biofilm matures. *J Antimicrob Chemother* 59: 59–65, 2007
- Takaishi Y, Ikeo T, Miki T, Nishizawa Y, Morii H: Suppression of alveolar bone resorption by etidronate treatment for periodontal disease: 4- to 5-year follow-up of four patients. *J Int Med Res* 31: 575–584, 2003
- Takaishi Y, Miki T, Nishizawa Y, Morii H: Clinical effect of etidronate on alveolar pyorrhoea associated with chronic marginal periodontitis: Report of four cases. *J Int Med Res* 29: 355–365, 2001
- Terveysportti: Lääkkeet ja hinnat (online). Available online: <https://www.terveysportti.fi/terveysportti/laakkeet.koti>. Accessed: January 19<sup>th</sup>, 2021
- Thomer L, Schneewind O, Missiakas D: Multiple ligands of von Willebrand factor-binding protein (vWbp) promote *Staphylococcus aureus* clot formation in human plasma. *J Biol Chem* 288: 28283–28292, 2013
- Thormann E, Simonsen AC, Hansen PL, Mouritsen OG: Interactions between a polystyrene particle and hydrophilic and hydrophobic surfaces in aqueous solutions. *Langmuir* 24: 7278–7284, 2008
- Tirapelli C, Panzeri H, Lara EH, Soares RG, Peitl O, Zanotto ED: The effect of a novel crystallised bioactive glass-ceramic powder on dentine hypersensitivity: A long-term clinical study. *J Oral Rehabil* 38: 253–262, 2011
- Tortora GJ, Funke BR, Case CL: *Microbiology: An Introduction*. 11<sup>th</sup> edition. Harlow: Pearson Education Limited, 2014
- Tran N, Kelley MN, Tran PA, Garcia DR, Jarrell JD, Hayda RA, Born CT: Silver doped titanium oxide-PDMS hybrid coating inhibits *Staphylococcus aureus* and *Staphylococcus epidermidis* growth on PEEK. *Mater Sci Eng C Mater Biol Appl* 49: 201–209, 2015
- Tunio SA, Oldfield NJ, Berry A, Ala'Aldeen DA, Wooldridge KG, Turner DP: The moonlighting protein fructose-1, 6-bisphosphate aldolase of *Neisseria meningitidis*: Surface localization and role in host cell adhesion. *Mol Microbiol* 76: 605–615, 2010
- Välimäki VV, Aro HT: Molecular basis for action of bioactive glasses as bone graft substitute. *Scand J Surg* 95: 95–102, 2006

- Välimäki VV, Moritz N, Yrjans JJ, Vuorio E, Aro HT: Effect of zoledronic acid on incorporation of a bioceramic bone graft substitute. *Bone* 38: 432–443, 2006
- Vanassche T, Peetermans M, Van Aelst LN, Peetermans WE, Verhaegen J, Missiakas DM, Schneewind O, Hoylaerts MF, Verhamme P: The role of staphylothrombin-mediated fibrin deposition in catheter-related *Staphylococcus aureus* infections. *J Infect Dis* 208: 92–100, 2013
- Veena HR, Prasad D: Evaluation of an aminobisphosphonate (alendronate) in the management of periodontal osseous defects. *J Indian Soc Periodontol* 14: 40–45, 2010
- Vijaranakul U, Nadakavukaren MJ, de Jonge BL, Wilkinson BJ, Jayaswal RK: Increased cell size and shortened peptidoglycan interpeptide bridge of NaCl-stressed *Staphylococcus aureus* and their reversal by glycine betaine. *J Bacteriol* 177: 5116–5121, 1995
- Voigt B, Albrecht D, Dalhoff A: Mode of action of MCB3681 in *Staphylococcus aureus* – A proteomic study. *Arch Clin Microbiol* 7: 1–4, 2016
- Vuong C, Voyich JM, Fischer ER, Braughton KR, Whitney AR, DeLeo FR, Otto M: Polysaccharide intercellular adhesin (PIA) protects *Staphylococcus epidermidis* against major components of the human innate immune system. *Cell Microbiol* 6: 269–275, 2004
- Waltimo T, Zehnder M, Söderling E: Bone powder enhances the effectiveness of bioactive glass S53P4 against strains of *Porphyromonas gingivalis* and *Actinobacillus actinomycetemcomitans* in suspension. *Acta Odontol Scand* 64: 183–186, 2006
- Weidenmaier C, Kokai-Kun JF, Kristian SA, Chanturiya T, Kalbacher H, Gross M, Nicholson G, Neumeister B, Mond JJ, Peschel A: Role of teichoic acids in *Staphylococcus aureus* nasal colonization, a major risk factor in nosocomial infections. *Nat Med* 10: 243–245, 2004
- Weinreb M, Quartuccio H, Sedor JG, Aufdemorte TB, Brunsvold M, Chaves E, Kornman KS, Rodan GA: Histomorphometrical analysis of the effects of the bisphosphonate alendronate on bone loss caused by experimental periodontitis in monkeys. *J Periodontal Res* 29: 35–40, 1994
- Winkler H: Treatment of orthopedic infections: Addressing the biofilm issue. In the book: Culture negative orthopedic biofilm infections, pp. 111–127. Eds. Ehrlich G, DeMeo P, Costerton J, Winkler H. Springer, Berlin, Heidelberg, Germany, 2012
- Wood NJ, Jenkinson HF, Davis SA, Mann S, O'Sullivan DJ, Barbour ME: Chlorhexidine hexametaphosphate nanoparticles as a novel antimicrobial coating for dental implants. *J Mater Sci Mater Med* 26: 201, 2015
- Wray LV Jr, Zalieckas JM, Fisher SH: *Bacillus subtilis* glutamine synthetase controls gene expression through a protein-protein interaction with transcription factor TnrA. *Cell* 107: 427–435, 2001
- Wuppermann FN, Mölleken K, Julien M, Jantos CA, Hegemann JH: *Chlamydia pneumoniae* GroEL1 protein is cell surface associated and required for infection of HEp-2 cells. *J Bacteriol* 190: 3757–3767, 2008
- Xolalpa W, Vallecillo AJ, Lara M, Mendoza-Hernandez G, Comini M, Spallek R, Singh M, Espitia C: Identification of novel bacterial plasminogen-binding proteins in the human pathogen *Mycobacterium tuberculosis*. *Proteomics* 7: 3332–3341, 2007
- Xu Y, Maltesen RG, Larsen LH, Schønheyder HC, Le VQ, Nielsen JL, Nielsen PH, Thomsen TR, Nielsen KL: *In vivo* gene expression in a *Staphylococcus aureus* prosthetic joint infection characterized by RNA sequencing and metabolomics: A pilot study. *BMC Microbiol* 16: 80, 2016

## 7. REFERENCES

- Yaacob M, Worthington HV, Deacon SA, Deery C, Walmsley AD, Robinson PG, Glenny AM: Powered versus manual toothbrushing for oral health. *Cochrane Database Syst Rev* 6: CD002281, 2014
- Yaffe A, Golomb G, Breuer E, Binderman I: The effect of topical delivery of novel bisacylphosphonates in reducing alveolar bone loss in the rat model. *J Periodontol* 71: 1607–1612, 2000
- Yamaguchi M, Ikeda R, Nishimura M, Kawamoto S: Localization by scanning immunoelectron microscopy of triosephosphate isomerase, the molecules responsible for contact-mediated killing of *Cryptococcus*, on the surface of *Staphylococcus*. *Microbiol Immunol* 54: 368–370, 2010
- Yang CK, Zhang XZ, Lu CD, Tai PC: An internal hydrophobic helical domain of *Bacillus subtilis* enolase is essential but not sufficient as a non-cleavable signal for its secretion. *Biochem Biophys Res Commun* 446: 901–905, 2014
- Yang W, Li E, Kairong T, Stanley SL Jr: *Entamoeba histolytica* has an alcohol dehydrogenase homologous to the multifunctional adhE gene product of *Escherichia coli*. *Mol Biochem Parasitol* 64: 253–260, 1994
- Yao C, Zhang Q, Li J, She P, Kong F, Du Y, Zhang F: Implantable zoledronate-PLGA microcapsules ameliorate alveolar bone loss, gingival inflammation and oxidative stress in an experimental periodontitis rat model. *J Biomater Appl* 35: 569–578, 2021
- Yates JL, Arfsten AE, Nomura M: *In vitro* expression of *Escherichia coli* ribosomal protein genes: Autogenous inhibition of translation. *Proc Natl Acad Sci U S A* 77: 1837–1841, 1980
- Zapotoczna M, McCarthy H, Rudkin JK, O’Gara JP, O’Neill E: An essential role for coagulase in *Staphylococcus aureus* biofilm development reveals new therapeutic possibilities for device-related infections. *J Infect Dis* 212: 1883–1893, 2015
- Zhang D, Hupa M, Hupa L: *In situ* pH within particle beds of bioactive glasses. *Acta Biomater* 4: 1498–1505, 2008
- Zhou C, Fey PD: The acid response network of *Staphylococcus aureus*. *Curr Opin Microbiol* 55: 67–73, 2020
- Zimmerli W, Trampuz A, Ochsner PE: Prosthetic-joint infections. *N Engl J Med* 351: 1645–1654, 2004
- Zimmerli W, Trampuz A: Implant-associated infection. In the book: *Biofilm infections*, pp. 69–90. Eds. Bjarnsholt T, Jensen P, Moser C, Høiby N. Springer, New York, US, 2011
- Zimmerli W: Clinical presentation and treatment of orthopaedic implant-associated infection. *J Intern Med* 276: 111–119, 2014
- Zmantar T, Kouidhi B, Miladi H, Mahdouani K, Bakhrouf A: A microtiter plate assay for *Staphylococcus aureus* biofilm quantification at various pH levels and hydrogen peroxide supplementation. *New Microbiol* 33: 137–145, 2010



## APPENDIX (SUPPLEMENTARY MATERIAL)

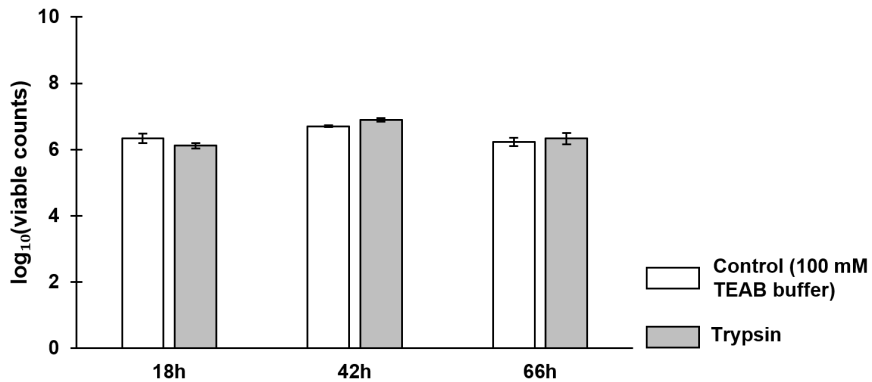


**Figure S1.** *S. aureus* ATCC 25923 biofilms on borosilicate glass coupons exposed to trypsin or 100 mM TEAB buffer (control). The number of viable cells is conveyed as  $\log_{10}$  values of CFU (mL·cm<sup>2</sup>)<sup>-1</sup>. The differences in the biofilm viabilities between the groups were not statistically significant (unpaired t-test with Welch's correction,  $p < 0.05$ ), demonstrating the absence of cell lysis and appropriateness of the trypsin-shaving method. Error bars denote the standard error of the mean (SEM) (n=2). Figure adapted from publication I, with permission from MDPI, to keep consistency of this document.

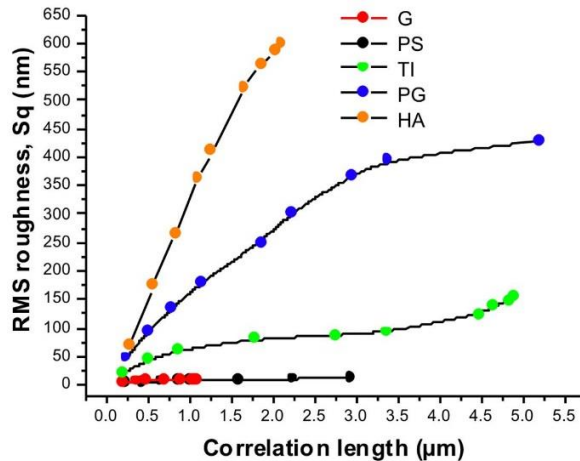


**Figure S2.** Length-scale dependent roughness of the substrate materials. G, borosilicate glass; PS, polystyrene; TI, titanium; PG, plexiglass; HA, hydroxyapatite. Figure originally included in publication I and reproduced with permission from MDPI.

